

# Goldberger-Treiman Relation and $g_{\pi NN}$ from the Three Quark BS/Faddeev Approach in the NJL Model

Noriyoshi ISHII

Institute for Theoretical Physics III,  
University of Erlangen-Nürnberg,  
Staudtstrasse 7, D-91058, Erlangen, GERMANY  
E-mail: ishii@theorie3.physik.uni-erlangen.de

Phone: +49 +9131 85 28466

FAX: +49 +9131 85 27704

## Abstract

A systematic evaluation method of matrix elements of quantum one-body operators between nucleon states in the three-quark Bethe-Salpeter(3qBS)/Faddeev approach in the NJL model is reviewed. We do not confine ourselves to a particular truncation scheme of the 3qBS kernel. One of our main aims is to derive a general condition to be imposed on a given BS kernel in order that the PCAC relation is satisfied correctly. We apply this condition to some particular 3qBS kernels. We numerically calculate  $g_{\pi NN}$  in the 3qBS /Faddeev approach to estimate the violation of the Goldberger-Treiman/PCAC relation due to the UV-regularization scheme. We finally consider the non-vanishing current quark mass effects on the Goldberger-Treiman relation.

## PACS Classification Codes:

12.39.-x, 12.39, Fe, 12.39.Ki

## Keywords:

Nucleon, Chiral Ward identity, Goldberger-Treiman Relation,  $g_{\pi NN}$ , Relativistic Faddeev Equation, Nambu-Jona-Lasinio (NJL) Model.

# 1 Introduction

The Nambu-Jona-Lasinio(NJL) model is a quantum field theoretical effective quark model based on QCD. While the confinement, which is one of the most important properties of the low energy QCD, is not incorporated, it is the simplest quantum field theoretical quark model respecting the chiral symmetry and providing us with explicit examples how the spontaneous breaking of the chiral symmetry plays an important role in hadronic phenomena[1], in particular, the interpretation of pion, K, and  $\eta$  as Nambu-Goldstone modes. Based on these advantages, not only mesons but also baryons have been extensively studied in the NJL model[2, 3]. The studies of baryons are mainly classified into the following two categories: (C1) the relativistic mean field approach[4], and (C2) the relativistic three-quark Bethe-Salpeter(3qBS)/Faddeev approach[5, 6, 7, 8, 9]. Since the NJL model is a second quantized field theory, it is, in principle, possible to consider the effects of  $q\bar{q}$  excitations in the nucleon. This is one of the most interesting targets in the studies of the nucleon structure beyond the non-relativistic constituent quark models. In this respect, on the one hand, the meanfield approach incorporates  $q\bar{q}$  effects through the mesonic hedgehog fields leading to the solitonic picture of the nucleon, where, however, the manifest Lorentz covariance is unfortunately missing. On the other hand, the 3qBS /Faddeev approach, which respects the manifest Lorentz covariance leading to the quark-diquark picture of baryons[10], approximates the 3qBS kernel according to the ladder truncation scheme, which prevents us from studying non-trivial  $q\bar{q}$  effects beyond the excitations of the “three-quark RPA vacuum”[11](the backward diagrams included in the ladder approximation).

It is thus necessary to extend the 3qBS kernel in order to study the non-trivial  $q\bar{q}$  effects in a Lorentz covariant manner, and therefore attempts have been (and are) made to go beyond the ladder truncation scheme [12]. To extend the NJL 3qBS kernels, chiral symmetry imposes important constraints. In particular, it would be very useful to have a criterion which tells us which kinds of kernels lead to the PCAC relation<sup>1</sup> correctly. One of the main aims of this paper is to derive such a criterion and to provide explicit examples of its application to some of the existing 3qBS kernels. We will first review how matrix elements of quantum one-body operators are evaluated systematically in the 3qBS framework by introducing classical external fields as a technical tool. Note that the evaluation of the bound state matrix elements in the 3qBS framework is not obvious beyond the diagrammatic argument. We will provide a direct formula to evaluate the matrix element in terms of the Faddeev framework. We then consider which properties of the 3qBS kernel are required to satisfy the PCAC relation correctly. We consider the relevant Feynman diagrams to calculate the matrix elements for several 3qBS kernels, and apply our criterion to these 3qBS kernels. Although we are going to restrict our attention only to the PCAC case, these considerations themselves can be extended to other cases straightforwardly such as the electromagnetic current, the isospin current, the baryon number current, etc —actually, the PCAC case is the most complicated one<sup>2</sup>.

---

<sup>1</sup>We mean by “PCAC relation” in the sense of Eq.(28).

<sup>2</sup>The proof of the electromagnetic Ward identity in the Faddeev approach to the NJL model in the

Even if the truncation scheme is consistent with the PCAC relation, the UV regularization schemes, which have been adopted so far in practical numerical calculations in the NJL model, usually, spoil it. It is thus worth while to evaluate  $g_{\pi NN}$  and  $g_A$  in the chiral limit in order to estimate explicitly the violation of the Goldberger-Treiman relation due to the UV regularization scheme. We will see that with the Euclidean sharp cut-off the violation is up to 4 %. The extracted value of  $g_{\pi NN}$  is 13.2. We will also estimate the PCAC violation due to the cutoff scheme off the chiral limit, which is again up to 4%. We will evaluate the off-shell  $g_{\pi NN}(\equiv \tilde{g}_{\pi NN})$  with the single-pole dominance approximation for the form factor  $h_A(q^2)$ . We obtain a very reasonable value  $\tilde{g}_{\pi NN} = 13.5$ . However  $g_A$  is 6 % larger than the experimental one. We will also consider the effect of the non-vanishing current quark mass on the Goldberger-Treiman relation, and find that it is in the opposite direction than expected from the experimental values. We will analyze this by including also the effect of the  $q\bar{q}$  interaction in the color singlet iso-vector axial-vector channel, providing an analytic expression for the deviation from the Goldberger-Treiman relation by assuming that the vacuum is approximated according to the mean-field approximation. We will find that the effect of this additional  $q\bar{q}$  channel works into the unwanted direction. We will see that, to resolve this problem, it is necessary either to improve the gap equation for the vacuum beyond the mean field approximation or to evaluate the on-shell  $g_{\pi NN}$ .

## 2 Bound State Matrix Elements and the Criterion (Sufficient Condition) for the PCAC Relation

We consider effective quark Lagrangians with global  $SU(2)_f \times SU(3)_c$  symmetries:

$$\mathcal{L} = \bar{\psi}(i\cancel{\partial} - m_0)\psi + \mathcal{L}_I, \quad (1)$$

where  $m_0$  is the current quark mass, and  $\psi$  and  $\bar{\psi}$  are the quark bispinor fields.  $\mathcal{L}_I$  is a local, chirally symmetric four-fermionic interaction Lagrangian of NJL type, i.e.,  $\mathcal{L}_I = \sum_{\Gamma} g_{\Gamma} (\bar{\psi}\Gamma\psi)^2$ , where  $\Gamma$  is a matrix with Dirac, isospin, and color indices. Examples are the original NJL type  $\mathcal{L}_I = g \left( (\bar{\psi}\psi)^2 - (\bar{\psi}\gamma_5\vec{\tau}\psi)^2 \right)$  and the color current interaction type  $\mathcal{L}_I = g \left( \bar{\psi}\gamma^{\mu}\frac{\lambda^a}{2}\psi \right)^2$ , etc. (For detail, see Appendix B.1.) Since interaction Lagrangians of this type can all be dealt with in the same manner, we will not confine ourselves to a particular one.

To evaluate a matrix element in the 3qBS framework is not really straight forward. This is because what is directly obtained in the 3qBS framework is not the nucleon eigenket  $|N\rangle$  but the 3qBS amplitude<sup>3</sup>, which itself is a matrix element of the type  $\langle 0|T\psi\psi\psi|N\rangle$ .

---

ladder truncation scheme can be found in ref.[9], which was applied to the quark-diquark model in [13]. Although these authors did not use the external field method, the results are consistent with our formalism. A systematic approach using the external field method can be found in ref.[14].

<sup>3</sup>The 3qBS amplitude is often referred to as the “wave function” due to historical reasons. However, we prefer to call it as “3qBS amplitude” to avoid unnecessary confusions[15].

We might thus suspect that a huge amount of information, which is contained in the ket vector  $|N\rangle$ , could be missing in the 3qBS amplitude. In the relativistic Faddeev framework, the situation is slightly more complicated —there are no immediate representations of the Faddeev amplitude in terms of the canonical operator formalism<sup>4</sup>. Therefore, we will first review how to evaluate a matrix element in the 3qBS framework based on the canonical operator formalism.

To this end, it is convenient to introduce space-time dependent external fields:

$$v_\mu(x) = v_\mu^a(x)\frac{\tau^a}{2}, \quad a_\mu(x) = a_\mu^a(x)\frac{\tau^a}{2}, \quad m(x) = s(x) + ip^a(x)\gamma_5\frac{\tau^a}{2}, \quad (2)$$

where  $v_\mu^a(x)$  is an isovector vector field,  $a_\mu^a(x)$  is an isovector axial-vector field,  $s(x)$  is a scalar isoscalar field, and  $p^a(x)$  is a pseudo-scalar isovector field. (The iso-spin index  $a$  runs over 1, 2, 3.) The following Lagrangian density characterizes how these external fields couple to the associated quantized one-body operators:

$$\begin{aligned} \mathcal{L}^{[e]} &= \bar{\psi}(i\not{\partial} - \not{v} - \not{a}\gamma_5 - m)\psi + \mathcal{L}_I \\ &= \bar{\psi}i\not{\partial}\psi + \mathcal{L}_I - v_\mu^a V^{a\mu} - a_\mu^a A^{a\mu} - \bar{\psi}m\psi, \end{aligned} \quad (3)$$

where  $V^{a\mu} \equiv \bar{\psi}\gamma^\mu\frac{\tau^a}{2}\psi$  and  $A^{a\mu} \equiv \bar{\psi}\gamma^\mu\gamma_5\frac{\tau^a}{2}\psi$ . The superscripts  $[e]$  or  $[0]$  will be used to indicate quantities in the presence or absence, respectively, of the external fields  $v, a, m - m_0$ . For simplicity, we include the current quark mass  $m_0$  in the definition of the external field  $m$ . We assume that these external fields,  $v, a, m$ , are localized in space-time, i.e., they vanish except for some finite space-time region. After performing the necessary manipulations, we will eventually set  $a(x) \equiv v(x) \equiv 0$  and  $m \equiv m_0$  in the whole space-time. This limit will be referred to as the “vanishing external fields limit”.

The 3qBS equation in the presence of the external fields is derived from the Schwinger-Dyson(SD) equation[15] by means of the same technique as for vanishing external fields:

$$G^{[e]} = G_0^{[e]} + G_0^{[e]}V^{[e]}G^{[e]}, \quad (4)$$

where  $V^{[e]}$  is the sum of 2PI and 3PI interactions, and  $G_0^{[e]}$  is an anti-symmetric combination of products of three constituent quark propagators in the presence of the external fields. For simplicity, we denote

$$K^{[e]} \equiv G_0^{[e]}V^{[e]}. \quad (5)$$

To avoid cumbersome notations, we often adopt the operator notation to suppress the explicit integration symbol  $\int d^4x_1 d^4x_2 d^4x_3$ , the explicit space-times coordinates  $(x_1, x_2, x_3)$  and the explicit indices of the quark fields.

Since the external fields are localized in space-time, a nucleon state “propagates” freely in the “past”. Therefore,  $G^{[e]}$  has an asymptotic initial nucleon pole. The residue

---

<sup>4</sup>The Faddeev amplitude provides the same amount of informations as the 3qBS amplitude does, as we show in Appendix A.

at this nucleon pole satisfies the following homogeneous 3qBS equation in the presence of the external fields:

$$\Psi[N_\alpha^a(\vec{P})]^{[e]} = K^{[e]}\Psi[N_\alpha^a(\vec{P})]^{[e]}, \quad (6)$$

where  $\Psi[N_\alpha^a(\vec{P})]^{[e]}$  is the 3qBS amplitude for the nucleon in the presence of the external fields with the isospin  $a$ , helicity  $\alpha$  and asymptotic four momentum  $P = (E_N(\vec{P}^2), \vec{P})$  with  $E_N(\vec{P}^2) = \sqrt{m_N^2 + \vec{P}^2}$  ( $m_N$  : nucleon mass). In terms of the canonical operator formalism, it is expressed as:

$$\begin{aligned} & \Psi[N_\alpha^a(\vec{P})]^{[e]}(x_1, x_2, x_3) \\ &= \langle 0 | T\psi(x_1)\psi(x_2)\psi(x_3) \\ & \quad \times \exp -i \int d^4x [v_\mu^a(x)V^{a\mu}(x) + a_\mu^a(x)A^{a\mu}(x) + \bar{\psi}(m(x) - m_0)\psi] | N_\alpha^a(\vec{P}) \rangle. \end{aligned} \quad (7)$$

$|0\rangle$  and  $|N_\alpha^a(\vec{P})\rangle$  are the vacuum and the nucleon state vectors, respectively. They are eigenstates of the ‘‘unperturbed’’ Hamiltonian  $H^{[0]}$  obtained by setting  $v = a = 0, m = m_0$ . We adopt the covariant normalizations:

$$\langle 0 | 0 \rangle = 1, \quad \langle N_{\alpha'}^a(\vec{P}') | N_\alpha^a(\vec{P}) \rangle = \frac{E_N(\vec{P}^2)}{m_N} (2\pi)^3 \delta^{(3)}(\vec{P}' - \vec{P}) \delta_{\alpha'\alpha} \delta_{a'a}. \quad (8)$$

Note that quantized operators are represented in the ‘‘interaction picture’’ in Eq.(7), where the ‘‘unperturbed Hamiltonian’’<sup>5</sup> is  $H^{[0]}$  and the ‘‘perturbing Hamiltonian’’ is

$$H_I \equiv \int d^3x (v_\mu^a(x)V_{a\mu}(x) + a_\mu^a(x)A^{a\mu}(x) + \bar{\psi}(x)(m(x) - m_0)\psi(x)). \quad (9)$$

We next consider the matrix element  $\langle N | A_\mu^b | N \rangle$ . Applying the functional derivative  $\frac{i\delta}{\delta a_\mu^a(x)}$  to both sides of Eq.(6), we obtain the following relation in the vanishing external field limit,

$$\left( \frac{i\delta\Psi[N_\alpha^a(\vec{P})]^{[e]}}{\delta a_\mu^b(x)} \right)^{[0]} = \left( \frac{i\delta K^{[e]}}{\delta a_\mu^b(x)} \right)^{[0]} \Psi[N_\alpha^a(\vec{P})]^{[0]} + K^{[0]} \left( \frac{i\delta\Psi[N_\alpha^a(\vec{P})]^{[e]}}{\delta a_\mu^b(x)} \right)^{[0]}. \quad (10)$$

The expressions for the ‘‘3qBS amplitudes’’ entering in Eq.(10) are given in terms of the canonical operator formalism as follows:

$$\begin{aligned} \Psi[N_\alpha^a(\vec{P})]^{[0]}(x_1, x_2, x_3) &= \langle 0 | T\psi(x_1)\psi(x_2)\psi(x_3) | N_\alpha^a(\vec{P}) \rangle \\ \bar{\Psi}[N_\alpha^a(\vec{P})]^{[0]}(x_1, x_2, x_3) &= \langle N_\alpha^a(\vec{P}) | T\bar{\psi}(x_1)\bar{\psi}(x_2)\bar{\psi}(x_3) | 0 \rangle \\ \left( \frac{i\delta\Psi[N_\alpha^a(\vec{P})]^{[e]}(x_1, x_2, x_3)}{\delta a_\mu^b(x)} \right)^{[0]} &= \langle 0 | T\psi(x_1)\psi(x_2)\psi(x_3)A^{b\mu}(x) | N_\alpha^a(\vec{P}) \rangle. \end{aligned} \quad (11)$$

---

<sup>5</sup> Note that  $H^{[0]}$  is the full Heisenberg Hamiltonian in the absence of the external fields.

By using the canonical operator analysis, i.e., by inserting into the Green's function the complete set relation in the baryon number 1 sector:

$$\mathbb{1} = \sum_{\alpha\alpha} \int \frac{d^3p}{(2\pi)^3} \frac{m_N}{E_N(\vec{p}^2)} |N_\alpha^a(\vec{p})\rangle \langle N_\alpha^a(\vec{p})| + \dots, \quad (12)$$

and by using the Fourier transform of the step function  $\theta(t)$ , we see that<sup>6</sup> the product  $\Psi^{[0]}\bar{\Psi}^{[0]}$  provides the residue of the Green's function at the nucleon pole, i.e.,

$$G^{[0]} = \sum_{\alpha\alpha} \int \frac{d^4p}{(2\pi)^4} \frac{m_N}{E_N(\vec{p}^2)} \frac{i}{p_0 - E_N(\vec{p}^2) + i\epsilon} \Psi[N_\alpha^a(\vec{p})]^{[0]}\bar{\Psi}[N_\alpha^a(\vec{p})]^{[0]} + \dots \quad (13)$$

In Appendix A, we explain how to obtain and normalize these two 3qBS amplitudes based on the relativistic Faddeev framework. In Appendix A, we prove that the residues  $\Psi^{[0]}$  and  $\bar{\Psi}^{[0]}$  satisfy the following 3qBS equation in the absence of the external fields(cf Eq.(6))

$$K^{[0]}\Psi^{[0]}[N_\alpha^a(\vec{P})] = \Psi^{[0]}[N_\alpha^a(\vec{P})], \quad \tilde{\Psi}^{[0]}[N_\alpha^a(\vec{P})]K^{[0]} = \tilde{\Psi}^{[0]}[N_\alpha^a(\vec{P})], \quad (14)$$

where a tilde is used to indicate an ‘‘amputation’’, i.e.,  $\tilde{\Psi}[N_\alpha^a(\vec{p})]^{[0]} = \bar{\Psi}[N_\alpha^a(\vec{p})]^{[0]}G_0^{[0]-1}$ . By rearranging Eq.(10), we obtain the following relation:

$$\left( \frac{i\delta\Psi[N_\alpha^a(\vec{P})]^{[e]}}{\delta a_\mu^b(x)} \right)^{[0]} = \frac{1}{1 - K^{[0]}} \left( \frac{i\delta K^{[e]}}{\delta a_\mu^b(x)} \right)^{[0]} \Psi[N_\alpha^a(\vec{P})]^{[0]}. \quad (15)$$

On the one hand, near the nucleon pole the resolvent is given as

$$\begin{aligned} \frac{1}{1 - K^{[0]}} &= G^{[0]}G_0^{[0]-1} \\ &\simeq \sum_{\alpha,\alpha'} \int \frac{d^4p}{(2\pi)^4} \frac{m_N}{E_N(\vec{p}^2)} \frac{i}{p^0 - E_N(\vec{p}^2) + i\epsilon} \Psi[N_\alpha^a(\vec{p})]^{[0]}\tilde{\Psi}[N_{\alpha'}^a(\vec{p})]^{[0]}. \end{aligned} \quad (16)$$

The l.h.s. of Eq.(15), on the other hand, is given near the nucleon pole as follows:

$$\begin{aligned} &\left( \frac{i\delta\Psi[N_\alpha^a(\vec{P})]^{[e]}}{\delta a_\mu^b(x)} \right)^{[0]} \\ &\simeq \sum_{\alpha'\alpha'} \int \frac{d^4p}{(2\pi)^4} \frac{m_N}{E_N(\vec{p}^2)} \frac{i}{p^0 - E_N(\vec{p}^2) + i\epsilon} \langle 0 | T\psi\psi\psi | N_{\alpha'}^a(\vec{p}) \rangle \langle N_{\alpha'}^a(\vec{p}) | A_\mu^b(x) | N_\alpha^a(\vec{P}) \rangle. \\ &= \sum_{\alpha'\alpha'} \int \frac{d^4p}{(2\pi)^4} \frac{m_N}{E_N(\vec{p}^2)} \frac{i}{p^0 - E_N(\vec{p}^2) + i\epsilon} \Psi[N_{\alpha'}^a(\vec{p})]^{[0]} \langle N_{\alpha'}^a(\vec{p}) | A_\mu^b(x) | N_\alpha^a(\vec{P}) \rangle. \end{aligned} \quad (17)$$

By comparing both sides of Eq.(15), we are left with:

$$\langle N_{\alpha'}^a(\vec{P}') | A_\mu^b(x) | N_\alpha^a(\vec{P}) \rangle = \tilde{\Psi}[N_{\alpha'}^a(\vec{P}')]^{[0]} \left( \frac{i\delta K^{[e]}}{\delta a_\mu^b(x)} \right)^{[0]} \Psi[N_\alpha^a(\vec{P})]^{[0]}. \quad (18)$$

---

<sup>6</sup>The argument is similar to the one given in p.92 in [15].

A similar consideration leads to the following relation:

$$\left\langle N_{\alpha'}^{a'}(\vec{P}') \left| i\bar{\psi}(x)\gamma_5\frac{\tau^b}{2}\psi(x) \right| N_{\alpha}^a(\vec{P}) \right\rangle = \tilde{\Psi}[N_{\alpha'}^{b'}(\vec{P}')]^{[0]} \left( \frac{i\delta K^{[e]}}{\delta p^b(x)} \right)^{[0]} \Psi[N_{\alpha}^a(\vec{P})]^{[0]}. \quad (19)$$

A combination of these two relations provides us with:

$$\begin{aligned} & \left\langle N^{a'}(\vec{P}') \left| \partial_{\mu}A^{b\mu}(x) - 2im_0\bar{\psi}(x)\gamma_5\tau^b\psi(x) \right| N^a(\vec{P}) \right\rangle \\ &= \tilde{\Psi}[N_{\alpha'}^{a'}(\vec{P}')]^{[0]} \left( \left( \partial_{\mu}\frac{i\delta}{\delta a_{\mu}^b(x)} - 2m_0\frac{i\delta}{\delta p^b(x)} \right) K^{[e]} \right)^{[0]} \Psi[N_{\alpha}^a(\vec{P})]^{[0]}. \end{aligned} \quad (20)$$

These expressions show that the 3qBS amplitudes provide enough informations to evaluate these matrix elements. Here the ‘‘relative time’’ dependence of the 3qBS amplitude surely plays a very important role. At any rate, we should keep in mind that, although bound state matrix elements are obtained by sandwiching one-body operators in the canonical operator formalism, it is these two-body operators shown on the r.h.s. of Eq.(20) that should be sandwiched in the 3qBS framework<sup>7</sup>, which leads to crucial differences[14]. The corresponding formula to evaluate the bound state matrix elements in the Faddeev framework is derived in Appendix A. Note that it is not hard to extend these arguments beyond the NJL model.

If the full 3qBS kernel were at our disposal, the chiral symmetry of the original Lagrangian should directly lead to the PCAC relation in the 3qBS framework. However, because the 3qBS kernel is in practice truncated such as to be manageable, it may happen that the truncation scheme spoils the chiral symmetry. We are thus interested in the criterion to decide which 3qBS kernel gives rise to the PCAC relation correctly. For this purpose, it is convenient to introduce the local ‘‘axial’’ gauge transformation of the external fields as follows:

$$\begin{aligned} i\cancel{\partial} - \not{v}^{(\omega)}(x) - \not{a}^{(\omega)}(x)\gamma_5 - m^{(\omega)} &= \Omega(x) \left( i\cancel{\partial} - \not{v}(x) - \not{a}(x)\gamma_5 - m \right) \Omega(x), \\ \Omega(x) &= e^{-i\gamma_5\omega(x)}; \quad \omega(x) = \omega^a(x)\frac{\tau^a}{2}, \end{aligned} \quad (21)$$

where  $v^{(\omega)}$ ,  $a^{(\omega)}$  and  $m^{(\omega)}$  are the gauge images of  $v$ ,  $a$  and  $m$ , respectively. We assume that  $\omega(x)$  is also localized in space-time. Infinitesimally, these gauge transformations are expressed as follows:

$$\begin{aligned} \frac{\delta v_{\mu}^a(y)}{\delta \omega^c(x)} &= \epsilon_{abc}a_{\mu}^b(y)\delta^{(4)}(x-y) \\ \frac{\delta a_{\mu}^a(y)}{\delta \omega^c(x)} &= \delta_{ac}\frac{\partial}{\partial x^{\mu}}\delta^{(4)}(x-y) + \epsilon_{abc}v_{\mu}^b(y)\delta^{(4)}(x-y) \\ \frac{\delta s(y)}{\delta \omega^c(x)} &= \frac{1}{2}p^c(y)\delta^{(4)}(x-y) \end{aligned} \quad (22)$$

---

<sup>7</sup>If 3PI interactions are included in the 3qBS kernel, there appear three-body operators in addition to the two-body operators in the 3qBS framework.

$$\frac{\delta p^b(y)}{\delta \omega^c(x)} = -2\delta_{bc}s(y)\delta^{(4)}(x-y),$$

where  $\epsilon_{abc}$  is the totally anti-symmetric tensor. Let  $F[v, a, m]$  be a functional. We define the functional derivative  $\frac{\delta}{\delta \omega^c(x)}$  through the following relation:

$$\frac{\delta F}{\delta \omega^c(x)} \equiv \frac{\delta F[v^{(\omega)}, a^{(\omega)}, m^{(\omega)}]}{\delta \omega^c(x)}. \quad (23)$$

By using the chain rule,  $\frac{i\delta}{\delta \omega^c(x)}$  is expressed as a linear combination of functional derivatives with respect to the external fields:

$$\begin{aligned} & \frac{i\delta}{\delta \omega^c(x)} \\ &= \int d^4y \left[ \frac{\delta a_\mu^b(y)}{\delta \omega^c(x)} \frac{i\delta}{\delta a_\mu^b(y)} + \frac{\delta v_\mu^b(y)}{\delta \omega^c(x)} \frac{i\delta}{\delta v_\mu^b(y)} + \frac{\delta s(y)}{\delta \omega^c(x)} \frac{i\delta}{\delta s(y)} + \frac{\delta p^b(y)}{\delta \omega^c(x)} \frac{i\delta}{\delta p^b(y)} \right] \\ &= \partial_\mu \frac{i\delta}{\delta a_\mu^c(x)} - \epsilon_{abc} v_\mu^a(x) \frac{i\delta}{\delta a_\mu^b(x)} - \epsilon_{abc} a_\mu^a(x) \frac{i\delta}{\delta v_\mu^b(x)} + \frac{1}{2} p^c(x) \frac{i\delta}{\delta s(x)} - 2s(x) \frac{i\delta}{\delta p^c(x)}. \end{aligned} \quad (24)$$

In particular, we have the following relation in the vanishing external field limit:

$$\left( \frac{i\delta K^{[e^{(\omega)}]}}{\delta \omega^b(x)} \right)^{[0]} = \partial_\mu \left( \frac{i\delta K^{[e]}}{\delta a_\mu^b(x)} \right)^{[0]} - 2m_0 \left( \frac{i\delta K^{[e]}}{\delta p^b(x)} \right)^{[0]}, \quad (25)$$

where  $[e^{(\omega)}]$  denotes the gauge transformed fields  $[v^{(\omega)}, a^{(\omega)}, m^{(\omega)}]$ . Now we state the sufficient condition for the validity of the PCAC relation as follows:

**Sufficient Condition:**

If a 3qBS kernel behaves in the following manner under a gauge transformation  $\Omega(x)$ :

$$\begin{aligned} & K^{[e^{(\omega)}]}(x_1, x_2, x_3; y_1, y_2, y_3) \\ &= \left( \Omega(x_1)^{-1} \otimes \Omega(x_2)^{-1} \otimes \Omega(x_3)^{-1} \right) K^{[e]} \left( \Omega(y_1) \otimes \Omega(y_2) \otimes \Omega(y_3) \right), \end{aligned} \quad (26)$$

then the PCAC relation is satisfied.

Our ‘‘criterion’’ is obtained from Eq.(26) by applying the functional derivative with respect to the gauge transformation on both sides, and using Eq.(25). We are left with the following chiral Ward identity, which is the ‘‘criterion’’ for the validity of the PCAC relation:

**Criterion:** (The Chiral Ward Identity for the 3qBS Kernel)

$$\begin{aligned} & \left[ \left( \partial_\mu \frac{i\delta}{\delta a_\mu^b(x)} - 2m_0 \frac{i\delta}{\delta p^b(x)} \right) K^{[e]} \right]^{[0]}(x_1, x_2, x_3; y_1, y_2, y_3) \\ &= K^{[0]} \left[ (\tau^b \gamma_5 \otimes 1 \otimes 1) \delta^{(4)}(x-y_1) + (1 \otimes \tau^b \gamma_5 \otimes 1) \delta^{(4)}(x-y_2) + (1 \otimes 1 \otimes \tau^b \gamma_5) \delta^{(4)}(x-y_3) \right] \\ & \quad - \left[ (\tau^b \gamma_5 \otimes 1 \otimes 1) \delta^{(4)}(x-x_1) + (1 \otimes \tau^b \gamma_5 \otimes 1) \delta^{(4)}(x-x_2) + (1 \otimes 1 \otimes \tau^b \gamma_5) \delta^{(4)}(x-x_3) \right] K^{[0]}. \end{aligned} \quad (27)$$



To see that this indeed leads to the PCAC relation, we sandwich Eq.(27) between  $\Psi[N_{\alpha'}^a(\vec{P}')]^{[0]}$  and  $\tilde{\Psi}[N_{\alpha}^a(\vec{P})]^{[0]}$  and use Eq.(14) and Eq.(20) to get

$$\langle N_{\alpha'}^a(\vec{P}') | \partial_{\mu} A^{b\mu}(x) - 2m_0 i \bar{\psi}(x) \gamma_5 \tau^b \psi(x) | N_{\alpha}^a(\vec{P}) \rangle = 0, \quad (28)$$

which is the desired relation.

We should comment here on the reason why we called Eq.(26) a ‘‘sufficient condition’’. If we try to extend our method to  $SU(3)_L \times SU(3)_R$ -QCD in the presence of external chiral gauge fields, the relation (26) is no longer valid due to the existence of the non-Abelian anomaly<sup>8</sup> [16]. Note, however, that, even if there is such a non-Abelian anomaly, because the anomalous contributions are polynomials of at least second order in the external chiral gauge fields, the infinitesimal form (the criterion Eq.(27)) is still valid. However, if more than two functional derivatives of the external chiral gauge fields are involved, one must pay full attention to the non-Abelian anomaly even for the infinitesimal form. At any rate, the chiral  $SU(2)_L \times SU(2)_R$  case, which is of most interest to us here, is known to be anomaly free.

### 3 Feynman Diagrams

The aim of this section is to see which kinds of Feynman diagrams are involved in the expression Eq.(18) of  $\langle N | A_{\mu}^b(x) | N \rangle$ , before applying the criterion/sufficient condition to particular 3qBS kernels.

We first consider the constituent quark propagator  $S_F^{[e]}(x, y)$  in the presence of the external fields. The self energy is, in principle, obtained from the sum of 1PI diagrams. However, in practice, it is approximated in the mean field (Hartree-Fock) treatment, as expressed by the following gap equation:

$$\begin{aligned} iS_F^{[e]}(x, y) &= iS_{0;F}^{[e]}(x, y) \\ &- \sum_{\Gamma} 2ig_{\Gamma}^{(q\bar{q})} \int d^4z iS_{0;F}^{[e]}(x, z) \Gamma iS_F^{[e]}(z, y) \text{Tr} \left( \Gamma iS_F^{[e]}(z, z) \right). \end{aligned} \quad (29)$$

$g_{\Gamma}^{(q\bar{q})}$  are the effective coupling constants in the  $q\bar{q}$  channels, which are defined in Appendix B.1.  $S_{0;F}^{[e]}(x, y)$  is the current quark propagator, which is defined through the following relation:

$$\left( i\cancel{\partial}^{(x)} - \cancel{d}(x)\gamma_5 - \cancel{\psi}(x) - m(x) \right) S_{0;F}^{[e]}(x, y) = \delta^{(4)}(x - y). \quad (30)$$

The solution to Eq.(29) is obtained as a self-consistent solution to the following equations:

$$\begin{aligned} S_F^{[e]}(x, y) &= \left( i\cancel{\partial} - \cancel{d}\gamma_5 - \cancel{\psi} - m - \Sigma^{[e]} \right)^{-1} (x, y) \\ \Sigma^{[e]}(z) &\equiv \sum_{\Gamma} 2ig_{\Gamma}^{(q\bar{q})} \text{Tr} \left( S_F^{[e]}(z, z) \Gamma \right) \Gamma. \end{aligned} \quad (31)$$

---

<sup>8</sup>This anomaly should not be confused with the  $U_A(1)$  anomaly, i.e., the Abelian anomaly.

$\Sigma^{[e]}(z)$  is the self-energy of the constituent quark. Now, several comments are in order. (1) Due to the presence of the external fields, there is no translational symmetry any more, and therefore the self-energy depends on the space-time point  $z$ . (The dependence on just a single space-time coordinate  $z$  is due to the mean field approximation.) (2) Non-vanishing external fields may lead to not only a non-vanishing scalar condensate, but also a non-vanishing pseudoscalar, vector, axial vector condensates. However, in the vanishing external field limit, we have  $m_0 + \Sigma^{[0]} = M$  (the constituent quark mass). (3) Because the NJL model is non-renormalizable, it is necessary to introduce a UV regularization in all loop integrals. Hereafter, whenever a loop integral is encountered, the integration is understood as a regularized one. (4) If this regularization respects the chiral symmetry,  $S_F^{[e]}(x, y)$  and  $\Sigma^{[e]}(z)$  should behave in the following way:

$$\begin{aligned} S_F^{[e(\omega)]}(x, y) &= \Omega(x)^{-1} S_F^{[e]}(x, y) \Omega(y)^{-1} \\ \Sigma^{[e(\omega)]}(z) &= \Omega(z) \Sigma^{[e]}(z) \Omega(z). \end{aligned} \quad (32)$$

For later convenience, the transformation of  $S_F$  is depicted in Fig.1.

All diagrammatically truncated 3qBS kernels  $K^{[e]}$  can be expressed as the product of several constituent quark propagators  $S_F^{[e]}$  and several elementary local vertices  $\Gamma$ . Because, in our case, these elementary local vertices do not depend on the external fields<sup>9</sup>,  $K^{[e]}$  depends on  $v, a$  and  $m$  only through  $S_F^{[e]}$ . In a symbolic notation, this may be denoted as  $K^{[e]} = K[\Gamma; S_F^{[e]}]$ , and the functional derivatives are then symbolically expressed by using the chain rule as follows:

$$\left[ \frac{i\delta K^{[e]}}{\delta a_\mu^b(x)} \right]^{[0]} = \sum_{\alpha\alpha'} \int d^4z d^4z' \left[ \frac{i\delta S_{F\alpha\alpha'}^{[e]}(z, z')}{\delta a_\mu^b(x)} \right]^{[0]} \left( \frac{\delta K[\Gamma; S_F^{[0]}]}{\delta S_{F\alpha\alpha'}^{[0]}(z, z')} \right), \quad (33)$$

where  $\alpha, \alpha'$  are triples of the Dirac, iso-spin, and color indices. This relation implies that the general rule to obtain the functional derivative of the 3qBS kernel is to replace each constituent quark propagator in turn by its derivative, and then sum up the resulting terms. Now all we need is  $\delta S_F^{[e]}/\delta a_\mu^b(x)$ , which is obtained by applying  $\delta/\delta a_\mu^b(x)$  to Eq.(31) as follows:

$$\begin{aligned} \left[ \frac{\delta S_F^{[e]}(x, y)}{\delta a_\mu^b(z)} \right]^{[0]} &= S_F^{[0]}(x, z) \left( \gamma^\mu \gamma_5 \frac{\tau^b}{2} \right) S_F^{[0]}(z, y) \\ &+ \int d^4z' S_F^{[0]}(x, z') \left[ \frac{\delta \Sigma^{[e]}(z')}{\delta a_\mu^b(z)} \right]^{[0]} S_F^{[0]}(z', y). \end{aligned} \quad (34)$$

$$\left[ \frac{\delta \Sigma^{[e]}(z')}{\delta a_\mu^b(z)} \right]^{[0]} = \sum_{\Gamma} 2ig_{\Gamma}^{(q\bar{q})} \text{Tr} \left( \left[ \frac{\delta S_F^{[e]}(z', z')}{\delta a_\mu^b(z)} \right]^{[0]} \Gamma \right) \Gamma. \quad (35)$$

---

<sup>9</sup>If derivative couplings are involved in the interaction Lagrangian, our argument is straightforwardly extended by replacing ordinary derivatives by chiral covariant derivatives. In this case,  $\delta/\delta a_\mu^b(x)$  also hits the argument  $\Gamma$  in  $K[\Gamma; S_F^{[e]}]$ . This is essential to extend the arguments given in the next section. In this case, it is not simply  $A^{b\mu}(x)$  but the conserved current operator, that is inserted in the r.h.s. in the 3rd line in Eq.(11) —  $A^{b\mu}(x)$  fails to be a conserved current in this case.

By inserting the first relation into the second, we obtain the following closed equation for  $\delta\Sigma/\delta a_\mu^b$ :

$$\begin{aligned} \left[ \frac{\delta\Sigma^{[e]}(z')}{\delta a_\mu^b(z)} \right]^{[0]} &= \sum_\Gamma 2ig_\Gamma^{(q\bar{q})} \text{Tr} \left( S^{[0]}(z', z) \left( \gamma^\mu \gamma_5 \frac{\tau^b}{2} \right) S^{[0]}(z, z') \Gamma \right) \Gamma \\ &+ \int d^4 z'' \sum_\Gamma 2ig_\Gamma^{(q\bar{q})} \text{Tr} \left( S^{[0]}(z', z'') \left[ \frac{\delta\Sigma^{[e]}(z'')}{\delta a_\mu^b(z)} \right]^{[0]} S^{[0]}(z'', z') \Gamma \right) \Gamma. \end{aligned} \quad (36)$$

For simplicity, we adopt<sup>10</sup> the effective  $q\bar{q}$  coupling constant in the iso-vector axialvector channel  $g_{\text{ax}} = 0$ . (For the precise meaning of  $g_{\text{ax}}$ , see Appendix B. We will discuss the general case, i.e.,  $g_{\text{ax}} \neq 0$ , in Appendix D.) We can parameterize our solution as follows:

$$\int d^4 z' e^{iq(z'-z)} \left[ \frac{\delta\Sigma^{[e]}(z')}{\delta a_\mu^b(z)} \right]^{[0]} = \tilde{H}(q^2) \left( q_\mu \gamma_5 \frac{\tau^b}{2} \right), \quad (37)$$

and from Eq.(36) we see that  $\tilde{H}(q^2)$  satisfies the following equation:

$$\tilde{H}(q^2) = -2ig_\pi \Pi_{5A}(q^2) - 2ig_\pi \Pi_{55}(q^2) \tilde{H}(q^2), \quad (38)$$

where  $\Pi_{5A}(q^2)$  and  $\Pi_{55}(q^2)$  are the bubble integrals which are defined in Appendix B.2. The solution is expressed as a geometric series:

$$\tilde{H}(q^2) = \frac{-2ig_\pi \Pi_{5A}(q^2)}{1 + 2ig_\pi \Pi_{55}(q^2)}. \quad (39)$$

$\delta S_F/\delta a_\mu^b(z)$  is depicted in Fig.2.(a). The two diagrams on the r.h.s. correspond to the two terms in Eq.(34), respectively, where the second one is proportional to  $q^\mu \tilde{H}(q^2)$  and has the pionic pole. Note that, whenever the quark propagator is obtained as a non-trivial solution to a self-consistent equation which leads to the chiral symmetry breaking,  $\delta S_F/\delta a_\mu^b$  always has a non-trivial ‘‘mesonic part’’  $\tilde{H}(q^2)$ .

Now we can consider particular 3qBS kernels and the associated diagrams relevant for the matrix element calculation. Our first example is the ladder truncated 3qBS kernel, which is depicted in Fig.3(a). Solid lines represent the constituent quark propagator. A slash indicates amputation of the constituent quark propagator. The interaction strengths in the various  $qq$  channels are obtained by applying the Fierz identity to the interaction Lagrangian. (See Appendix B.) In this case, Eq.(33) leads to the diagram in Fig.3(b), where the insertion on the quark line indicated by the ‘‘ $\otimes$ ’’ has been defined in Fig.2. (Diagrams with the same topologies are omitted.)

The second example is the  $qq$  interaction involving the exchange of  $q\bar{q}$  pairs in the t-channel (‘‘meson exchange interaction’’), which is depicted in Fig.4(a). In this case, Eq.(33) leads to the diagrams depicted in Fig.4(b). We see that, in addition to the

---

<sup>10</sup>The non-vanishing effective  $q\bar{q}$  coupling constant in the iso-vector axial-vector channel  $g_{\text{ax}}$  does not change the chiral symmetry properties[1].

coupling of the external field to the external quark propagators, couplings to internal quark propagators are also involved (the second diagram), which are often referred to as the “meson exchange current” contributions.

It is straightforward to extend these considerations to more complicated and realistic cases. A moral is that, once the 3qBS kernel is specified, a unique set of Feynman diagrams exists to determine the matrix element of the axial vector current.

## 4 Applications of the Criterion/Sufficient Condition

The aims of this section are to see whether the 3qBS kernels presented in the previous section satisfy the criterion Eq.(27)/sufficient condition Eq.(26), and to provide examples how to use the general considerations of Section 2 practically.

We first consider the chiral transformation properties of the elementary local vertices in the Lagrangian. The global chiral symmetry of the interaction Lagrangian  $\mathcal{L}_I = \sum_{\Gamma} g_{\Gamma} (\bar{\psi} \Gamma \psi)^2$  implies the following identity:

$$\sum_{\Gamma} g_{\Gamma} \left( e^{i\gamma_5 \tau^b \Theta^b} \Gamma e^{i\gamma_5 \tau^b \Theta^b} \right)_{ij} \left( e^{i\gamma_5 \tau^b \Theta^b} \Gamma e^{i\gamma_5 \tau^b \Theta^b} \right)_{kl} = \sum_{\Gamma} g_{\Gamma} \Gamma_{ij} \Gamma_{kl}. \quad (40)$$

Since  $\mathcal{L}_I$  is a contact interaction without any derivative terms, this identity remains valid even if  $\Theta^b$  acquires space-time dependence, i.e.,

$$\sum_{\Gamma} g_{\Gamma} \left( \Omega(x) \Gamma \Omega(x) \right)_{ij} \left( \Omega(x) \Gamma \Omega(x) \right)_{kl} = \sum_{\Gamma} g_{\Gamma} \Gamma_{ij} \Gamma_{kl}. \quad (41)$$

Actually, these  $q\bar{q}$  interactions consist of several “closed chiral multiplet sectors”, and the identity of the type Eq.(41) holds in each such sector separately. For example, the  $q\bar{q}$  interaction in the  $\pi$  and  $\sigma$  mesonic channel forms a closed chiral multiplet under the local axial gauge transformation, i.e., the following identity holds:

$$\begin{aligned} \delta_{ij} \delta_{kl} - \sum_{a=1}^3 (\gamma_5 \tau^a)_{ij} (\gamma_5 \tau^a)_{kl} &= \left( \Omega(x) \Omega(x) \right)_{ij} \left( \Omega(x) \Omega(x) \right)_{kl} \\ &\quad - \sum_{a=1}^3 \left( \Omega(x) \gamma_5 \tau^a \Omega(x) \right)_{ij} \left( \Omega(x) \gamma_5 \tau^a \Omega(x) \right)_{kl}. \end{aligned} \quad (42)$$

We need to establish similar relations in the  $qq$  sector. For this purpose, it is convenient to use the following Fierz identity (for details, see Appendix B.1.):

$$\mathcal{L}_I = \sum_{\Gamma} g_{\Gamma} (\bar{\psi} \Gamma \psi)^2 = \sum_{\Gamma'} g_{\Gamma'}^{(qq)} (\bar{\psi} \Gamma' \bar{\psi}^T) (\psi^T \Gamma' \psi). \quad (43)$$

In this representation, the identity Eq.(41) is expressed in the following way:

$$\sum_{\Gamma'} g_{\Gamma'}^{(qq)} \left( \Omega(x) \Gamma' \Omega(x)^T \right)_{ij} \left( \Omega(x)^T \Gamma' \Omega(x) \right)_{kl} = \sum_{\Gamma'} g_{\Gamma'}^{(qq)} \Gamma'_{ij} \Gamma'_{kl}. \quad (44)$$

These  $qq$  interactions also consist of several closed chiral multiplet sectors, and in each sector Eq.(44) is valid separately. In particular, the  $qq$  interaction in the scalar diquark channel ( $J^\pi = 0^+$ , isoscalar, color  $\bar{\mathbf{3}}$ ) forms a closed chiral singlet, i.e.,

$$\begin{aligned} & \sum_{A=2,5,7} \left( (\gamma_5 C^{-1}) \tau_2 \beta_A \right)_{ij} \left( (C \gamma_5) \tau_2 \beta_A \right)_{kl} \\ &= \sum_{A=2,5,7} \left( \Omega(x) \left( (\gamma_5 C^{-1}) \tau_2 \beta_A \right) \Omega(x)^T \right)_{ij} \left( \Omega(x)^T \left( (C \gamma_5) \tau_2 \beta_A \right) \Omega(x) \right)_{kl}, \end{aligned} \quad (45)$$

where  $\beta^A$  is the rescaled color Gell-Mann matrix  $\beta_A = \sqrt{\frac{3}{2}} \lambda_A$  with the normalization  $\text{tr}(\beta_A \beta_B) = 3 \delta_{AB}$ . Note that  $\beta_A$  for  $A = 2, 5, 7$  are anti-symmetric matrices corresponding to the color  $\bar{\mathbf{3}}_c$  diquark channels. The  $qq$  interaction in the axial vector diquark ( $J^\pi = 1^+$ , isovector, color  $\bar{\mathbf{3}}$ ) together with the vector diquark ( $J^\pi = 1^-$ , isoscalar, color  $\bar{\mathbf{3}}$ ) channel forms a closed chiral multiplet, i.e.,

$$\begin{aligned} & \sum_{A=2,5,7} \left[ \sum_{a=1}^3 \left( (\gamma_\mu C^{-1}) (\tau_a \tau_2) \beta_A \right)_{ij} \left( (C \gamma^\mu) (\tau_2 \tau_a) \beta_A \right)_{kl} \right. \\ & \quad \left. - \left( (\gamma_\mu \gamma_5 C^{-1}) \tau_2 \beta_A \right)_{ij} \left( (C \gamma_5 \gamma^\mu) \tau_2 \beta_A \right) \right] \\ &= \sum_{A=2,5,7} \left[ \sum_{a=1}^3 \left( \Omega(x) \left( (\gamma_\mu C^{-1}) (\tau_a \tau_2) \beta_A \right) \Omega(x)^T \right)_{ij} \left( \Omega(x)^T \left( (C \gamma^\mu) (\tau_2 \tau_a) \beta_A \right) \Omega(x) \right)_{kl} \right. \\ & \quad \left. - \left( \Omega(x) \left( (\gamma_\mu \gamma_5 C^{-1}) \tau_2 \beta_A \right) \Omega(x)^T \right)_{ij} \left( \Omega(x)^T \left( (C \gamma_5 \gamma^\mu) \tau_2 \beta_A \right) \Omega(x) \right)_{kl} \right] \end{aligned} \quad (46)$$

We give a list of these closed chiral multiplets in Appendix B.1.

Now we consider whether the sufficient condition Eq.(26) is satisfied in the case of the ladder truncation scheme, i.e., the 3qBS kernel of the type Fig.3. In this case, the 2PI interaction consists of only an elementary contact interaction. In practical numerical calculations, it is further truncated according to the quantum numbers of the diquark channels, i.e., the scalar diquark channel, the axialvector diquark channel, etc. We assume that the truncated vertex corresponds to a sum of closed chiral multiplets. Fig.5 shows the steps involved in the analysis of the gauge transformation properties of the kernel. In the first step, we apply the local gauge transformation  $\Omega(x)$  in order to get the transformed kernel (l.h.s. of Eq.(26)). Only the constituent quark propagators transform, and their transformation is given by Eq.(32). In the second step, we use Eq.(44), and the last step is due to the fact that amputated propagators are delta functions. As a result, the condition Eq.(26) is satisfied by the kernel in the ladder approximation, provided that the truncation of  $qq$  channels is done such as to have closed chiral multiplets. In particular, since the  $qq$  interaction in the scalar diquark channel forms a chiral singlet, the 3qBS framework in the ladder truncation scheme keeping only the  $qq$  interaction in the scalar diquark channel gives rise the PCAC relation correctly. However, if the  $qq$  interaction in the axialvector diquark channel is further included, it is in principle necessary to include also the  $qq$  interaction in the vector diquark channel. In practice, however, the vector

diquark channel can be expected to have small effects, at least on the nucleon mass, from the nonrelativistic analogy.

Next we consider whether the sufficient condition is satisfied in the case of the kernel involving  $q\bar{q}$  exchange, i.e., the 3qBS kernel of the type Fig.4. Fig.6 shows the argument for one of the infinite terms involved in the ladder sum. We assume that each vertex corresponds to a sum of closed chiral multiplets. In the first step we apply the gauge transformation using Eq.(32) to transform the constituent quark propagator. In the second step we use Eq.(41). Note that all the phase factors, which appear around the internal vertices, cancel themselves. The last step is due to the fact that the amputated propagator is just a delta function. This demonstrates the validity of Eq.(26) for the kernel involving  $q\bar{q}$  exchange. Several comments are in order. First, since the mass of the pion is so small, the  $q\bar{q}$  exchange in the pionic channel will contribute much more than the one in the sigma mesonic channel. However, in principle, it is necessary to include both channels in order to get the PCAC relation correctly. Second, if we include the  $q\bar{q}$  exchange interaction in the 3qBS kernel, it is necessary to take into account also the “meson exchange current contributions” in the calculation of the matrix element of the axial current, since the l.h.s. of our criterion Eq.(27) involves also the second diagram in Fig.4.(b), as discussed in Section 3.

These examples are straightforwardly extended to more general, complicated and realistic cases (for example, to the expansion scheme of [12]). We may consider these 3qBS kernel as a formal sum of 2PI and 3PI diagrams. It is thus not hard to convince ourselves that the chiral symmetry in the original interaction Lagrangian leads to the PCAC relation correctly in our formalism, provided the truncation of the kernel is done consistent with the condition (26).

## 5 The Goldberger-Treiman Relation and $g_{\pi NN}$

In this section, we give the explicit numerical results for  $g_{\pi NN}$  in the chiral limit together with the off-shell  $g_{\pi NN}$  off the chiral limit. We restrict our attention to the ladder truncation scheme keeping only the  $qq$  interaction in the scalar diquark channel. Although this truncation scheme of 3qBS kernel should lead to the correct Goldberger-Treiman relation, the UV regularization (the Euclidean cutoff in our case) unfortunately violates the chiral symmetry. One of the aims of this section is therefore to estimate the degree of violation of the PCAC/Goldberger-Treiman relation due to the UV-regularization. In this section, unless explicitly indicated for the more general case, *the external fields are understood to be absent*, i.e.,  $v = a = 0$ ,  $m = m_0$ . For consistency reason, we prefer to use the axial current operator  $A_\mu^b(x)$  as an interpolating field for the pion in this paper. For those readers who prefer to use  $\bar{\psi}(x)\gamma_5\frac{\tau^b}{2}\psi(x)$  as an interpolating field for the pion, the following relation would be convenient<sup>11</sup>:

$$A_\mu^b(x) = f_\pi\partial_\mu\pi_{\text{as}}^b(x) + \cdots, \quad (47)$$

---

<sup>11</sup>We will not use this relation explicitly in this paper.

where  $\pi_{\text{as}}^b(x)$  is the asymptotic field operator for the pion.

## 5.1 The Extraction of $g_{\pi NN}$ in the Chiral Limit

In this subsection,  $m_0 = 0$  is understood. The axial form factors  $g_A(q^2)$  and  $h_A(q^2)$  are defined through the following relation:

$$\bar{u}^{(\alpha)a}(\vec{P}) \frac{\tau^b}{2} \left( g_A(q^2) \gamma^\mu \gamma_5 + q^\mu h_A(q^2) \gamma_5 \right) u^{(\beta)c}(\vec{L}) = \left\langle N^{(\alpha)a}(\vec{P}) \left| A^{b\mu}(x=0) \right| N^{(\beta)c}(\vec{L}) \right\rangle, \quad (48)$$

where  $\bar{u}^{(\alpha)a}(\vec{P})$  and  $u^{(\beta)c}(\vec{L})$  are the final and initial nucleon bispinors with the isospins  $a, c$ , the helicities  $\alpha, \beta$  and the momenta  $P, L$  ( $P^2 = L^2 = m_N^2$ ), respectively.  $q = P - L$  is the momentum transfer.  $g_A$  and  $g_{\pi NN}$  are extracted as follows[15]:

$$g_A = g_A(q^2 = 0), \quad h_A(q^2) = \frac{-2f_\pi g_{\pi NN}}{q^2} + \dots \quad (49)$$

A multiplication of  $q_\mu$  on both sides of Eq.(48) leads to

$$0 = \bar{u}^{(\alpha)a}(\vec{P}) \frac{\tau^b}{2} \left( g_A(q^2) \not{q} \gamma_5 + q^2 h_A(q^2) \gamma_5 \right) u^{(\beta)c}(\vec{L}) \quad (50)$$

$$= \bar{u}^{(\alpha)a}(\vec{P}) \frac{\tau^b}{2} \left( 2m_N g_A(q^2) \gamma_5 + q^2 h_A(q^2) \gamma_5 \right) u^{(\beta)c}(\vec{L})$$

$$0 = 2m_N g_A(q^2) + q^2 h_A(q^2), \quad (51)$$

where we used the PCAC relation (28) for  $m_0 = 0$ . As is well-known[15], due to the pion pole of  $h_A(q^2)$  at  $q^2 = 0$ , this relation leads to the Goldberger–Treiman(GT) relation:

$$m_N g_A = f_\pi g_{\pi NN}. \quad (52)$$

We expand the both sides of Eq.(48) with respect to a small  $q^2$  to extract  $g_{\pi NN}$ . The l.h.s. is expanded as follows:

$$\begin{aligned} & \bar{u}^{(\alpha)a}(\vec{P}) \frac{\tau^b}{2} \left( g_A(q^2) \gamma^\mu \gamma_5 + q^\mu h_A(q^2) \gamma_5 \right) u^{(\beta)c}(\Lambda^{-1} \vec{P}) \quad (53) \\ &= \bar{u}^{(\alpha)a}(\vec{P}) \frac{\tau^b}{2} \left( g_A(q^2) \gamma^\mu \gamma_5 + q^\mu h_A(q^2) \gamma_5 \right) \hat{S}(\Lambda^{-1}) u^{(\beta)c}(\vec{P}) \\ &\simeq \left( \bar{u}^{(\alpha)a}(\vec{P}) \frac{\tau^b}{2} \gamma^\mu \gamma_5 u^{(\beta)b}(\vec{P}) \right) g_A + \left( \bar{u}^{(\alpha)a}(\vec{P}) \frac{\tau^b}{2} \gamma_5 S(-\lambda) u^{(\beta)c}(\vec{P}) \right) q^\mu \frac{-2f_\pi g_{\pi NN}}{q^2} + O(q), \end{aligned}$$

where  $(\Lambda^{-1})_\mu^\nu = (e^{-\lambda})_\mu^\nu$  is a boost matrix, i.e.,  $L_\mu = (\Lambda^{-1})_\mu^\nu P_\nu$ ,  $\hat{S}(\Lambda^{-1}) = e^{S(-\lambda)}$  is the boost matrix in the Dirac bispinor space with  $S(-\lambda) = (-\lambda)_{\mu\nu} \frac{-i}{4} \sigma^{\mu\nu}$ . Note that  $q_\mu = P_\mu - (\Lambda^{-1})_\mu^\nu P_\nu \simeq \lambda_\mu^\nu P_\nu + O(\lambda^2)$ . We thus have  $\lambda = O(q)$ . Hence we have

$$\left( \bar{u}^{(\alpha)a}(\vec{P}) \frac{\tau^b}{2} \gamma_5 S(-\lambda) u^{(\beta)c}(\vec{P}) \right) q^\mu = O(q^2), \quad (54)$$

which cancels the pion pole of  $h_A(q^2)$  at  $q^2 = 0$ .

The r.h.s. of Eq.(48) is evaluated by the 3qBS /Faddeev expression Eq.(18) and Eq.(93) of the nucleon matrix element:

$$\begin{aligned} \langle N^{(\alpha)a}(\vec{P}) | A^{b\mu}(x=0) | N^{(\beta)c}(\vec{L}) \rangle &= \tilde{\Psi}[N_\alpha^a(\vec{P})] \left[ \frac{i\delta K^{[e]}}{\delta a_\mu^b(x=0)} \right]^{[0]} \Psi[N_\beta^c(\vec{L})] \quad (55) \\ &= \bar{\psi}[N_\alpha^a(\vec{P})] \left[ \frac{i\delta K_F^{[e]}}{\delta a_\mu^b(x=0)} \right]^{[0]} \psi[N_\beta^c(\vec{L})], \end{aligned}$$

where  $\psi[N_\beta^c(\vec{L})]$ ,  $\bar{\psi}[N_\alpha^a(\vec{P})]$  and  $K_F^{[e]}$  are the Faddeev amplitudes and the Faddeev kernel, respectively. These quantities are defined in Appendix A, where also their relation to the 3qBS quantities is explained. The Faddeev equation is depicted in Fig.7. Since we adopted the ladder truncation scheme in this section, the  $qq$  interaction in Fig.7 is understood to be point-like and separable. Hence the double line in Fig.7 can be expressed as a geometric series of  $qq$  bubble integrals. In addition, since the  $qq$  interaction is truncated to the scalar diquark channel, the double line in Fig.7 now stands for the following t-matrix  $t_{\text{sd}}(q^2)$  in the scalar diquark channel:

$$t_{\text{sd}}(q^2) = 2 \times \frac{2ig_{\text{sd}}}{1 - 2ig_{\text{sd}}\Pi_{\text{sd}}(q^2)}, \quad (56)$$

with

$$\Pi_{\text{sd}}(q^2)\delta_{AB} = \int \frac{d^4k}{(2\pi)^4} \text{tr} \left( (C\gamma_5\tau_2\beta_A)iS_F(q+k)(\gamma_5C^{-1}\tau_2\beta_B)iS_F(-k)^T \right). \quad (57)$$

Since the second line in Eq.(55) involves the functional derivative of the Faddeev kernel, the contributions are classified as the following three types<sup>12</sup>(cf. Appendix A.3): (a) the quark current contribution[Fig.8.(a)], (b) the exchange current contribution[Fig.8.(b)], (c) the diquark current contribution[Fig.8.(c)]. Note that, due to the iso-scalar nature of the scalar diquark, the diquark current contribution to the matrix element of the iso-vector axial current vanishes identically.

The evaluation of the diagram Fig.8.(a) poses a problem, since there appears a delta function  $\delta^{(4)}(p-l-q/2)$  in addition to the delta function associated with the total momentum conservation. Therefore, depending on the momentum transfer  $q$ , the evaluation involves the values of the Faddeev amplitude at points which are outside the mesh used for the solution of the Faddeev equation<sup>13</sup>. To avoid this problem, we use the homogeneous Faddeev equation Eq.(87)[Fig.7] to iterate the Faddeev amplitude in the final state. The diagram Fig.8.(a) is thus exactly equivalent to Fig.8.(a'), which is free from the additional delta function. We therefore have to evaluate the diagrams of Fig.8.(a') and Fig.8.(b). Since the operator insertion on a constituent quark line has been given in Eqs. (34) –

<sup>12</sup>In the diagrams of Fig.8, we adopted the relative momenta of the spectator quark and the diquark, which are defined in Eq.(121), with the value  $\eta = 1/2$ .

<sup>13</sup>The numerical procedure to obtain the mass and the associated Faddeev amplitudes is explained in detail in [6, 7, 8].



(39) and Fig.2.(a), we are led to the four diagrams shown in Fig.8.(d). Here, we used the identity Eq.(127) to express the matrix element only in terms of the Faddeev amplitudes in the rest frame, and used also the identity

$$\gamma^\mu(\Lambda p)_\mu = S(\Lambda)\not{p}S(\Lambda^{-1}). \quad (58)$$

Note that, since we truncated the  $qq$  interaction to the scalar diquark channel, two of the boost matrices  $\hat{S}(\Lambda^{-1})$  out of the three ( $\hat{S}(\Lambda^{-1})^{\otimes 3}$ ) in Eq.(127) cancel. The remaining  $\hat{S}(\Lambda^{-1})$  is found in Fig.8.(d) at the point where the operator is inserted, which is a consequence of the manipulation Eq.(58). By using the following relations, which express the first order deviations due to the non-vanishing momentum transfer  $q$ :

$$\begin{aligned} \delta(S(\Lambda^{-1})) &= S(-\lambda) \\ \delta(\gamma^\mu(\Lambda p)_\mu) &= [S(\lambda), \not{p}] \\ \delta(S_F(P - \Lambda^{-1}(P/2 - l))) &= S_F(P/2 + l) [S(-\lambda), \not{P}/2 - \not{l}] S_F(P/2 + l), \quad \text{etc.}, \end{aligned} \quad (59)$$

we can consider the limit  $q \rightarrow 0$ . After using the homogeneous Faddeev equation Eq.(87), we are left with the eight diagrams depicted in Fig.9. Note that the equality Fig.8.(a) + Fig.8.(b) (= Fig.8.(d)) = Fig.9 holds only in the limit  $q \rightarrow 0$ , which is emphasized in Fig.9 by “ $q \rightarrow 0$ ”. By comparing both sides of Eq.(48) in the limit  $q \rightarrow 0$ , the explicit spin-parity projection<sup>14</sup> shows that the first two diagrams are proportional to  $\bar{u}^{(\alpha)a}(\vec{P}) \frac{\tau^b}{2} \gamma^\mu \gamma_5 u^{(\beta)b}(\vec{P})$ , which contribute to  $g_A$ , and the other diagrams are proportional to  $\bar{u}^{(\alpha)a}(\vec{P}) \frac{\tau^b}{2} \gamma_5 S(-\lambda) u^{(\beta)b}(\vec{P})$ , which contribute to  $g_{\pi NN}$ . Note that the 1st, the 3rd, the 4th and the 5th diagrams in Fig.9 come from the quark current contribution[Fig.8.(a)], and the others come from the exchange current contribution[Fig.8.(b)].

## 5.2 Numerical Results in the Chiral Limit

We first have to explain the choice of the parameters. There are four parameters: the cutoff  $\Lambda$  (Euclidean sharp cutoff), the current quark mass  $m_0$ , the effective coupling constant in the pionic channel  $g_\pi$  and the effective coupling constant in the  $qq$  scalar diquark channel  $g_{sd}$ . We fix the first three parameters ( $\Lambda, m_0, g_\pi$ ) by solving the gap equation Eq.(101) for the constituent quark mass  $M$ , and Eq.(107) for the pion mass  $m_\pi$  and decay constant  $f_\pi$ , imposing the following three conditions: (1)  $m_\pi = 140$  MeV, (2)  $f_\pi = 93$  MeV, (3)  $M = 400$  MeV. The resulting values are  $\Lambda = 739$  MeV,  $g_\pi = 10.42$  GeV<sup>-2</sup>,  $m_0 = 8.99$  MeV. Once these parameters are fixed, we consider the chiral limit by taking  $m_0 \rightarrow 0$  keeping  $\Lambda, g_\pi$  fixed. Eq.(101) provides the  $m_0$  dependences of  $M = M(m_0)$ . We treat  $g_{sd}$  as a free parameter (independent of  $m_0$ ) to generate different nucleon masses. Note that, in the case  $m_\pi = 140$  MeV,  $g_{sd}/g_\pi = 0.66$  gives the experimental value of the nucleon mass  $m_N = 940$  MeV. For convenience, we plot the nucleon mass  $m_N$  (for

<sup>14</sup>The spin-parity projection is performed by using the helicity formalism. (See for detail[8])

$g_{sd}/g_\pi = 0.66$ ), the quark-diquark threshold( $m_N + m_{sd}$ ) where  $m_{sd}$  is the scalar diquark mass, the pion mass  $m_\pi$ , the pion decay constant  $f_\pi$ , and the constituent quark mass  $M$  against the current quark mass  $m_0$  in Fig.10. We also plot the nucleon mass in the chiral limit against  $g_{sd}/g_\pi$  [solid line], together with the physical case( $m_\pi = 140$  MeV) [dashed line] in Fig.11.

Our results for  $g_{\pi NN}$  and  $g_A$  in the chiral limit are plotted against  $g_{sd}/g_\pi$  by the solid line in Fig.12 and Fig.13, respectively. We obtain  $g_{\pi NN} = 13.2$  and  $g_A = 1.32$  for  $g_{sd}/g_\pi = 0.66$  compared to the experimental values  $g_{\pi NN}^{(\text{exp})} = 13.5$  and  $g_A^{(\text{exp})} = 1.26$ . We will discuss the extension off the chiral limit in the next subsection.

To estimate the violation of the GT relation, it is convenient to define a quantity:

$$\Delta_G \equiv \frac{f_\pi g_{\pi NN}}{m_N g_A}. \quad (60)$$

In the chiral limit, the deviation of  $\Delta_G$  from 1 is solely due to the cutoff artifact. We plot  $\Delta_G$  against  $g_{sd}/g_\pi$  in Fig.14 in the chiral limit [solid line]. It is seen that the violation of the GT relation is up to 4 %. In particular, for the reasonable case  $g_{sd}/g_\pi = 0.66$ , the violation is only 2 % in the chiral limit.

### 5.3 PCAC Violation off the Chiral Limit

In the chiral limit,  $\Delta_G$  works as the measure of the violation of the PCAC relation due to the cutoff artifact. However, off the chiral limit,  $\Delta_G$  does not work as the measure any more, since it contains, in addition to the unphysical cutoff artifact which we are going to estimate here, the physical effect of the non-vanishing current quark mass. Therefore, in order to estimate the cutoff artifact, we need to construct a quantity which picks up only the cutoff artifact for any values of  $m_0 > 0$ . To this end, we introduce another form factor  $i_A(q^2)$  through the following relation:

$$\left\langle N_\alpha^a(\vec{P}) \left| i\bar{\psi}(x)\gamma_5\frac{\tau^b}{2}\psi(x) \right| N_\beta^c(\vec{L}) \right\rangle = e^{iqx}\bar{u}_\alpha^a(\vec{P}) \left( i\gamma_5\frac{\tau^b}{2} \right) u_\beta^c(\vec{L}) \times i_A(q^2). \quad (61)$$

Eq.(51) generalizes in the following way:

$$2m_N g_A(q^2) + q^2 h_A(q^2) = 2m_0 i_A(q^2). \quad (62)$$

In particular, in the limit  $q^2 \rightarrow 0$ , since now  $m_\pi \neq 0$ , we have

$$2m_N g_A = 2m_0 i_A(q^2 = 0). \quad (63)$$

Now we define a quantity  $\Delta_P$  as follows:

$$\Delta_P = \frac{m_0 i_A(q^2 = 0)}{m_N g_A}. \quad (64)$$

By construction, the deviation of  $\Delta_P$  from 1 is solely due to the cutoff artifact for any value of  $m_0$ . To evaluate  $i_A(q^2)$ , we first have to solve the following equation for the operator insertion on a constituent quark line similar to Eq.(34):

$$\begin{aligned} \left[ \frac{\delta S_F^{[e]}(x, y)}{\delta p^b(z)} \right]^{[0]} &= S_F^{[0]}(x, z) \left( i\gamma_5 \frac{\tau^b}{2} \right) S_F^{[0]}(z, y) \\ &+ \int d^4 z' S_F^{[0]}(x, z') \left[ \frac{\delta \Sigma^{[e]}(z')}{\delta p^b(z)} \right]^{[0]} S_F^{[0]}(z', y). \\ \left[ \frac{\delta \Sigma^{[e]}(z')}{\delta p^b(z)} \right]^{[0]} &= \sum_{\Gamma} 2i g_{\Gamma}^{(q\bar{q})} \text{Tr} \left( \left[ \frac{\delta S_F^{[e]}(z', z')}{\delta p^b(z)} \right]^{[0]} \Gamma \right) \Gamma. \end{aligned} \quad (65)$$

Since  $g_{\text{ax}} = 0$ , we can parameterize  $\delta \Sigma / \delta p^b$  as

$$\int d^4 z' e^{iq(z'-z)} \left[ \frac{\delta \Sigma^{[e]}(z')}{\delta p^b(z)} \right] = I(q^2) \left( i\gamma_5 \frac{\tau^b}{2} \right). \quad (66)$$

$I(q^2)$  then satisfies the following equation:

$$I(q^2) = -2ig_{\pi} \Pi_{55}(q^2) - 2ig_{\pi} \Pi_{55}(q^2) I(q^2), \quad (67)$$

with the solution

$$I(q^2) = \frac{-2ig_{\pi} \Pi_{55}(q^2)}{1 + 2ig_{\pi} \Pi_{55}(q^2)}. \quad (68)$$

Note that this quantity of course has the pion pole. The evaluation of  $i_A(q^2 = 0)$  amounts to the 2nd to the 8th diagrams given in Fig.9, where  $q_{\mu} \tilde{H}(q^2)$  is replaced by  $1 + I(q^2)$ . In Fig.15, we plot  $\Delta_P$  against the current quark mass  $m_0$  for  $g_{\text{sd}}/g_{\pi} = 0.66$  case [dashed line]. It is seen that the cutoff artifact is again within 4%.

## 5.4 The Off-shell $g_{\pi NN}$ off the Chiral Limit

We next evaluate  $g_{\pi NN}$  off the chiral limit ( $m_{\pi} = 140$  MeV). In this case, whereas the definition of  $g_A = g_A(q^2 = 0)$  does not change<sup>15</sup>, since the pion pole of  $h_A(q^2)$  is shifted,  $g_{\pi NN}$  is extracted according to:

$$h_A(q^2) = \frac{-2f_{\pi} g_{\pi NN}}{q^2 - m_{\pi}^2} + \dots. \quad (69)$$

In order to extract  $g_{\pi NN}$  from the nucleon matrix element of the axial current, it is necessary to evaluate the form factor  $h_A(q^2)$ . However, at this stage it is still difficult to evaluate  $h_A(q^2)$  for non-vanishing momentum transfer in the relativistic Faddeev approach<sup>16</sup>. We

<sup>15</sup>The evaluation of the iso-vector  $g_A$  off the chiral limit was already done in ref. [9] in the case of  $g_{\text{ax}} = 0$ .

<sup>16</sup>The numerical evaluation of the on-shell  $g_{\pi NN}$  off the chiral limit is currently under consideration.

confine ourselves to evaluate the off-shell  $g_{\pi NN}(q^2 = 0) \equiv \tilde{g}_{\pi NN}$  defined by the single-pole dominance approximation to  $h_A(q^2)$  as

$$\tilde{g}_{\pi NN} \equiv \frac{m_\pi^2}{2f_\pi} h_A(q^2 = 0). \quad (70)$$

Note that, whereas the nearest cut in the physical  $h_A(q^2)$  is the three pion cut ( $q^2 > 9m_\pi^2$ ), the Cutkosky rule(cf. p.315 in [15]) suggests that the nearest cut in our  $h_A(q^2)$  is the  $q\bar{q}$  cut ( $q^2 > 4M^2$ ). This is mainly due to the mean field approximation for the vacuum, and due to also the leak of the confinement in the NJL model. Since  $4M^2$  is larger than  $9m_\pi^2$ , the single-pole dominance approximation may work better in our case. We note that, although we could subtract the  $q\bar{q}$  cut contributions from  $\tilde{H}(q^2)$ , it is impossible to subtract it from the remaining part, because the calculation refers only to  $q = 0$ . The explicit evaluation shows that the subtraction of the  $q\bar{q}$  cut contributions from  $\tilde{H}(q^2)$  leads to only a small difference. We note that the quantity  $\tilde{g}_{\pi NN}$  is not only one of the possible off-shell extensions of the on-shell  $g_{\pi NN}$ , but also the value of the axial form factor  $h_A(q^2)$  at  $q^2 = 0$  up to the well-defined numerical factor given by Eq.(70). This enables us to derive an analytical expression of  $\Delta_G$  which follows from the PCAC relation by neglecting the small cutoff artifact. (See Appendix D.)

We plot  $\tilde{g}_{\pi NN}$  against  $g_{sd}/g_\pi$  in Fig.12 [dashed line], and  $g_A$  in Fig.13 [dashed line]. The value of  $\tilde{g}_{\pi NN}$  is 13.5 for  $g_{sd}/g_\pi = 0.66$ . This value is quite reasonable compared to the experimental value. We also plot  $\Delta_G$  off the chiral limit [dotted line] and  $\Delta_P$  [dashed line] against  $g_{sd}/g_\pi$  in Fig.14. The reader might suspect why the validity of the GT relation could be improved by going off the chiral limit. The reason is that the effect of non-vanishing  $m_0$  works into the opposite direction compared to the UV-cutoff artifact. To see this, we plot  $\Delta_G$  against the current quark mass  $m_0$  [solid line] in Fig.15 for the case  $g_{sd}/g_\pi = 0.66$ . We also plot  $\Delta_P$  against  $m_0$  [dashed line], which is used to indicate the size of the cutoff artifact contained in  $\Delta_G$ . It is seen that  $\Delta_G$  is a monotonically decreasing function of  $m_0$ . However, the experimental data  $\Delta_G = 1.06$  suggests that, as far as we believe that  $m_\pi = 140$  MeV is really close to the chiral limit,  $\Delta_G$  should be an increasing function in the vicinity of  $m_0 \simeq 0$ . We investigate this problem further in Appendix D by taking into account also the effects of non-vanishing coupling constant in the isovector axial vector  $q\bar{q}$  channel  $g_{ax}$ . (We leave this analysis for the appendix, because the non-vanishing  $g_{ax}$  makes things quite complicated.) The main conclusions there are summarized as follows: (1)  $g_A$  and  $\tilde{g}_{\pi NN}$  both decrease with increasing  $g_{ax}/g_\pi$ , and increase with increasing  $m_0$ . (2) The best fit of  $g_A$  and  $\tilde{g}_{\pi NN}$  could be obtained in the region  $0 \leq g_{ax}/g_\pi < 0.1$ , which, however, would depend on the quantity which we prefer to adjust. From this point of view,  $g_{ax} = 0$  is actually a rather good choice, because  $\tilde{g}_{\pi NN}$  is very reasonable and  $g_A = 1.33$  is still close to the experimental value  $g_A^{(\text{exp})} = 1.26$ . (3) For those values of  $g_{ax}$  which we examine,  $\Delta_G$  remains to be a decreasing function of  $m_0$ . (4) An analytic expression of  $\Delta_G$  (Eq.(137)) is derived by neglecting the small cut-off artifact and by assuming that the vacuum is approximated by the mean-field approximation. All the baryonic quantities disappear from this expression. In particular, this expression is valid even beyond the ladder truncation scheme for the 3qBS kernel. The discrepancy

between the analytic and the numeric  $\Delta_G$  is due to the cutoff artifact. It is found to be within 3 %. (5) As a consequence, to make  $\Delta_G$  to be an increasing function of  $m_0$  and to obtain  $\Delta_G = 1.06$ , we have to go beyond the validity of this analytic expression of  $\Delta_G$ . Therefore, all we can do is either to improve the gap equation for the vacuum beyond the mean field approximation or to estimate the on-shell  $g_{\pi NN}$ . We do not further investigate this problem in this paper.

## 6 Summary and Discussions

In this work we reviewed how to evaluate expectation values of quantum one-body operators in the framework of the 3qBS /Faddeev equation by introducing classical external fields as a technical tool. In the 3qBS approach, the expectation values are obtained by sandwiching, the functional derivative of the 3qBS kernel with respect to the corresponding external field between the 3qBS amplitudes. In the Faddeev approach, the expectation values are obtained by sandwiching, between the Faddeev amplitudes, the functional derivative of the Faddeev kernel with respect to the corresponding external field. We gave the criterion for 3qBS kernels to give rise to the PCAC relation correctly. For practical purpose, we also gave the sufficient condition for the validity of this criterion by introducing the local “axial” gauge transformation of the external fields. We applied the sufficient condition to several 3qBS kernels. The main results are as follows: (1) If the 3qBS kernel is truncated in the ladder truncation scheme keeping only the  $qq$  interaction in the scalar diquark channel, the PCAC relation is obtained correctly. (2) If the  $qq$  interaction in the axial-vector diquark channel is included, it is necessary to include also the  $qq$  interaction in the vector diquark channel to give rise to the PCAC relation correctly. (3) Even if the  $qq$  interaction due to the  $q\bar{q}$  exchange in both the pionic and the sigma mesonic channel is included, the correct PCAC relation is obtained. Concerning the point (2), we note that the vector diquark channel is often considered to be not important. This is because the non-relativistic quark model suggests that the contribution from this channel to the nucleon mass is suppressed in the non-relativistic limit. However, to respect the chiral  $SU(2)_L \times SU(2)_R$  symmetry, the  $qq$  interaction in the vector diquark channel should be included, even if it is expected to give a negligible contribution to the nucleon mass. We should note, however, that the relativistic Faddeev equation including all the  $qq$  interactions in the scalar, axial-vector and vector diquark channel amounts to a two-dimensional integral equation with  $14 \times 14$  matrix structure even after the spin-parity projection is carried out, which requires a tremendous effort to be solved.

Although these truncation schemes give rise to the PCAC relation correctly, the regularization scheme, which has been adopted in practical numerical calculations so far, does not respect the chiral symmetry, leading to the violation of the Goldberger-Treiman relation. To estimate this violation, we carried out the numerical evaluations of  $g_A$  and  $g_{\pi NN}$  in the chiral limit in the simplest case, i.e., the ladder truncation scheme keeping only the  $qq$  interaction in the scalar diquark channel. We found that the violations are up to 4 %. In particular, for the case  $g_s/g_\pi = 0.66$ , which reproduces the experimental

nucleon mass, the violation is only 2 %. The value of  $g_{\pi NN}$  in the chiral limit is 13.2 which is quite close to the experimental value 13.5, and  $g_A$  becomes 1.32 compared to the experimental value 1.26. We next estimated the PCAC violation due to the cutoff artifact off the chiral limit. We found that this violation is again within 4%.

In the relativistic Faddeev method, it is still difficult to calculate form factors for non-vanishing momentum transfer, which is needed to extract the on-shell  $g_{\pi NN}$  off the chiral limit. So we defined the off-shell  $\tilde{g}_{\pi NN}$  by means of the single-pole dominance approximation to  $h_A(q^2)$ . Although we obtained a very reasonable result  $\tilde{g}_{\pi NN} = 13.5$  for the case  $g_{sd}/g_\pi = 0.66$ , the effect of non-vanishing current quark mass  $m_0$  on the Goldberger-Treiman violation ( $\Delta_G(m_0)$ ) was found to be in the “wrong” direction: Whereas the experimental value of  $\Delta_G$  is 1.06, which suggests that  $\Delta_G$  should be an increasing function of  $m_0$  in the vicinity of  $m_0 = 0$ , our  $\Delta_G(m_0)$  is a decreasing function of  $m_0$ . We tried to resolve this problem (Appendix D) by taking into account the effect of non-vanishing effective coupling constant in the iso-vector axial-vector mesonic channel  $g_{ax}$ . The main results are as follows: (1)  $g_A$  and  $\tilde{g}_{\pi NN}$  both decrease with increasing  $g_{ax}/g_\pi$ , and increase with increasing  $m_0$ . (2) The best fit of  $g_A$  and  $\tilde{g}_{\pi NN}$  could be obtained in the region  $0 \leq g_{ax}/g_\pi < 0.1$ , which, however, would depend on the quantity which we prefer to adjust. From this point of view,  $g_{ax} = 0$  is actually a rather good choice, since  $\tilde{g}_{\pi NN} = 13.5$  is a very reasonable result and  $g_A = 1.33$  is still close to the experimental value  $g_A^{(\text{exp})} = 1.26$ . (3) For those values of  $g_{ax}$  which we examined,  $\Delta_G$  remains to be a decreasing function of  $m_0$ . (4) An analytic expression of  $\Delta_G$  was derived by neglecting the small cutoff artifact and by assuming that the vacuum is approximated by the mean-field method. All the baryonic quantities disappear from this expression. In particular, this expression is valid even beyond the ladder truncation scheme for the 3qBS kernel. The discrepancy between the analytic and the numeric  $\Delta_G$  is due to the cutoff artifact. It was found to be within 3 %. (5) As a consequence, to make  $\Delta_G$  to be an increasing function of  $m_0$ , we have to take into account the effects which are beyond the validity of the analytic expression of  $\Delta_G$ . Hence, all we can do are either to improve the vacuum beyond the meanfield approximation or to estimate the on-shell  $g_{\pi NN}$ .

We finally give a comment on the iso-scalar  $g_A^{(0)}$ . It is straightforward to extend our formalism to the chiral  $U(1)_L \times U(1)_R$  case. The  $U_A(1)$  anomaly in QCD is simulated in the NJL model as an explicit  $U_A(1)$  symmetry breaking. It is easy to see that, whereas the vector, axial-vector and tensor diquark channels form closed chiral  $U(1)_L \times U(1)_R$  singlets separately, only a combination of the scalar diquark and the pseudo scalar diquark forms a closed chiral  $U(1)_L \times U(1)_R$  doublet. To isolate the  $U_A(1)$  breaking contribution, one can parameterize the two coupling constants  $g_{sd}$  and  $g_{pd}$  as  $g_{sd} = \lambda + \delta\lambda$ ,  $g_{pd} = -\lambda + \delta\lambda$ . Now, in the ladder truncation scheme, it is only  $\delta\lambda$  that can provide the  $U_A(1)$  breaking effects to 3qBS amplitudes, because  $\lambda$  and the other  $qq$  interactions respect the  $U_A(1)$  symmetry. The  $qq$  interaction in the pseudo-scalar diquark channel is often considered to be irrelevant from the non-relativistic analogy. However, setting  $g_{pd} = 0$  corresponds to a particular choice of  $U_A(1)$  breaking, i.e.,  $\delta\lambda = g_{sd}/2$ , and this particular choice is not based on any of the underlying physics of  $U_A(1)$  breaking. Due to this reason, we suggest that the  $qq$  interaction in the pseudoscalar diquark channel should be included

for a reasonable estimate of the iso-scalar  $g_A^{(0)}$ , even if it is expected to give a negligible contribution to the nucleon mass.

### **Acknowledgment**

The author thanks K. Yazaki, W. Bentz, H. Asami, L. v. Smekal and H. Terazawa for their extensive discussions and encouraging suggestions. He also thanks the unknown referee of his previous paper[11] for giving him the main motivation for the current work.

# Appendices

## A The Faddeev Equation

The aim of this appendix is to summarize the notations of the relativistic Faddeev equation and to provide the derivations of some of the relevant relations involving the Faddeev method which are essential to the other parts of this paper in a self-contained manner. In this appendix, *summations over repeated indices are not implied*, and, unless explicitly indicated, *the external fields are understood to be absent*, i.e.,  $v \equiv a \equiv 0$ ,  $m \equiv m_0$ .

### A.1 The Relativistic Faddeev Equation<sup>17</sup> and the Green's Function

We begin with the 3qBS equation (see Eq.(4)) in the absence of the external fields:

$$G = G_0 + KG; \quad K = K_1 + K_2 + K_3, \quad (71)$$

where the index  $i$  of  $K_i$  refers to the spectator quark. The formal solution of  $G$  is expressed by using the resolvent of  $K$  as follows:

$$G = \frac{1}{1 - K} G_0. \quad (72)$$

Note that the resolvent exists in a mathematical sense. However, because  $K$  is an unbounded operator, it is difficult to interpret it as it stands. Therefore, we adopt the Faddeev prescription. We introduce the following Faddeev decomposition of the Green's function:

$$G = G_0 + G^1 + G^2 + G^3; \quad G^i \equiv K_i G. \quad (73)$$

We insert the following resolvent identity of  $K$  into Eq.(72):

$$\frac{1}{1 - K} = \frac{1}{1 - K_i} + \frac{1}{1 - K_i} \left( \sum_{j \neq i} K_j \right) \frac{1}{1 - K}. \quad (74)$$

We obtain

$$G = \frac{1}{1 - K_i} G_0 + \frac{1}{1 - K_i} \sum_{j \neq i} G^j, \quad (75)$$

which is further inserted into the defining relation of  $G^i$  in Eq.(73). We are left with the following closed equations for  $G^1, G^2, G^3$  (the Faddeev equations):

$$G^i = \frac{K_i}{1 - K_i} G_0 + \frac{K_i}{1 - K_i} \sum_{j \neq i} G^j. \quad (76)$$

---

<sup>17</sup>A rather good pedagogical introduction to the Faddeev equation is found in [17].



It is possible to simplify these coupled equations into a single closed equation for  $G^3$  by using the identical particle nature of the three quarks.  $G^1$  and  $G^2$  are obtained from  $G^3$  by means of simple permutation operations. For this purpose, it is convenient to introduce the cyclic permutation operator  $Z$ , which is defined as follows:

$$(Z\psi)(x_1, x_2, x_3) = \psi(x_2, x_3, x_1). \quad (77)$$

Note that  $Z$  is easily implemented by using delta functions. We give a list of obvious relations:

$$\begin{aligned} Z^3 &= 1, & Z(1 + Z + Z^2) &= (1 + Z + Z^2)Z = 1 + Z + Z^2, \\ K_i &= Z^i K_3 Z^{-i}, & ZG &= GZ = G, & ZG_0 &= G_0 Z = G_0, & G^i &= Z^i G^3. \end{aligned} \quad (78)$$

Now Eq.(76) reduces to the following closed integral equation for  $G^3$  (the reduced Faddeev equation):

$$G^3 = \frac{K_3}{1 - K_3} G_0 + \frac{K_3}{1 - K_3} (Z + Z^2) G^3, \quad (79)$$

which is depicted in Fig.7.(a). The two-quark resolvent  $\frac{K_3}{1 - K_3}$  is depicted in Fig.7.(b). (cf. Eq.(5)) It is not so hard to identify the so-called ‘‘Z-diagram’’ structure (the quark exchange diagram), which is provided by a combination of the permutation operator  $Z$  (or  $Z^2$ ) and two external quark propagators of the two-quark resolvent  $\frac{K_3}{1 - K_3}$ . We refer to the kernel of this integral equation as the Faddeev kernel  $K_F$ :

$$K_F \equiv \frac{K_3}{1 - K_3} (Z + Z^2). \quad (80)$$

Now the formal solution of  $G^3$  to Eq.(79) is given as:

$$G^3 = \frac{1}{1 - K_F} \frac{K_3}{1 - K_3} G_0. \quad (81)$$

By inserting this into the first relation in Eq.(73), we have another formal representation of the Green’s function  $G$ :

$$G = G_0 + (1 + Z + Z^2) \frac{1}{1 - K_F} \frac{K_3}{1 - K_3} G_0. \quad (82)$$

## A.2 The 3qBS Amplitude and the Faddeev Amplitude

To obtain the form of the Green’s function  $G$  near the nucleon pole, we first diagonalize the Faddeev kernel  $K_F$ , regarding the total four momentum  $p_\mu$  as a parameter<sup>18</sup>:

$$K_F \psi[n; p] = \lambda_n(p^2) \psi[n; p], \quad \bar{\psi}[n; p] K_F = \lambda_n(p^2) \bar{\psi}[n; p]. \quad (83)$$

---

<sup>18</sup>The numerical procedure to solve this homogeneous Faddeev equation is explained into detail in [6].

We adopt the following normalization condition:

$$\bar{\psi}[n'; p']\psi[n; p] = \mathcal{N}_n(p^2)(2\pi)^4\delta^{(4)}(p' - p)\delta_{n'n}; \quad \mathcal{N}_n(p^2) \equiv \frac{i}{2\sqrt{p^2}\lambda'_n(p^2)}, \quad (84)$$

where  $\lambda'_n(p^2) \equiv d\lambda_n(p^2)/d(p^2)$ . Now the Faddeev kernel is expressed as:

$$K_F = \sum_n \int \frac{d^4p}{(2\pi)^4\mathcal{N}_n(p^2)}\lambda_n(p^2)\psi[n; p]\bar{\psi}[n; p]. \quad (85)$$

Note that, in reasonable cases, the eigen-modes associated with the largest eigenvalue are four-fold degenerate—they correspond to the nucleon (the ground states in the sector of the baryon number 1). The degeneracy is due to the iso-spin 1/2 and spin up/down. We refer to these eigen-modes as the (off-shell) eigenvalues and Faddeev amplitudes for the nucleon and denote them as  $\lambda_N(p^2)$ ,  $\psi[N_\alpha^a(p)]$  and  $\bar{\psi}[N_\alpha^a(p)]$ . The nucleon mass  $m_N$  is obtained by solving the following equation:

$$\lambda_N(p^2 = m_N^2) = 1. \quad (86)$$

The associated eigenvectors satisfy the homogeneous Faddeev equations:

$$\psi[N_\beta^c(\vec{L})] = \frac{K_3}{1 - K_3}(Z + Z^2)\psi[N_\beta^c(\vec{L})], \quad \bar{\psi}[N_\alpha^a(\vec{P})] = \bar{\psi}[N_\alpha^a(\vec{P})]\frac{K_3}{1 - K_3}(Z + Z^2). \quad (87)$$

For simplicity, we suppress the time components of the total four momenta in the on-shell Faddeev amplitudes. We define the 3qBS amplitudes for nucleon states by:

$$\begin{aligned} \Psi[N_\alpha^a(\vec{P})] &\equiv (1 + Z + Z^2)\psi[N_\alpha^a(\vec{P})] \\ \bar{\Psi}[N_\alpha^a(\vec{P})] &\equiv \bar{\psi}[N_\alpha^a(\vec{P})]\frac{K_3}{1 - K_3}G_0 \\ &= \bar{\psi}[N_\alpha^a(\vec{P})]\frac{K_3}{1 - K_3}\frac{1 + Z + Z^2}{3}G_0. \end{aligned} \quad (88)$$

In order to see that these definitions of the 3qBS amplitudes are reasonable and that the normalization scheme adopted in Eq.(84) is consistent with the covariant normalization of the ket vectors in Eq.(8), we first consider the form of the Green's function near the nucleon pole as follows (cf. Eq.(82)):

$$\begin{aligned} G &\simeq (1 + Z + Z^2) \sum_{a,\alpha} \int \frac{d^4P}{(2\pi)^4\mathcal{N}_N(P^2)} \frac{\psi[N_\alpha^a(P)]\bar{\psi}[N_\alpha^a(P)]}{1 - \lambda_N(P^2)} \frac{K_3}{1 - K_3} G_0 \\ &\simeq \sum_{a,\alpha} \int \frac{d^4P}{(2\pi)^4\mathcal{N}_N(P^2)} \Psi[N_\alpha^a(\vec{P})] \frac{1}{1 - \lambda_N(P^2)} \bar{\Psi}[N_\alpha^a(\vec{P})] \\ &\simeq \sum_{a,\alpha} \int \frac{d^4P}{(2\pi)^4\mathcal{N}_N(m_N^2)} \times \frac{1}{-\lambda'_N(m_N^2)} \frac{\Psi[N_\alpha^a(\vec{P})]\bar{\Psi}[N_\alpha^a(\vec{P})]}{P^2 - m^2 + i\epsilon} \\ &\simeq \sum_{a,\alpha} \int \frac{d^4P}{(2\pi)^4} \frac{m_N}{E_N(\vec{P}^2)} \frac{i}{P_0 - E_N(\vec{P}^2) + i\epsilon} \Psi[N_\alpha^a(\vec{P})]\bar{\Psi}[N_\alpha^a(\vec{P})]. \end{aligned} \quad (89)$$

This result is consistent with the expression which is expected from the canonical operator analysis. Note that the above manipulations are exact at the nucleon pole.

Next, we show that these 3qBS amplitudes satisfy the homogeneous 3qBS equation Eq.(14):

$$\begin{aligned}
K\Psi[N_\alpha^a(\vec{P})] &= \sum_{i=1,2,3} Z^i K_3 Z^{-i} (1+Z+Z^2) \psi[N_\alpha^a(\vec{P})] & (90) \\
&= (1+Z+Z^2) K_3 (1+Z+Z^2) \psi[N_\alpha^a(\vec{P})] \\
&= (1+Z+Z^2) \frac{K_3}{1-K_3} (Z+Z^2) \psi[N_\alpha^a(\vec{P})] = \Psi[N_\alpha^a(\vec{P})] \\
\tilde{\Psi}[N_\alpha^a(\vec{P})]K &= \bar{\psi}[N_\alpha^a(\vec{P})] \frac{K_3}{1-K_3} \frac{1+Z+Z^2}{3} \sum_{i=1,2,3} Z^i K_3 Z^{-i} & (91) \\
&= \bar{\psi}[N_\alpha^a(\vec{P})] \frac{K_3}{1-K_3} (1+Z+Z^2) K_3 \frac{1+Z+Z^2}{3} \\
&= \bar{\psi}[N_\alpha^a(\vec{P})] \frac{K_3}{1-K_3} \frac{1+Z+Z^2}{3} = \tilde{\Psi}[N_\alpha^a(\vec{P})],
\end{aligned}$$

where, to obtain the 3rd lines of Eq.(90) and Eq.(91), we used the following identities:

$$\begin{aligned}
\bar{\psi} \frac{K_3}{1-K_3} (1+Z+Z^2) &= \bar{\psi} \frac{K_3}{1-K_3} + \bar{\psi} = \bar{\psi} \frac{1}{1-K_3} & (92) \\
(1+Z+Z^2)\psi &= \frac{K_3}{1-K_3} (Z+Z^2)\psi + (Z+Z^2)\psi = \frac{1}{1-K_3} (Z+Z^2)\psi,
\end{aligned}$$

which immediately follow from the homogeneous Faddeev equations Eq.(87).

### A.3 The Matrix Elements in terms of the Faddeev Amplitude

Here, we derive an explicit expression for the matrix element of the axial vector current operator in terms of the Faddeev amplitudes, which is, in the practical applications, more convenient than the expression in terms of the 3qBS amplitudes. To avoid cumbersome

notations, we introduce a shorthand notation:  $O_{i;\mu}^b \equiv \left[ \frac{i\delta K_i^{[e]}}{\delta a_\mu^b(x=0)} \right]^{[0]}$  ( $i=1,2,3$ ) and  $O_\mu^b = \sum_{i=1,2,3} O_{i;\mu}^b$ , where the index  $i$  refers to the spectator quark. Note that  $O_{i;\mu}^b = Z^i O_{3;\mu}^b Z^{-i}$ .

Now we have from Eq.(18):

$$\begin{aligned}
&\langle N_\alpha^a(\vec{P}) | A_\mu^b(x=0) | N_\beta^c(\vec{L}) \rangle \\
&= \tilde{\Psi}[N_\alpha^a(\vec{P})] O_\mu^b \Psi[N_\beta^c(\vec{L})] \\
&= \bar{\psi}[N_\alpha^a(\vec{P})] \frac{K_3}{1-K_3} (1+Z+Z^2) O_{3;\mu}^b (1+Z+Z^2) \psi[N_\beta^c(\vec{L})] \\
&= \bar{\psi}[N_\alpha^a(\vec{P})] \frac{1}{1-K_3} O_{3;\mu}^b \frac{1}{1-K_3} (Z+Z^2) \psi[N_\beta^c(\vec{L})]
\end{aligned}$$

$$= \bar{\psi}[N_\alpha^a(\vec{P})] \left[ \frac{i\delta K_F^{[e]}}{\delta a_\mu^a(x=0)} \right]^{[0]} \psi[N_\beta^c(\vec{L})], \quad (93)$$

where, to obtain the fourth line, we used Eq.(92). Since the permutation operator  $Z$  does not depend on the external fields,  $\delta/\delta a_\mu^b$  only hits one the constituent quark propagators in the two-quark resolvent  $\frac{K_3}{1-K_3}$  in  $K_F$ . (cf. Eq.(80))

We comment on the ladder truncation scheme. In this case, the  $qq$  interaction is point-like. By combining the diagrammatic expressions of  $K_3$  [Fig.3.(a)] and the two-quark resolvent  $\frac{K_3}{1-K_3}$  [Fig.7.(b)], we see that the diagrams involved in  $i\delta K_F/\delta a_\mu^a$  are classified into two types, i.e., (1)  $\delta/\delta a_\mu^a$  hits one of the internal quark propagators (i.e., in the  $qq$  bubble diagram) in the ladder sum, (2)  $\delta/\delta a_\mu^a$  hits one of the two external quark propagators. With the aid of this classification, a straight forward diagrammatic argument shows that the diagrammatic expression of Eq.(93) is given by the three diagrams Fig.8.(a), Fig.8.(b) and Fig.8.(c). The first type leads to Fig.8.(c), which we refer to as the ‘‘diquark current’’ contribution, and the second type leads to Fig.8.(a) and Fig.8.(b), which we refer to as the ‘‘quark current’’ contribution and the ‘‘exchange current’’ contribution, respectively.

## B Notations of the NJL Model

The aims of this section are to define some of the relevant quantities with explicit examples, and to summarize the notations of the NJL model. In this section, *the external fields are understood to be absent*, i.e.,  $v_\mu^a(x) \equiv a_\mu^a(x) \equiv 0$ ,  $m(x) \equiv m_0$ .

### B.1 The Elementary Effective Coupling Constants and the Closed Chiral Multiplets

Here we define the elementary effective coupling constants in  $q\bar{q}$  and  $qq$  channels. We start with the Lagrangian density Eq.(1). For definiteness, we virtually distinguish the two  $\psi$ 's and the two  $\bar{\psi}$ 's from each other, respectively, i.e.,

$$\mathcal{L}_I = \sum_{\Gamma} g_{\Gamma} (\bar{\psi}_1 \Gamma \psi_2) (\bar{\psi}_3 \Gamma \psi_4). \quad (94)$$

The elementary interaction, which is depicted in Fig.16.(a), can be classified into the following three types: (i)  $q\bar{q}$  direct channel [Fig.16.(b)], (ii)  $q\bar{q}$  exchange channel [Fig.16.(c)], (iii)  $qq$  diquark channel [Fig.16.(d)]. They are related by Fierz identities to each other. We define the effective coupling constants  $g^{(q\bar{q}\text{dir})}$ ,  $g^{(q\bar{q}\text{exch})}$  and  $g^{(qq)}$  through the following relations:

$$\mathcal{L}_I = \sum_{\alpha} \sum_{i=0}^3 \sum_{A=0}^8 g_{\alpha i A}^{(q\bar{q}\text{dir})} (\bar{\psi}_1 \Gamma_{\alpha} \tau_i \beta_A \psi_2) (\bar{\psi}_3 \Gamma^{\alpha} \tau_i \beta_A \psi_4) \quad (95)$$

$$\begin{aligned}
&= \sum_{\alpha} \sum_{i=0}^3 \sum_{A=0}^8 g_{\alpha i A}^{(q\bar{q}\text{exch})} \left( \bar{\psi}_1 \Gamma_{\alpha} \tau_i \beta_A \psi_4 \right) \left( \bar{\psi}_3 \Gamma^{\alpha} \tau_i \beta_A \psi_2 \right) \\
&= \sum_{\alpha} \sum_{i=0}^3 \sum_{A=0}^8 g_{\alpha i A}^{(qq)} \left( \bar{\psi}_1 (\Gamma_{\alpha} \gamma_5 C^{-1}) (\tau_i \tau_2) \beta_A \bar{\psi}_3^T \right) \left( \psi_2^T (C \gamma_5 \Gamma^{\alpha}) (\tau_2 \tau_i) \beta_A \psi_4 \right).
\end{aligned}$$

$\Gamma_{\alpha}, \Gamma^{\alpha}$  are Dirac gamma matrices, where  $\alpha$  runs over S(scalar), V(vector), T(tensor), A(axial-vector) and P(pseudo-scalar), i.e.,

$$\begin{aligned}
(\Gamma_{\alpha})_{\alpha=S,V,T,A,P} &= (1, \gamma_{\mu}, \sigma_{\mu\nu}, \gamma_{\mu} \gamma_5, \gamma_5) \\
(\Gamma^{\alpha})_{\alpha=S,V,T,A,P} &= (1, \gamma^{\mu}, \sigma^{\mu\nu}, \gamma_5 \gamma^{\mu}, \gamma_5).
\end{aligned} \tag{96}$$

$\tau_i$  ( $i = 0, 1, 2, 3$ ) are the iso-spin Pauli matrices with  $\tau_0 = 1$ . They are normalized according to  $\text{tr}(\tau_i \tau_j) = 2\delta_{ij}$ . Note that, both in  $q\bar{q}$  and  $qq$  representations,  $\tau_0$  corresponds to the iso-scalar, and  $\tau_i$  ( $i = 1, 2, 3$ ) correspond to the iso-vector channels.  $\beta_A$  are the rescaled Gell-Mann color matrices, i.e.,  $\beta_0 = 1$ ,  $\beta_A = \sqrt{\frac{3}{2}} \lambda_A$  ( $A = 1, 2, \dots, 8$ ) with the normalization  $\text{tr}(\beta_A \beta_B) = 3\delta_{AB}$ . In  $q\bar{q}$  representations,  $\beta_0$  corresponds to the  $1_c$  mesonic channels, and  $\beta_A$  for  $A = 1, 2, \dots, 8$  corresponds to  $8_c$  mesonic channels. Note that  $\beta_A$  for  $A = 2, 5, 7$  are anti-symmetric and the others are symmetric. Therefore, in  $qq$  representation,  $\beta_A$  for  $A = 2, 5, 7$  correspond to  $\bar{3}_c$  diquark channels, and  $\beta_A$  for  $A = 0, 1, 3, 4, 6, 8$  correspond to  $6_c$  diquark channels. We define the effective coupling constants  $g^{(q\bar{q})}$  as follows:

$$g_{\alpha i A}^{(q\bar{q})} = g_{\alpha i A}^{(q\bar{q}\text{dir})} + g_{\alpha i A}^{(q\bar{q}\text{exch})}. \tag{97}$$

We consider two examples (i) the original NJL type interaction Lagrangian:

$$\mathcal{L}_I = g \left( (\bar{\psi} \psi)^2 - \sum_{i=1}^3 (\bar{\psi} \gamma_5 \tau_i \psi)^2 \right), \tag{98}$$

where  $\tau_i$  is the isospin Pauli matrix, and (ii) the color current type interaction Lagrangian:

$$\mathcal{L}_I = -g \sum_{a=1}^8 \left( \bar{\psi} \gamma_{\mu} \frac{\lambda_a}{2} \psi \right)^2, \tag{99}$$

where  $\lambda_a$  is the color Gell-Mann matrix. We give a list of these effective coupling constants  $g^{(q\bar{q})} = g^{(q\bar{q}\text{dir})} + g^{(q\bar{q}\text{exch})}$  and  $g^{(qq)}$  for these two interaction Lagrangians:

Original NJL Type	S	V	T	A	P
$1_c(q\bar{q}), I=0$	$g + g/12$	$0 - g/6$	$0 + g/12$	$0 - g/6$	$0 + g/12$
$1_c(q\bar{q}), I=1$	$0 - g/12$	$0 + 0$	$0 - g/12$	$0 + 0$	$-g - g/12$
$8_c(q\bar{q}), I=0$	$0 + g/12$	$0 - g/6$	$0 + g/12$	$0 - g/6$	$0 + g/12$
$8_c(q\bar{q}), I=1$	$0 - g/12$	$0 + 0$	$0 - g/12$	$0 + 0$	$0 - g/12$
$\bar{3}_c(qq), I=0$	$g/6$	$-g/12$	$g/6$ (!)	$-g/12$ (!)	$g/6$
$\bar{3}_c(qq), I=1$	$0$ (!)	$g/12$ (!)	$0$	$g/12$	$0$ (!)
$6_c(qq), I=0$	$g/6$ (!)	$-g/12$ (!)	$g/6$	$-g/12$	$g/6$ (!)
$6_c(qq), I=1$	$0$	$g/12$	$0$ (!)	$g/12$ (!)	$0$
Color Current Type	S	V	T	A	P
$1_c(q\bar{q}), I=0$	$0 + 2g/9$	$0 - g/9$	$0 + 0$	$0 + g/9$	$0 - 2g/9$
$1_c(q\bar{q}), I=1$	$0 + 2g/9$	$0 - g/9$	$0 + 0$	$0 + g/9$	$0 - 2g/9$
$8_c(q\bar{q}), I=0$	$0 - g/36$	$-g + g/72$	$0 + 0$	$0 - g/72$	$0 + g/36$
$8_c(q\bar{q}), I=1$	$0 - g/36$	$0 + g/72$	$0 + 0$	$0 - g/72$	$0 + g/36$
$\bar{3}_c(qq), I=0$	$g/9$	$-g/18$	$0$ (!)	$g/18$ (!)	$-g/9$
$\bar{3}_c(qq), I=1$	$g/9$ (!)	$-g/18$ (!)	$0$	$g/18$	$-g/9$ (!)
$6_c(qq), I=0$	$-g/18$ (!)	$g/36$ (!)	$0$	$-g/36$	$g/18$ (!)
$6_c(qq), I=1$	$-g/18$	$g/36$	$0$ (!)	$-g/36$ (!)	$g/18$

For completeness, we also presented the effective couplings in the  $6_c$  diquark channels, which do not contribute directly to the color singlet baryon states. Note that the two  $\bar{\psi}$  fields and the two  $\psi$  fields are originally undistinguished Grassmann fields. Therefore, in  $qq$  representation, unless  $\Gamma_\alpha \gamma_5 C^{-1} \tau_i \tau_2 \beta_A$  is anti-symmetric, the contribution vanishes. Due to this reason, half of the effective coupling constants in the  $qq$  channels actually vanish, and these cases are indicated by “(!)” in the list.

Due to the chiral  $SU(2)_L \times SU(2)_R$  symmetry of the interaction Lagrangian, it can be already seen from the above list that some of the effective coupling constants are grouped together. In fact, the straight forward application of the chiral  $SU(2)_L \times SU(2)_R$

transformation leads us to the following list of “closed chiral multiplets”<sup>19</sup>:

$q\bar{q}(1_c)$	$(V, I = 0)$	$q\bar{q}(8_c)$	$(V, I = 0)$
	$(A, I = 0)$		$(A, I = 0)$
	$((S, I = 0) - (P, I = 1))$		$((S, I = 0) - (P, I = 1))$
	$((S, I = 1) - (P, I = 0))$		$((S, I = 1) - (P, I = 0))$
	$((T, I = 0) - (T, I = 1))$		$((T, I = 0) - (T, I = 1))$
	$((V, I = 1) - (A, I = 1))$		$((V, I = 1) - (A, I = 1))$
$qq(\bar{3}_c)$	$(S, I = 0)$	$qq(6_c)$	$(S, I = 1)$
	$(T, I = 1)$		$(T, I = 0)$
	$(P, I = 0)$		$(P, I = 1)$
	$((V, I = 0) - (A, I = 1))$		$((V, I = 1) - (A, I = 0))$

Note that the total number of independent coupling constants of the chiral  $SU(2)_L \times SU(2)_R$  symmetric NJL type interaction Lagrangian is at most eight. Therefore, if we fix all the eight coupling constants in the  $qq$  channels, all the effective coupling constants in the  $q\bar{q}$  channels are obtained as their linear combinations. In the ladder truncation scheme of the 3qBS kernel, we can fix the coupling constants in the  $\bar{3}_c$  ( $qq$ ) channels based on the calculations for color singlet baryons. However, the coupling constants in the  $6_c$  ( $qq$ ) channels remain free. One can then use these remaining coupling constants (related to the  $q\bar{q}$  coupling constants) to reproduce the mesonic properties.

To avoid cumbersome notations, we introduce the following abbreviations:

$$g_\pi = -g_{P,I=1,1_c}^{(q\bar{q})} = g_{S,I=0,1_c}^{(q\bar{q})}, \quad g_{\text{sd}} = g_{S,I=0,\bar{3}_c}^{(qq)}, \quad g_{\text{ax}} = g_{A,I=1,1_c}^{(q\bar{q})} = -g_{V,I=1,1_c}^{(q\bar{q})}. \quad (100)$$

## B.2 The Vacuum of the NJL model at the Mean Field Level

Here, we summarize some of the notations of the NJL model in the vacuum and the mesonic sectors.

### B.2.1 $g_{\text{ax}} = 0$ Case

The gap equation is given by:

$$M = m_0 + 2ig_\pi \int \frac{d^4p}{(2\pi)^4} \text{Tr} S_F(p), \quad S_F(p) \equiv \frac{1}{\not{p} - M}, \quad (101)$$

<sup>19</sup>For the precise meaning, see Section.4.

which provides the spontaneous breaking of the chiral symmetry in the NJL model at the level of mean field approximation.  $M$  is the constituent quark mass. The pion mass and the pion decay constant are obtained from the two-point axial current correlator as follows:

$$\int d^4x e^{iqx} \langle 0 | T A_\mu^a(x) A_\nu^b(0) | 0 \rangle = \frac{i q_\mu q_\nu f_\pi^2}{q^2 - m_\pi^2 + i\epsilon} + \text{continuum}. \quad (102)$$

Here we adopted the following definition of the pion decay constant:

$$\langle 0 | A_\mu^a(x) | \pi^b(\vec{p}) \rangle = i p_\mu f_\pi \delta_{ab} e^{-ipx}, \quad (103)$$

where the covariant normalization  $\langle \pi^a(\vec{p}) | \pi^b(\vec{k}) \rangle = 2\sqrt{m_\pi^2 + \vec{p}^2} (2\pi)^3 \delta^{(3)}(\vec{p} - \vec{k}) \delta_{ab}$  is adopted. The explicit form of the axial current correlator can be easily obtained in the ladder approximation. However, in order to emphasize the consistency between the vacuum, the mesonic sector and the baryonic sector in our formulation, we prefer to use the external field method. Since the canonical operator expression of  $\delta S_F / \delta a_\nu^b$  is

$$\left[ \frac{i \delta i S_F^{[e]}(x, z)_{\alpha\beta}}{\delta a_\nu^b(y)} \right]^{[0]} = \langle 0 | T \psi_\alpha(x) \bar{\psi}_\beta(z) A_\nu^b(y) | 0 \rangle, \quad (104)$$

the explicit form of the axial current correlator is obtained in the following way (cf. eqs. (36) - (39)):

$$\begin{aligned} & \int d^4x e^{iq(x-y)} \langle 0 | T A_\mu^a(x) A_\nu^b(y) | 0 \rangle \\ &= \int d^4x e^{iq(x-y)} \text{Tr} \left( (\gamma_\mu \gamma_5 \frac{\tau^a}{2}) \left[ \frac{\delta S_F^{[e]}(x, x)}{\delta a_\mu^b(y)} \right]^{[0]} \right) \\ &= -\frac{1}{4} \delta_{ab} \Pi_{\mu\nu}(q) - \frac{1}{4} q_\mu q_\nu \delta_{ab} \Pi_{5A}(q^2) \tilde{H}(q^2) \\ &= -\frac{1}{4} \Pi_{\mu\nu}(q) \delta_{ab} - \frac{1}{4} q_\mu q_\nu \delta_{ab} \frac{\Pi_{5A}(q^2) (-2i g_\pi) \Pi_{5A}(q^2)}{1 + 2i g_\pi \Pi_{55}(q^2)}, \end{aligned} \quad (105)$$

where

$$\begin{aligned} \Pi_{55}(q^2) \delta_{ab} &\equiv - \int \frac{d^4k}{(2\pi)^4} \text{Tr} \left( (\gamma_5 \tau^a) i S_F(k+q) (\gamma_5 \tau^b) i S_F(k) \right) \\ q_\mu \Pi_{5A}(q^2) \delta_{ab} &\equiv - \int \frac{d^4k}{(2\pi)^4} \text{Tr} \left( (\gamma_5 \tau^a) i S_F(k+q) (\gamma_\mu \gamma_5 \tau^b) i S_F(k) \right) \\ &= - \int \frac{d^4k}{(2\pi)^4} \text{Tr} \left( (\gamma_5 \gamma_\mu \tau^b) i S_F(k+q) (\gamma_5 \tau^a) i S_F(k) \right) \\ \Pi_{\mu\nu}(q) \delta_{ab} &\equiv - \int \frac{d^4k}{(2\pi)^4} \text{Tr} \left( (\gamma_\mu \gamma_5 \tau^a) i S_F(k+q) (\gamma_5 \gamma_\nu \tau^b) i S_F(k) \right) \\ &\equiv \delta_{ab} \left( \frac{q_\mu q_\nu}{q^2} \right) \Pi_1(q^2) + \delta_{ab} \left( g_{\mu\nu} - \frac{q_\mu q_\nu}{q^2} \right) \Pi_2(q^2). \end{aligned} \quad (106)$$



The explicit expressions for  $m_\pi$  and  $f_\pi$  are obtained from:

$$0 = 1 + 2ig_\pi \Pi_{55}(m_\pi^2), \quad f_\pi = \frac{-i\Pi_{5A}(m_\pi^2)}{2\sqrt{-i\Pi'_{55}(m_\pi^2)}}, \quad (107)$$

where  $\Pi'_{55}(q^2) \equiv \frac{d\Pi_{55}(q^2)}{d(q^2)}$ .

### B.2.2 $g_{\text{ax}} \neq 0$ Case

Even if we switch on  $g_{\text{ax}} \neq 0$ , the gap equation does not change. However, the axial current correlator changes in the following way:

$$\begin{aligned} & \int d^4x e^{iq(x-y)} \langle 0 | T A_\mu^a(x) A_\nu^b(y) | 0 \rangle \\ &= -\frac{1}{4} \delta_{ab} \Pi_{\mu\nu}(q) - \frac{1}{4} \delta_{ab} \left( g_{\mu\nu} - \frac{q_\nu q_\mu}{q^2} \right) \Pi_2(q^2) G_2(q^2) \\ & \quad - \frac{1}{4} \delta_{ab} \left( \frac{q_\mu q_\nu}{q^2} \right) \left( q^2 H(q^2) \Pi_{5A}(q^2) + G(q^2) \Pi_1(q^2) \right) \\ &= -\frac{1}{4} \delta_{ab} \Pi_{\mu\nu}(q) - \frac{1}{4} \delta_{ab} \left( g_{\mu\nu} - \frac{q_\nu q_\mu}{q^2} \right) \frac{2ig_{\text{ax}} \Pi_2(q^2)}{1 - 2ig_{\text{ax}} \Pi_2(q^2)} - \frac{1}{4} \delta_{ab} \left( \frac{q_\mu q_\nu}{q^2} \right) \frac{N(q^2)}{D(q^2)}, \end{aligned} \quad (108)$$

where  $H(q^2)$ ,  $G_1(q^2)$ ,  $G_2(q^2)$  and  $D(q^2)$  are defined in Appendix D, and  $N(q^2)$  is given as follows:

$$\begin{aligned} N(q^2) &= -\frac{1}{4} q^2 (-2ig_\pi) \left( \Pi_{5A}(q^2) \right)^2 \left( 1 + 2ig_{\text{ax}} \Pi_1(q^2) \right) \\ & \quad - \frac{1}{4} \left( 1 + 2ig_\pi \Pi_{55}(q^2) \right) \left( 2ig_{\text{ax}} \Pi_1(q^2) \right) \end{aligned} \quad (109)$$

The explicit expressions for  $m_\pi$  and  $f_\pi$  are obtained from:

$$0 = D(m_\pi^2), \quad f_\pi = \sqrt{\frac{N(m_\pi^2)}{im_\pi^2 D'(m_\pi^2)}}, \quad (110)$$

where  $D'(q^2) \equiv \frac{dD(q^2)}{d(q^2)}$ .

## B.3 The Regularized Bubble Integrals

The regularized expressions for the bubble integrals with the sharp Euclidean cut-off are as follows:

$$\Pi_{55}(q^2) = 24i \int^\Lambda \frac{d^4 k_E}{(2\pi)^4} \int_0^1 dx \frac{k_E^2 + M^2 + q^2 x(1-x)}{(k_E^2 + M^2 - q^2 x(1-x))^2} \quad (111)$$

$$\Pi_{5A}(q^2) = 24iM \int^\Lambda \frac{d^4 k_E}{(2\pi)^4} \int_0^1 dx \frac{1}{(k_E^2 + M^2 - q^2 x(1-x))^2} \quad (112)$$

$$\Pi_{\mu\nu}(q) = 48i \int^\Lambda \frac{d^4 k_E}{(2\pi)^4} \int_0^1 dx \frac{M^2 g_{\mu\nu} - x(1-x)(q^2 g_{\mu\nu} - q_\mu q_\nu)}{(k_E^2 + M^2 - q^2 x(1-x))^2}. \quad (113)$$

These expressions satisfy the following identities:

$$\Pi_{5A}(0) = 2M\Pi'_{55}(0) \quad (114)$$

$$q^\nu \Pi_{\mu\nu}(q) = 2Mq_\mu \Pi_{5A}(q^2) \quad (115)$$

$$\Pi_1(0) = \Pi_2(0). \quad (116)$$

We comment here on the expression for  $\Pi_{\mu\nu}(q)$ . In order to obtain the above expression for  $\Pi_{\mu\nu}(q)$ , we have to use the following prescription:

$$\int \frac{d^4 k}{(2\pi)^4} \int_0^1 dx \frac{2k_\mu k_\nu + g_{\mu\nu}(M^2 - k^2 - q^2 x(1-x))}{(M^2 - k^2 - q^2 x(1-x))^2} \Rightarrow 0 \quad (117)$$

This is due to the following reason. The straight forward application of the sharp Euclidean cut-off leads, rather than to Eq.(115), to the following identity:

$$q^\nu \Pi_{\mu\nu}(q) = -q^\nu \Pi_{\mu\nu}^{(V)}(q) + 2Mq_\mu \Pi_{5A}(q^2), \quad (118)$$

where  $\Pi_{\mu\nu}^{(V)}(q)$  is

$$\Pi_{\mu\nu}^{(V)}(q)\delta_{ab} \equiv - \int \frac{d^4 k}{(2\pi)^4} \text{Tr} \left( (\gamma_\mu \tau^a) iS_F(k+q) (\gamma_\nu \tau^b) iS_F(k) \right). \quad (119)$$

Since the non-vanishing longitudinal part of  $\Pi_{\mu\nu}^{(V)}(q)$  is an unphysical cutoff artifact, which spoils the significance of the outputs, the prescription Eq.(117) is often used to suppress it. (See p.178 in ref. [18].) Note that, if the dimensional regularization is applied, the expression Eq.(117) vanishes identically. Now the analogous subtraction should be performed on the l.h.s. in Eq.(118), otherwise the Gell-Mann-Oakes-Renner relation would be terribly violated in the case  $g_{ax} \neq 0$ . Note that, once we use this prescription, the Gell-Mann-Oakes-Renner violations are less than 1% for  $m_\pi \leq 140$  MeV.

## C Matrix Element in terms of the 3qBS/Faddeev Amplitudes in the Rest Frame

In principle, we can use any Lorentz frames to calculate the Lorentz invariant form factors of a matrix element. But in practice, it is convenient to make use of the rest frame, because this frame is often used in the calculation of the mass and the 3qBS amplitudes. The aim of this appendix is to give expressions for the matrix element in terms of the 3qBS /Faddeev amplitudes in the rest frame by using the Lorentz covariance. Unless

the opposite is explicitly indicated, *the external fields are understood to be absent*, i.e.,  $v = a = 0$ ,  $m = m_0$ . To make the Lorentz transformation of the spinor simpler, we select the final momentum  $P = (m_N, \vec{0})$  and the initial momentum  $L^\mu = (\Lambda^{-1})^\mu{}_\nu P^\nu$ , where  $\Lambda^\mu{}_\nu = (e^\omega)^\mu{}_\nu$  represents the boost. We introduce the Fourier transforms of the 3qBS amplitudes and of  $O_\mu^b \equiv \left[ \frac{i\delta K^{[e]}}{\delta a_\mu^b(0)} \right]^{[0]}$ :

$$\begin{aligned}
& \Psi[N_\beta^c(L)](l, l') (2\pi)^4 \delta^{(4)}(L - \bar{L}) \tag{120} \\
&= \int d^4 y_1 d^4 y_2 d^4 y_3 e^{-i \sum l_i y_i} \Psi[N_\beta^c(L)](y_1, y_2, y_3) \\
& \tilde{\Psi}[N_\alpha^a(P)](p, p') (2\pi)^4 \delta^{(4)}(\bar{P} - P) \\
&= \int d^4 x_1 d^4 x_2 d^4 x_3 \tilde{\Psi}[N_\alpha^a(P)](x_1, x_2, x_3) e^{i \sum p_i x_i} \\
& O_\mu^b(\bar{P}, p, p'; \bar{L}, l, l') \\
&= \int d^4 x_1 d^4 x_2 d^4 x_3 \int d^4 y_1 d^4 y_2 d^4 y_3 e^{-i \sum p_i x_i} O_\mu^b(x_1, x_2, x_3; y_1, y_2, y_3) e^{i \sum l_i y_i} \\
& O_\mu^b(P, L; p, p', l, l') \\
&= \int \frac{d^4 \bar{P}}{(2\pi)^4} \int \frac{d^4 \bar{L}}{(2\pi)^4} (2\pi)^4 \delta^{(4)}(\bar{P} - P) O_\mu^b(\bar{P}, p, p'; \bar{L}, l, l') (2\pi)^4 \delta^{(4)}(L - \bar{L})
\end{aligned}$$

$\bar{P}, \bar{L}$  are the total momenta and  $p, p', l, l'$  are the relative momenta, which are defined though the following relations:

$$\begin{aligned}
\bar{P} &= \sum p_i & p &= \eta p_3 - (1 - \eta)(p_1 + p_2), & p' &= \eta' p_1 - (1 - \eta') p_2 \tag{121} \\
\bar{L} &= \sum l_i & l &= \eta l_3 - (1 - \eta)(l_1 + l_2), & l' &= \eta' l_1 - (1 - \eta') l_2,
\end{aligned}$$

where  $0 < \eta, \eta' < 1$  are arbitrary real numbers. We note that, unlike the nonrelativistic approaches, the choice of  $\eta$  and  $\eta'$  is almost completely arbitrary in the relativistic quantum field theory<sup>20</sup>. The delta functions in the first two relations in Eq.(120) are due to the translational invariance. It is important to note that the Jacobians associated with the variable change, i.e.,  $(p_1, p_2, p_3) \mapsto (\bar{P}, p, p')$  and  $(l_1, l_2, l_3) \mapsto (\bar{L}, l, l')$  are 1, i.e.,

$$\frac{d^4 p_1}{(2\pi)^4} \frac{d^4 p_2}{(2\pi)^4} \frac{d^4 p_3}{(2\pi)^4} = \frac{d^4 \bar{P}}{(2\pi)^4} \frac{d^4 p}{(2\pi)^4} \frac{d^4 p'}{(2\pi)^4}, \quad \frac{d^4 l_1}{(2\pi)^4} \frac{d^4 l_2}{(2\pi)^4} \frac{d^4 l_3}{(2\pi)^4} = \frac{d^4 \bar{L}}{(2\pi)^4} \frac{d^4 l}{(2\pi)^4} \frac{d^4 l'}{(2\pi)^4}. \tag{122}$$

Now the matrix element reduces to the following expression:

$$\begin{aligned}
& \left\langle N_\alpha^a(P) \left| A_\mu^b(0) \right| N_\beta^c(L) \right\rangle \left( \equiv \tilde{\Psi}[N_\alpha^a(P)] O_\mu^b \Psi[N_\beta^c(L)] \right) \tag{123} \\
&= \int \frac{d^4 p}{(2\pi)^4} \frac{d^4 p'}{(2\pi)^4} \int \frac{d^4 l}{(2\pi)^4} \frac{d^4 l'}{(2\pi)^4} \\
& \quad \times \tilde{\Psi}[N_\alpha^a(P)](p, p') O_\mu^b(P, L; p, p', l, l') \Psi[N_\beta^c(L)](l, l')
\end{aligned}$$

<sup>20</sup>For complete expositions, see [15].

$$\begin{aligned}
&= \int \frac{d^4 p}{(2\pi)^4} \frac{d^4 p'}{(2\pi)^4} \int \frac{d^4 l}{(2\pi)^4} \frac{d^4 l'}{(2\pi)^4} \\
&\quad \times \tilde{\Psi}[N_\alpha^a(P)](p, p') O_\mu^b(P, L; p, p', l, l') \hat{S}(\Lambda^{-1})^{\otimes 3} \Psi[N_\beta^c(P)](\Lambda l, \Lambda l') \\
&= \int \frac{d^4 p}{(2\pi)^4} \frac{d^4 p'}{(2\pi)^4} \int \frac{d^4 l}{(2\pi)^4} \frac{d^4 l'}{(2\pi)^4} \\
&\quad \times \tilde{\Psi}[N_\alpha^a(P)](p, p') O_\mu^b(P, L; p, p', \Lambda^{-1}l, \Lambda^{-1}l') \hat{S}(\Lambda^{-1})^{\otimes 3} \Psi[N_\beta^c(P)](l, l'),
\end{aligned}$$

where the second equality follows from the following Lorentz transformation property of the 3qBS amplitude of the rest frame:

$$\begin{aligned}
&\langle 0 | T\psi(x_1)\psi(x_2)\psi(x_3) | N_\beta^c(\Lambda^{-1}P) \rangle \\
&= \langle 0 | [T\psi(x_1)\psi(x_2)\psi(x_3)] \check{S}(\Lambda^{-1}) | N_\beta^c(P) \rangle \\
&= \hat{S}(\Lambda^{-1})^{\otimes 3} \langle 0 | T\psi(\Lambda x_1)\psi(\Lambda x_2)\psi(\Lambda x_3) | N_\beta^c(P) \rangle,
\end{aligned} \tag{124}$$

where  $(\Lambda^{-1})_\mu^\nu = (e^{-\lambda})_\mu^\nu$  is the pure boost matrix,  $\check{S}(\Lambda^{-1})$  is the boost operator in the Fock space,  $\hat{S}(\Lambda^{-1}) = e^{S(-\lambda)}$ ,  $(S(-\lambda) = \frac{-i}{4}\sigma_{\mu\nu}(-\lambda)^{\mu\nu})$  the boost matrix in the Dirac bispinor space, and  $\hat{S}(\Lambda)^{\otimes 3} = \hat{S}(\Lambda) \otimes \hat{S}(\Lambda) \otimes \hat{S}(\Lambda)$ . In the last line of Eq.(123), with the aid of the Lorentz invariance of the Jacobian, we rotate the integration variables  $l, l'$  by the boost  $\Lambda$ , i.e.,  $l \mapsto \Lambda^{-1}l, l' \mapsto \Lambda^{-1}l'$ . The problem thus reduces to the ‘‘matrix element’’ calculation of  $O_\mu^b(P, \Lambda^{-1}P; p, p', \Lambda^{-1}l, \Lambda^{-1}l')\hat{S}(\Lambda^{-1})^{\otimes 3}$  between two 3qBS amplitudes in the rest frame.

By using the homogeneous Faddeev equation Eq.(87), the Faddeev amplitude is expressed by the 3qBS amplitude as follows:

$$\psi[N_\alpha^a(\vec{P})] = K_3 \Psi[N_\alpha^a(\vec{P})]. \tag{125}$$

Hence, the Lorentz transformation property of the 3qBS amplitude implies the following Lorentz transformation property of the Faddeev amplitude:

$$\psi[N_\alpha^a(\Lambda^{-1}P)](x_1, x_2, x_3) = \hat{S}(\Lambda^{-1})^{\otimes 3} \psi[N_\alpha^a(P)](\Lambda x_1, \Lambda x_2, \Lambda x_3). \tag{126}$$

By repeating almost the same arguments, we are left with the following expression of the matrix element in terms of the Faddeev amplitudes in the rest frame:

$$\begin{aligned}
&\langle N_\alpha^a(P) | A_\mu^b(x=0) | N_\beta^c(L) \rangle \\
&= \int \frac{d^4 p}{(2\pi)^4} \frac{d^4 p'}{(2\pi)^4} \int \frac{d^4 l}{(2\pi)^4} \frac{d^4 l'}{(2\pi)^4} \\
&\quad \times \bar{\psi}[N_\alpha^a(P)](p, p') O_{F;\mu}^b(P, L; p, p', \Lambda^{-1}, \Lambda^{-1}l') \hat{S}(\Lambda^{-1})^{\otimes 3} \psi[N_\beta^c(P)](l, l'),
\end{aligned} \tag{127}$$

where the Fourier transforms  $\psi[N_\beta^c(P)](p, p')$ ,  $\bar{\psi}[N_\alpha^a(P)](p, p')$  are defined from  $\psi[N_\beta^c(P)](x_1, x_2, x_3)$ ,  $\bar{\psi}[N_\alpha^a(P)](x_1, x_2, x_3)$  similar to Eq.(120), and  $O_{F;\mu}^b(P, L; p, p', l, l')$  is defined from:

$$O_{F;\mu}^b(x_1, x_2, x_3; y_1, y_2, y_3) \equiv \left[ \frac{i\delta K_F^{[e]}(x_1, x_2, x_3; y_1, y_2, y_3)}{\delta a_\mu^b(x=0)} \right]^{[0]}. \tag{128}$$

## D Non-vanishing $g_{\text{ax}}$

### D.1 General Formalism

The aim of this appendix is to consider how to extract  $g_A$  and  $\tilde{g}_{\pi NN}$  in the case  $g_{\text{ax}} \neq 0$  providing an analytical expression of the GT violation  $\Delta_G(m_0)$ . Instead of repeating the argument similar to the one given in Section 5.1, which would become quite lengthy, we derive the expression of the form factors in a different manner, which would be easier for the readers to understand.

We first have to consider functional derivatives of the constituent quark propagator, i.e.,  $\delta S_F/\delta a_\mu^b$  and  $\delta S_F/\delta p^b$ , which are obtained as the solutions to Eq.(34) and Eq.(65). We parameterize  $\delta\Sigma/\delta a_\mu^b$  and  $\delta\Sigma/\delta p^b$  as follows:

$$\begin{aligned}
& \int d^4 z' e^{iq(z'-z)} \left[ \frac{\delta\Sigma^{[e]}(z')}{\delta a_\mu^b(z)} \right]^{[0]} & (129) \\
& = H(q^2) \left( q^\mu \gamma_5 \frac{\tau^b}{2} \right) + G_1(q^2) \left( \frac{q^\mu \not{q}}{q^2} \gamma_5 \frac{\tau^b}{2} \right) + G_2(q^2) \left( \gamma^\mu - \frac{q^\mu \not{q}}{q^2} \right) \gamma_5 \frac{\tau^b}{2} \\
& \int d^4 z' e^{iq(z'-z)} \left[ \frac{\delta\Sigma^{[e]}(z')}{\delta p^b(z)} \right]^{[0]} \\
& = I_1(q^2) \left( i\gamma_5 \frac{\tau^b}{2} \right) + I_2(q^2) \left( i\not{q} \gamma_5 \frac{\tau^b}{2} \right).
\end{aligned}$$

$H(q^2)$ ,  $G_1(q^2)$ ,  $G_2(q^2)$ ,  $I_1(q^2)$  and  $I_2(q^2)$  satisfy the following coupled equations:

$$\begin{aligned}
G_2(q^2) &= 2ig_{\text{ax}}\Pi_2(q^2) + 2ig_{\text{ax}}\Pi_2(q^2)G_2(q^2) & (130) \\
\begin{pmatrix} H(q^2) \\ G_1(q^2) \end{pmatrix} &= \begin{pmatrix} -2ig_\pi\Pi_{5A}(q^2) \\ 2ig_{\text{ax}}\Pi_1(q^2) \end{pmatrix} + \begin{pmatrix} -2ig_\pi\Pi_{55}(q^2) & -2ig_\pi\Pi_{5A}(q^2) \\ q^2 2ig_{\text{ax}}\Pi_{5A}(q^2) & 2ig_{\text{ax}}\Pi_1(q^2) \end{pmatrix} \begin{pmatrix} H(q^2) \\ G_1(q^2) \end{pmatrix} \\
\begin{pmatrix} I_1(q^2) \\ I_2(q^2) \end{pmatrix} &= \begin{pmatrix} -2ig_\pi\Pi_{55}(q^2) \\ 2ig_{\text{ax}}\Pi_{5A}(q^2) \end{pmatrix} + \begin{pmatrix} -2ig_\pi\Pi_{55}(q^2) & q^2(-2ig_\pi)\Pi_{5A}(q^2) \\ 2ig_{\text{ax}}\Pi_{5A}(q^2) & 2ig_{\text{ax}}\Pi_1(q^2) \end{pmatrix} \begin{pmatrix} I_1(q^2) \\ I_2(q^2) \end{pmatrix},
\end{aligned}$$

with the following solutions:

$$\begin{aligned}
H(q^2) &= \frac{-2ig_\pi\Pi_{5A}(q^2)}{D(q^2)} & (131) \\
G_1(q^2) &= \frac{q^2 \left( 2ig_{\text{ax}}\Pi_{5A}(q^2) \right) \left( -2ig_\pi\Pi_{5A}(q^2) \right) + \left( 1 + 2ig_\pi\Pi_{55}(q^2) \right) \left( 2ig_{\text{ax}}\Pi_1(q^2) \right)}{D(q^2)} \\
G_2(q^2) &= \frac{2ig_{\text{ax}}\Pi_2(q^2)}{1 - 2ig_{\text{ax}}\Pi_2(q^2)} \\
I_1(q^2) &= \frac{\left( 1 - 2ig_{\text{ax}}\Pi_1(q^2) \right) \left( -2ig_\pi\Pi_{55}(q^2) \right) + q^2 \left( -2ig_\pi\Pi_{5A}(q^2) \right) \left( 2ig_{\text{ax}}\Pi_{5A}(q^2) \right)}{D(q^2)} \\
I_2(q^2) &= \frac{2ig_{\text{ax}}\Pi_{5A}(q^2)}{D(q^2)}
\end{aligned}$$

$$D(q^2) = \left(1 + 2ig_\pi\Pi_{55}(q^2)\right) \left(1 - 2ig_{\text{ax}}\Pi_1(q^2)\right) - q^2 \left(-2ig_\pi\Pi_{5A}(q^2)\right) \left(2ig_{\text{ax}}\Pi_{5A}(q^2)\right).$$

We define ‘‘baryonic parts’’  $B_P(q^2)$  and  $B_A(q^2)$  of the form factors through Fig.17. Now the matrix elements are expressed as follows:

$$\langle N(P) | A_\mu^b(x=0) | N(L) \rangle = \bar{u}(P) \frac{\tau^b}{2} \left( g_A(q^2)(\gamma_\mu\gamma_5) + h_A(q^2)(q_\mu\gamma_5) \right) u(L) \quad (132)$$

$$\begin{aligned} &= \left( \bar{u}(P) \frac{\tau^b}{2} \gamma_\mu \gamma_5 u(L) \right) B_A(q^2) (1 + G_2(q^2)) \\ &+ \left( \bar{u}(P) \frac{\tau^b}{2} \not{q} \gamma_5 u(L) \right) B_A(q^2) q_\mu \frac{G_1(q^2) - G_2(q^2)}{q^2} \\ &+ \left( \bar{u}(P) \frac{\tau^b}{2} \gamma_5 u(L) \right) B_P(q^2) q_\mu H(q^2) \end{aligned}$$

$$\langle N(P) | i\bar{\psi}(0)\gamma_5 \frac{\tau^b}{2} \psi(0) | N(L) \rangle = \bar{u}(P) \frac{\tau^b}{2} \left( i_A(q^2)(i\gamma_5) \right) u(L) \quad (133)$$

$$= \left( \bar{u}(P) \frac{\tau^b}{2} i\gamma_5 u(L) \right) B_P(q^2) (1 + I_1(q^2)) + \left( \bar{u}(P) \frac{\tau^b}{2} i\not{q} \gamma_5 u(L) \right) B_A(q^2) I_2(q^2),$$

where the isospin and the helicity indices of the initial and the final nucleons are suppressed for simplicity. The form factors are expressed as

$$g_A(q^2) = B_A(q^2) (1 + G_2(q^2)) \quad (134)$$

$$h_A(q^2) = B_P(q^2) H(q^2) + 2m_N B_A(q^2) \frac{G_1(q^2) - G_2(q^2)}{q^2}$$

$$i_A(q^2) = B_P(q^2) (1 + I_1(q^2)) + 2m_N B_A(q^2) I_2(q^2).$$

$\tilde{g}_{\pi NN}$  is extracted according to Eq.(69) and  $g_A$  by  $g_A = g_A(q^2 = 0)$ . Note that, due to Eq.(116),  $G_1(q^2) - G_2(q^2)$  is proportional to  $q^2$ , which cancel  $q^2$  in the denominator in the expression of  $h_A(q^2)$ .

By neglecting the small cut-off artifact, the PCAC relation Eq.(28) leads to the relation:

$$2m_N g_A(q^2) + q^2 h_A(q^2) = 2m_0 i_A(q^2), \quad (135)$$

which provides the following relation between  $B_P(q^2)$  and  $B_A(q^2)$ :

$$2m_N B_A(q^2) (1 + G_1(q^2) - 2m_0 I_2(q^2)) + B_P(q^2) (q^2 H(q^2) - 2m_0 (1 + I_1(q^2))) = 0. \quad (136)$$

By using Eq.(131), Eq.(134) and Eq.(136), we are left with the following analytical expression of  $\Delta_G(m_0)$ :

$$\begin{aligned} \Delta_G(m_0) &= \frac{f_\pi \tilde{g}_{\pi NN}}{m_N g_A} \\ &= \frac{m_\pi^2}{2m_0} \frac{-2ig_\pi\Pi_{5A}(0)}{1 - 2ig_{\text{ax}}\Pi_1(0)} + m_\pi^2 \frac{2ig_{\text{ax}}}{1 - 2ig_A\Pi_1(0)} \left( \Pi_1'(0) - \Pi_2'(0) \right), \end{aligned} \quad (137)$$

where  $\Pi'_1(q^2) \equiv \frac{d\Pi_1(q^2)}{d(q^2)}$ ,  $\Pi'_2(q^2) \equiv \frac{d\Pi_2(q^2)}{d(q^2)}$ . All the baryonic quantities disappear from  $\Delta(m_0)$ . Note that, once the mean-field approximation for the vacuum is adopted, this expression is valid even beyond the ladder truncation scheme of the 3qBS kernel, as far as the kernel satisfies our criterion of PCAC relation<sup>21</sup>. This, in particular, implies that, to improve  $\Delta_G(m_0)$ , we have to improve the vacuum or to evaluate the on-shell  $g_{\pi NN}$ . Therefore, the easiest way to improve the result of  $\Delta_G(m_0)$  in Section 5.4 is to improve the vacuum by including the effect of  $g_{\text{ax}} \neq 0$ , since it is not so easy to treat the vacuum beyond the meanfield approximation.

## D.2 The Numerical Results

We first have to explain the choice of the parameters. There are five parameters: the cutoff  $\Lambda$  (Euclidean sharp cutoff), the current quark mass  $m_0$ , the effective coupling constant in the pionic channel  $g_\pi$ , the effective coupling constant in the iso-vector axial-vector mesonic channel  $g_{\text{ax}}$  and the effective coupling constant in the  $qq$  scalar diquark channel  $g_{\text{sd}}$ . We treat  $g_{\text{ax}}$  as a free parameter, and fix the first three parameters ( $\Lambda, m_0, g_\pi$ ) by solving the gap equation Eq.(101) for the constituent quark mass  $M$ , and Eq.(110) for the pion mass  $m_\pi$  and the pion decay constant  $f_\pi$  imposing the following three conditions: (1)  $m_\pi = 140$  MeV, (2)  $f_\pi = 93$  MeV, (3)  $M = 400$  MeV. We fix  $g_{\text{sd}}$  by requiring that  $m_N = 940$  MeV. We give our numerical results for the three cases (1)  $g_{\text{ax}}/g_\pi = 0$ , (2)  $g_{\text{ax}}/g_\pi = 0.25$ , (3)  $g_{\text{ax}}/g_\pi = 0.5$ . The explicit values of the parameters are listed as follows:

1.  $g_{\text{ax}}/g_\pi = 0$ :  $\Lambda = 739$  MeV,  $m_0 = 8.99$  MeV,  $g_\pi = 10.4$  GeV<sup>-2</sup>,  $g_s/g_\pi = 0.66$ .
2.  $g_{\text{ax}}/g_\pi = 0.25$ :  $\Lambda = 812$  MeV,  $m_0 = 6.99$  MeV,  $g_\pi = 8.13$  GeV<sup>-2</sup>,  $g_s/g_\pi = 0.694$ .
3.  $g_{\text{ax}}/g_\pi = 0.5$ :  $\Lambda = 874$  MeV,  $m_0 = 5.75$  MeV,  $g_\pi = 6.71$  GeV<sup>-2</sup>,  $g_s/g_\pi = 0.72$ .

Once these parameters are fixed, we consider the chiral limit by taking  $m_0 \rightarrow 0$  keeping  $\Lambda, g_\pi, g_{\text{ax}}$  and  $g_{\text{sd}}$  fixed. Eq.(101) provides the  $m_0$  dependences of  $M = M(m_0)$ . We confine ourselves to non-negative values of  $g_{\text{ax}}/g_\pi$  because of the following reasons: (1) our examples of the interaction Lagrangians give non-negative values, i.e.,  $g_{\text{ax}}/g_\pi = 0$  in the original NJL type, and  $g_{\text{ax}}/g_\pi = 0.5$  in the color current type. (2) As we shall see below,  $g_A$  and  $\tilde{g}_{\pi NN}$  increase with decreasing  $g_{\text{ax}}/g_\pi$ . If  $g_{\text{ax}} < 0$ , we cannot adjust either  $g_A$  nor  $\tilde{g}_{\pi NN}$ . (3) The increase of  $g_A$  with decreasing  $g_{\text{ax}}$  is due to the fact that the negative  $g_{\text{ax}}/g_\pi$  works as an attraction in the transversal iso-vector axial-vector mesonic channel ( $a_1$  channel), which makes  $G_2(q^2 = 0)$  to grow up, leading to the rapid increase of  $g_A = g_A(q^2 = 0)$ . (cf. Eq.(134)) This ‘‘anti-screening’’ of  $g_A$  does not seem to be reasonable[2].

Now we present our numerical results. In Fig.18, we plot  $g_{\pi NN}$  against the current quark mass  $m_0$  for these three cases of  $g_{\text{ax}}$ . It is seen that  $\tilde{g}_{\pi NN}$  decreases with increasing

<sup>21</sup>Although the baryonic parts  $B_P(q^2)$  and  $B_A(q^2)$  change, they still satisfy Eq.(136). Hence Eq.(137) remains to be valid.

$g_{\text{ax}}/g_\pi$ , and increases with increasing  $m_0$ . The crosses in the figure are used to indicate  $m_0$  which correspond to  $m_\pi = 140$  MeV. We use the diamonds to indicate  $m_0$  which correspond to  $m_\pi = 2 \times 140$  MeV, which is used to indicate the validity of the single pole dominance approximation of  $\tilde{g}_{\pi NN}$ . Note that the distance between 0 and  $4M^2$ , i.e., the  $q\bar{q}$  cut, is still 10 times larger than  $m_\pi^2$ , as long as  $m_\pi \leq 2 \times 140$  MeV. In Fig.19, we plot  $g_A$  against  $m_0$  for the three cases of  $g_{\text{ax}}$ . We see that  $g_A$  decreases with increasing  $g_{\text{ax}}/g_\pi$  and increases with increasing  $m_0$ . Note that, if  $g_{\text{ax}}/g_\pi = 0.1$ , then  $g_A = 1.23$  and  $\tilde{g}_{\pi NN} = 12.5$ . So the best fit of  $\tilde{g}_{\pi NN}$  and  $g_A$  could be obtained in the region  $0 \leq g_{\text{ax}}/g_\pi < 0.1$ , which, however, would depend on the quantity which we prefer to adjust. From this point of view,  $g_{\text{ax}} = 0$  is actually a rather good choice. In this case,  $\tilde{g}_{\pi NN} = 13.5$  is very reasonable and  $g_A = 1.33$  is still close to the experimental value  $g_A^{(\text{exp})} = 1.26$ . Note that, due to the chiral symmetry, positive  $g_{\text{ax}}/g_\pi$  implies an attractive interaction in the iso-vector vector mesonic channel ( $\rho$  meson). In order to describe  $\rho$  meson in the NJL model, however, we need stronger  $g_{\text{ax}}$  [2, 19], but, stronger  $g_{\text{ax}}$  leads to smaller  $g_A$  and  $\tilde{g}_{\pi NN}$  in our calculation. (The situation could be improved by including  $qq$  interactions in the axial-vector diquark channel, which enhance  $g_{\pi NN}$  [20]. In this case, one should also include the  $qq$  interaction in the vector diquark channel for the Goldberger-Treiman and the PCAC relation.) In Fig.20, we plot the numerical  $\Delta_G$  together with the analytic  $\Delta_G$  (Eq.(137)) against  $m_0$ . It is seen that they are monotonically decreasing functions of  $m_0$  independent of  $g_{\text{ax}}/g_\pi$ . We see that the discrepancy between the analytic and the numeric  $\Delta_G$  is within 3 %. Recall that, when deriving Eq.(137), we neglected the small cut-off artifact. Hence this discrepancy is solely due to the cut-off artifact. Note that the analytic  $\Delta_G$  approaches 1 as  $m_0 \rightarrow 0$  in Fig.20. In fact, based on Eq.(114), Eq.(115), Eq.(116) and the Gell-Mann-Oakes-Renner relation, it is possible to prove that the analytic  $\Delta_G$  approaches to 1 as  $m_0 \rightarrow 0$ . To make  $\Delta_G$  an increasing function of  $m_0$ , it is necessary to go beyond the validity of the analytic  $\Delta_G$  (Eq.(137)). This implies that all we can do is either to improve the gap equation for the vacuum beyond the meanfield approximation or to evaluate the on-shell  $g_{\pi NN}$ . In Fig.21, we plot the PCAC violation  $\Delta_P$  against  $m_0$  for the three cases of  $g_{\text{ax}}/g_\pi$ . The deviation of  $\Delta_P$  from 1 is solely due to the cutoff artifact. We see that the PCAC violations are only within 3%, which suggests the practical validity of our results.

## References

- [1] Y. Nambu, G. Jona-Lasinio, Phys. Rev. **122** (1960) 345; **124** (1961) 246.
- [2] U. Vogl, W. Weise, Prog. Part. Nucl. Phys. **27**(1991)195.
- [3] S. Klevansky. Rev. Mod. Phys. **64** (1992) 649.  
T. Hatsuda, T. Kunihiro, Phys. Rep. **247** (1994) 221.  
R. Alkofer, H. Reinhardt, H. Weigel, Phys. Rep. **265** (1996) 139.  
C. Christov et al., Prog. Part. Nucl. Phys. **37** (1996) 1.
- [4] M. Kato, W. Bentz, K. Yazaki, K. Tanaka, Nucl. Phys. **A551** (1993) 541.  
S. Kahana, G. Ripka, Nuch. Phys. **A429** (1984) 462.



- D. I. Diakonov, V. Yu. Petrov, P. V. Poboylitsa, Nucl. Phys. **B306** (1988) 809.  
R. Alkofer, Nucl. Phys. **B306** (1990) 310.  
Th. Meissner, F. Grümmer, K. Goeke, Phys. Lett. **B 227** (1989) 296.  
P. Sieber, Th. Meissner, F. Grümmer, K. Goeke, Nucl. Phys. **A 547** 459.
- [5] A. Buck, R. Alkofer, H. Reinhardt, Phys. Lett. **B 286** (1992) 29.
- [6] N. Ishii, W. Bentz, K. Yazaki, Phys. Lett. **B301** (1993) 165.
- [7] N. Ishii, W. Bentz, K. Yazaki, Phys. Lett. **B318** (1993) 26.
- [8] N. Ishii, W. Bentz, K. Yazaki, Nucl. Phys. **A587** (1995) 617.
- [9] H. Asami, N. Ishii, W. Bentz, K. Yazaki, Phys. Rev. **C51** (1995) 3388.
- [10] M. Oettel, G. Hellstern, R. Alkofer, and H. Reinhardt, Phys. Rev. **C58** (1998) 2549.  
H. Mineo, W. Bentz, K. Yazaki, Phys. Rev. **C60** (1999) 065201
- [11] N. Ishii, Phys. Lett. **B431** (1998) 1.
- [12] A. Bender, C. D. Roberts, L. v. Smekal, Phys. Lett. **B380** (1996) 7.
- [13] M. Oettel, M. A. Pichowsky, L. v. Smekal, nucl-th/9909082.
- [14] A. N. Kvinikhidze, B. Blankleider, Phys. Rev. **C60** (1999) 044004, 044003, and personal communication.
- [15] C. Itzykson, J.-B. Zuber, “Quantum field theory”, McGraw-Hill International Editions (1985).
- [16] S. Pokorski, Section 12 in “Gauge Field Theories”, Cambridge University Press (1990).
- [17] I. R. Afnan, A. W. Thomas, in “Modern Three-Hadron Physics” (Springer-Verlag, Berlin (1977), ed. A. W. Thomas).
- [18] K. Huang, “Quarks, Leptons and Gauge Fields”.
- [19] M. Takizawa, K. Kubodera, F. Myhrer, Phys. Lett. **B261** (1991) 221.
- [20] C. Fischer, Diploma thesis, Eberhard-Karls-Universität Tübingen (1999).  
R. Alkofer, personal communication.

## Figure Captions

1. The gauge transformation property of  $S_F^{[e]}$  is depicted. A single line represents a propagator of the constituent quark in the presence of the external fields. The gauge transformation reduces to the multiplication of the phase factors  $\Omega(x)$  and  $\Omega(y)$ .
2. The functional derivative of the propagator, i.e.,  $\left[ \frac{i\delta S_F^{[e]}}{\delta a_\mu^b(z)} \right]^{[0]}$  is depicted. A single line is a constituent quark propagator. Dashed lines are used to indicate the momentum transfer  $q$ . Fig.2.(a) corresponds to  $g_{ax} = 0$  case, and Fig.2.(b) corresponds to  $g_{ax} \neq 0$  case.
3. (a) The 3qBS kernel in the ladder truncation scheme is depicted. A single line represents a quark propagator. A slash indicates an amputation, i.e., removal of the quark leg.  
 (b) The diagram used to evaluate the nucleon matrix element for 3qBS kernel of the type Fig.3.(a) is depicted. “ $\otimes$ ” is understood in the sense of Fig.2. Diagrams of the same topologies are omitted.
4. (a) The  $q\bar{q}$  exchange improved 3qBS kernel is depicted. A single line represents a quark propagator. A slash indicates an amputation. A wavy line represents a ladder sum of  $q\bar{q}$  bubbles as is depicted in the second line. Diagrams of the same topologies are omitted.  
 (b) The diagrams with which to obtain the nucleon matrix element for 3qBS kernel of the type Fig.4.(a) are depicted. The second term is often referred to as the “meson exchange current” contribution. The diagrams of the same topologies are omitted.
5. The proof that the ladder truncated 3qBS kernel gives rise to the PCAC relation correctly is diagrammatically explained. In the first step, the local gauge transformation  $\Omega(x) = e^{i\gamma_5\omega(x)}$  is applied. Only the constituent quark propagators transform. In the next step, Eq.(44) is used. The last step is due to the fact that amputated propagators are delta functions. It is seen that the sufficient condition is satisfied.
6. The proof that the  $q\bar{q}$  exchange improved 3qBS kernel gives rise to the PCAC relation correctly is diagrammatically explained. In the first step, we applied the gauge transformation. In the second step, Eq.(41) is used. Note that all the phase factors, which appear at the internal vertices, cancel themselves. The last step is due to the fact that the amputated propagators are delta functions. It is seen that the sufficient condition is satisfied.
7. (a) The Faddeev equation Eq.(79) is depicted. A single line is a constituent quark propagator. A double line is a t-matrix in the  $qq$  diquark channel. (For precise meaning, see Fig.7.(b).) (b) The diagrammatic expression of the two-quark resolvent

$\frac{K_3}{1 - K_3}$  is depicted. A single line is a constituent quark propagator. A slash indicates an amputation.

8. The diagrams which contribute to the matrix element  $\langle N|A_\mu^b(x)|N\rangle$  are depicted. A blob with “N” which is followed by a triple line is a quark-diquark Faddeev amplitude of the nucleon. A single line is a constituent quark propagator, and a double line is a t-matrix in the  $qq$  scalar diquark channel. A dashed line indicates a momentum transfer  $q_\mu$ . Fig.8.(a) is referred to as the “quark current” contribution, and Fig.8.(b) the “exchange current” contribution. Fig.8.(c) is referred to as the “diquark current” contribution. If the  $qq$  interaction is truncated to the scalar diquark channel, Fig.8.(c) does not contribute to  $g_A$ , due to the iso-scalar nature of the scalar diquark. Fig.8.(a’) is equivalent to Fig.8.(a), which is obtained by once iterating the Faddeev amplitude in the final state by using the homogeneous Faddeev equation. By using Eq.(127) and  $\gamma^\mu(\Lambda p)_\mu = S(\Lambda)\not{p}S(\Lambda^{-1})$ , Fig.8.(a’) and Fig.8.(b) reduce to the four diagrams depicted in Fig.8.(d).
9. Diagrams which contribute to  $g_A$  and  $g_{\pi NN}$  are depicted. These eight diagrams are equivalent to four diagrams in Fig.8.(d) in the limit  $q \rightarrow 0$ , which is indicated by “ $q \rightarrow 0$ ”. The explicit spin-parity projection shows that the first two contribute to  $g_A$ , and the others to  $g_{\pi NN}$ .
10. The nucleon mass  $m_N$  (for  $g_{sd}/g_{pi} = 0.66$ ) (solid line), the quark-diquark threshold  $M + m_{sd}$  ( $g_{sd}/g_\pi = 0.66$  case) (dotted line), the pion mass  $m_\pi$  (dashed line), the pion decay constant  $f_\pi$  (dot-dashed line), the constituent quark mass  $M$  (dot-dot-dashed line) are plotted against the current quark mass  $m_0$ . The points which corresponds to  $m_\pi = 140$  MeV are indicated by the vertical dotted line.
11. The nucleon mass is plotted against  $g_{sd}/g_\pi$  for the two cases (1) the chiral limit (solid line), (2) off the chiral limit [ $m_\pi = 140$  MeV] (dashed line). The vertical dotted line indicates  $g_{sd}/g_\pi = 0.66$ , where  $m_N$  becomes 940 MeV for the case  $m_\pi = 140$  MeV.
12.  $g_{\pi NN}$  is plotted against  $g_{sd}/g_\pi$  for the two cases (1) the chiral limit (solid line), (2) off the chiral limit [ $m_\pi = 140$  MeV] (dashed line). The vertical dotted line indicates  $g_{sd}/g_\pi = 0.66$ , where  $m_N$  becomes 940 MeV for the case  $m_\pi = 140$  MeV.
13. The iso-vector  $g_A$  is plotted against  $g_{sd}/g_\pi$  for the two cases (1) the chiral limit (solid line), (2) off the chiral limit [ $m_\pi = 140$  MeV] (dashed line). The vertical dotted line indicates  $g_{sd}/g_\pi = 0.66$ , where  $m_N$  becomes 940 MeV for the case  $m_\pi = 140$  MeV.
14. The violation of the GT relation  $\Delta_G$  is plotted against  $g_{sd}/g_\pi$  for the two cases (1) the chiral limit (solid line), (2) off the chiral limit [ $m_\pi = 140$  MeV] (dotted line). The dashed line is the plot of the violation of the PCAC relation  $\Delta_P$  off the chiral limit. The vertical dotted line indicates  $g_{sd}/g_\pi = 0.66$ , where  $m_N$  becomes 940 MeV for the case  $m_\pi = 140$  MeV.

15. The violation of the GT relation  $\Delta_G$  (solid line) and the violation of the PCAC relation  $\Delta_P$  (dashed line) are plotted against the current quark mass  $m_0$  for the case  $g_{sd}/g_\pi = 0.66$ . The vertical dotted line indicates the current quark mass  $m_0$  which corresponds to  $m_\pi = 140$  MeV.
16. The interaction Lagrangian  $\mathcal{L}_I$  is depicted in Fig.16.(a). The diagrammatic interpretations of this interaction in the  $q\bar{q}$  channel are classified into the two types: the direct channel [Fig.16.(b)] and the exchange channel (Fig.16.(c)). Fig.16.(b) is obtained from Fig.16.(a) by using the Fierz identity. Another Fierz identity leads to the diagrammatic representation of the interaction in the  $qq$  channel which is depicted in Fig.16.(d).
17. The baryonic parts  $B_P(q^2)$  and  $B_A(q^2)$  of the form factors are defined diagrammatically. A blob with “N” which is followed by a triple line is a quark-diquark Faddeev amplitude of the nucleon. A single line is the constituent quark propagator, and a double line is a t-matrix in the  $qq$  scalar diquark channel. A dashed line indicates a momentum transfer  $q_\mu$ .
18.  $g_{\pi NN}$  is plotted against the current quark mass  $m_0$  for the three cases (1)  $g_{ax}/g_\pi = 0$  (solid line), (2)  $g_{ax}/g_\pi = 0.25$  (dotted line), (3)  $g_{ax}/g_\pi = 0.5$  (dashed line). The crosses indicate the points which correspond to  $m_\pi = 140$  MeV, and the diamonds indicate the points which correspond to  $m_\pi = 280$  MeV.
19.  $g_A$  is plotted against the current quark mass  $m_0$  for the three cases (1)  $g_{ax}/g_\pi = 0$  (solid line), (2)  $g_{ax}/g_\pi = 0.25$  (dotted line), (3)  $g_{ax}/g_\pi = 0.5$  (dashed line). The crosses indicate the points which correspond to  $m_\pi = 140$  MeV, and the diamonds indicate the points which correspond to  $m_\pi = 280$  MeV.
20. The numerical  $\Delta_G$  is plotted against the current quark mass  $m_0$  for the three cases (1)  $g_{ax}/g_\pi = 0$  (solid line), (2)  $g_{ax}/g_\pi = 0.25$  (dashed line), (3)  $g_{ax}/g_\pi = 0.5$  (dot-dot-dashed line). The analytic  $\Delta_G$  is also plotted for these three cases (1) by dotted line, (2) by dot-dashed line, (3) by dot-dash-dashed line. The crosses indicate the points which correspond to  $m_\pi = 140$  MeV, and the diamonds indicate the points which correspond to  $m_\pi = 280$  MeV.
21. The violation of the PCAC relation  $\Delta_P$  is plotted against the current quark mass  $m_0$  for the three cases (1)  $g_{ax}/g_\pi = 0$  (solid line), (2)  $g_{ax}/g_\pi = 0.25$  (dotted line), (3)  $g_{ax}/g_\pi = 0.5$  (dashed line). The crosses indicate the points which correspond to  $m_\pi = 140$  MeV, and the diamonds indicate the points which correspond to  $m_\pi = 280$  MeV.

Fig.18

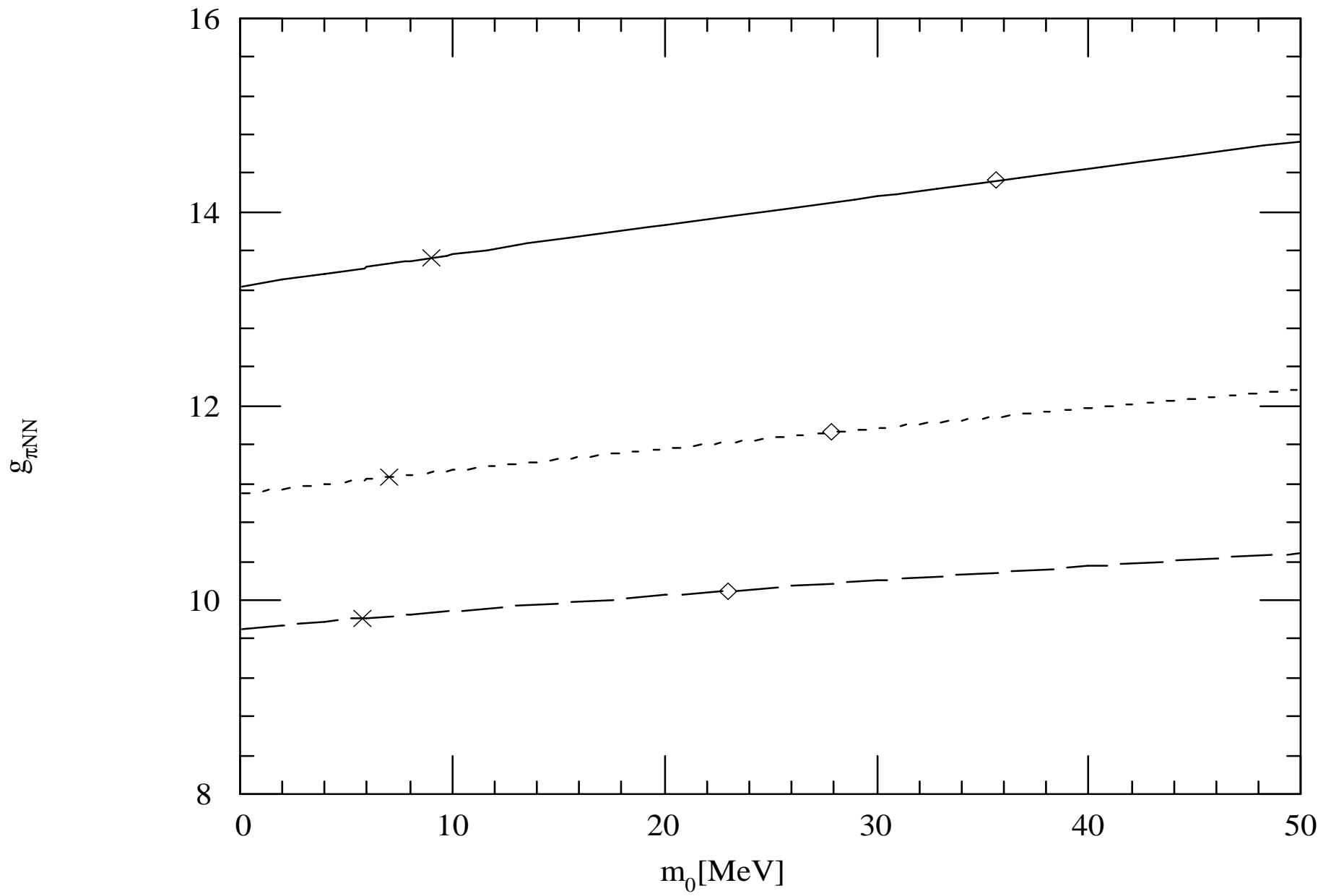


Fig.10

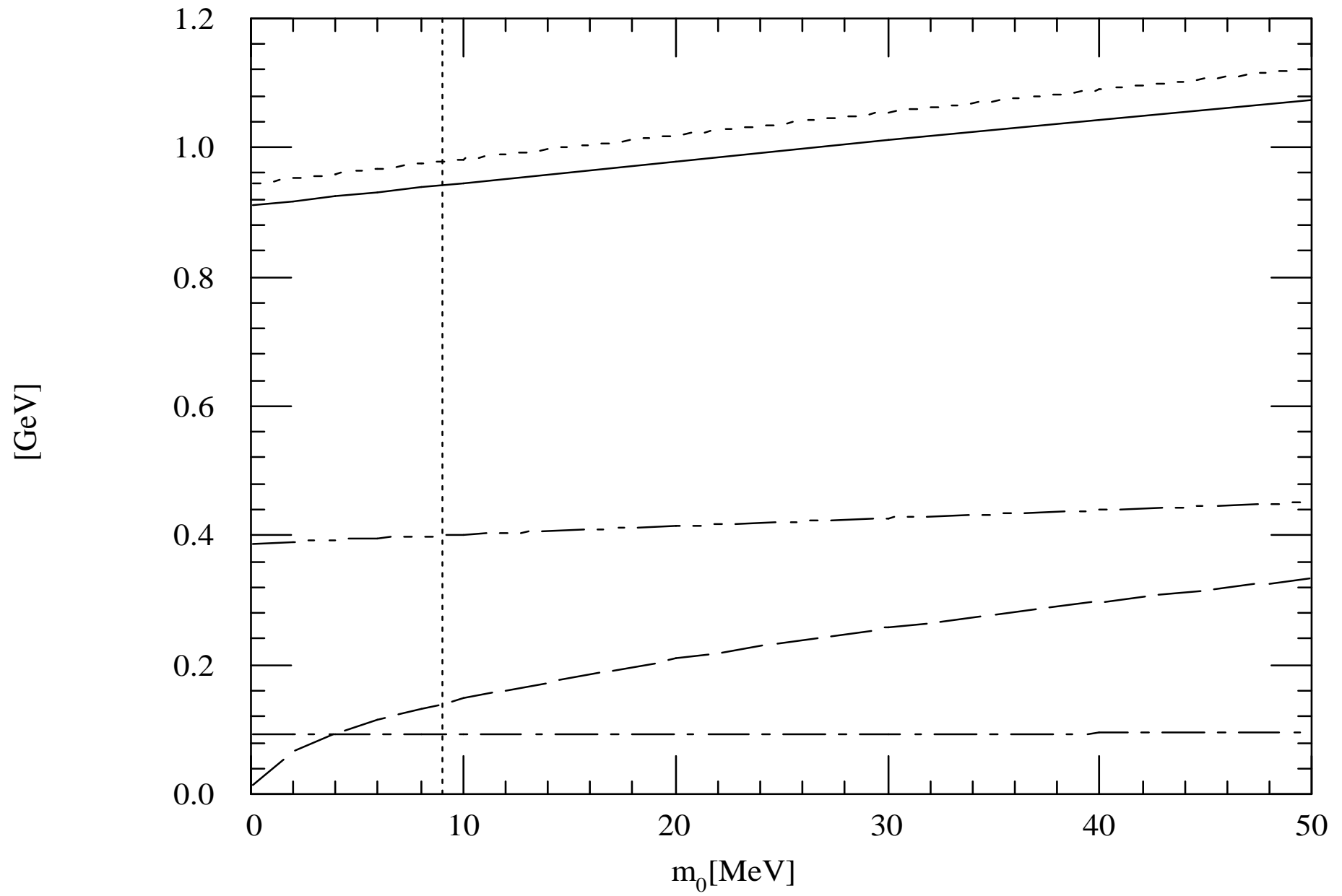


Fig.19

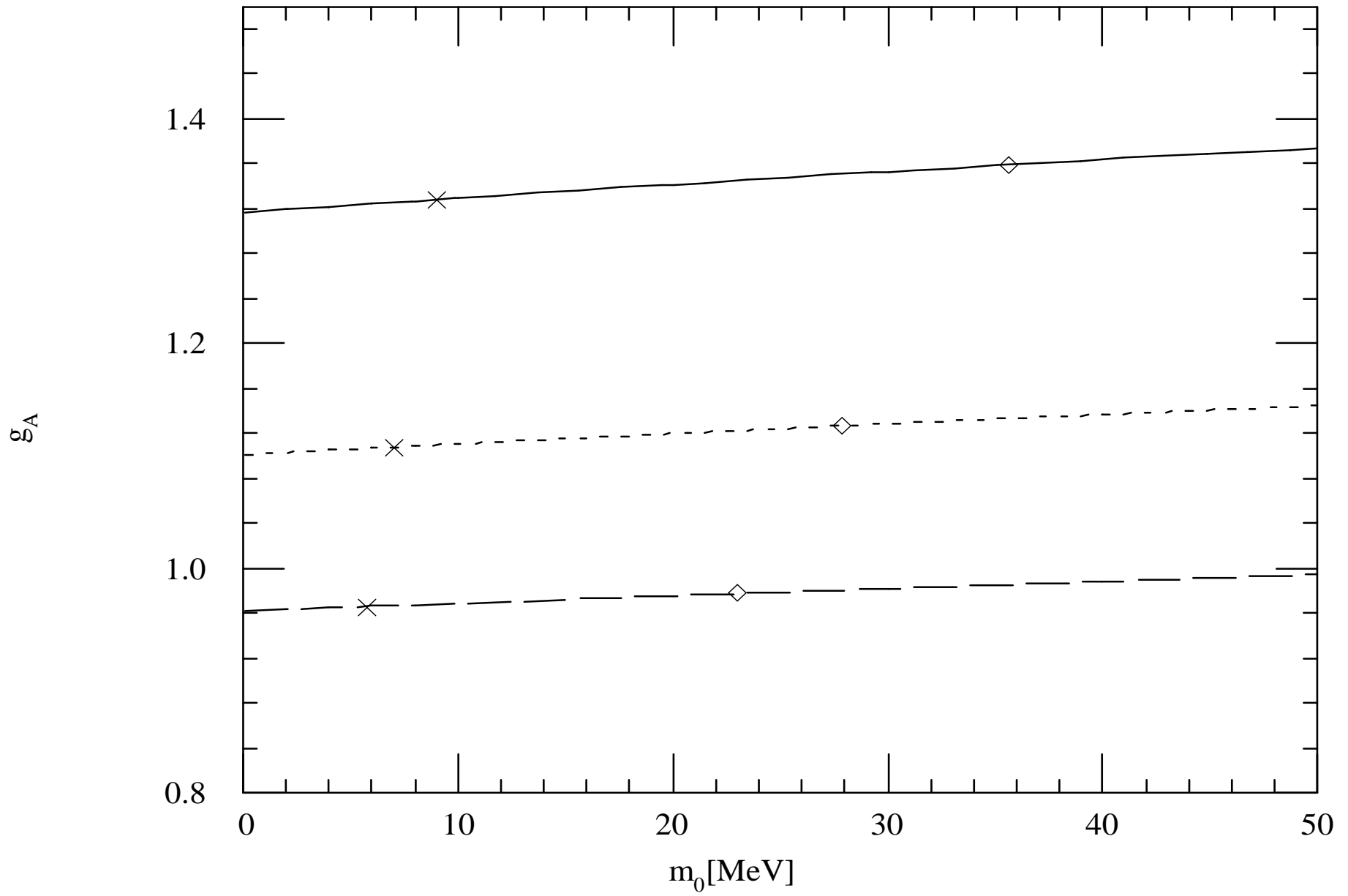


Fig.11

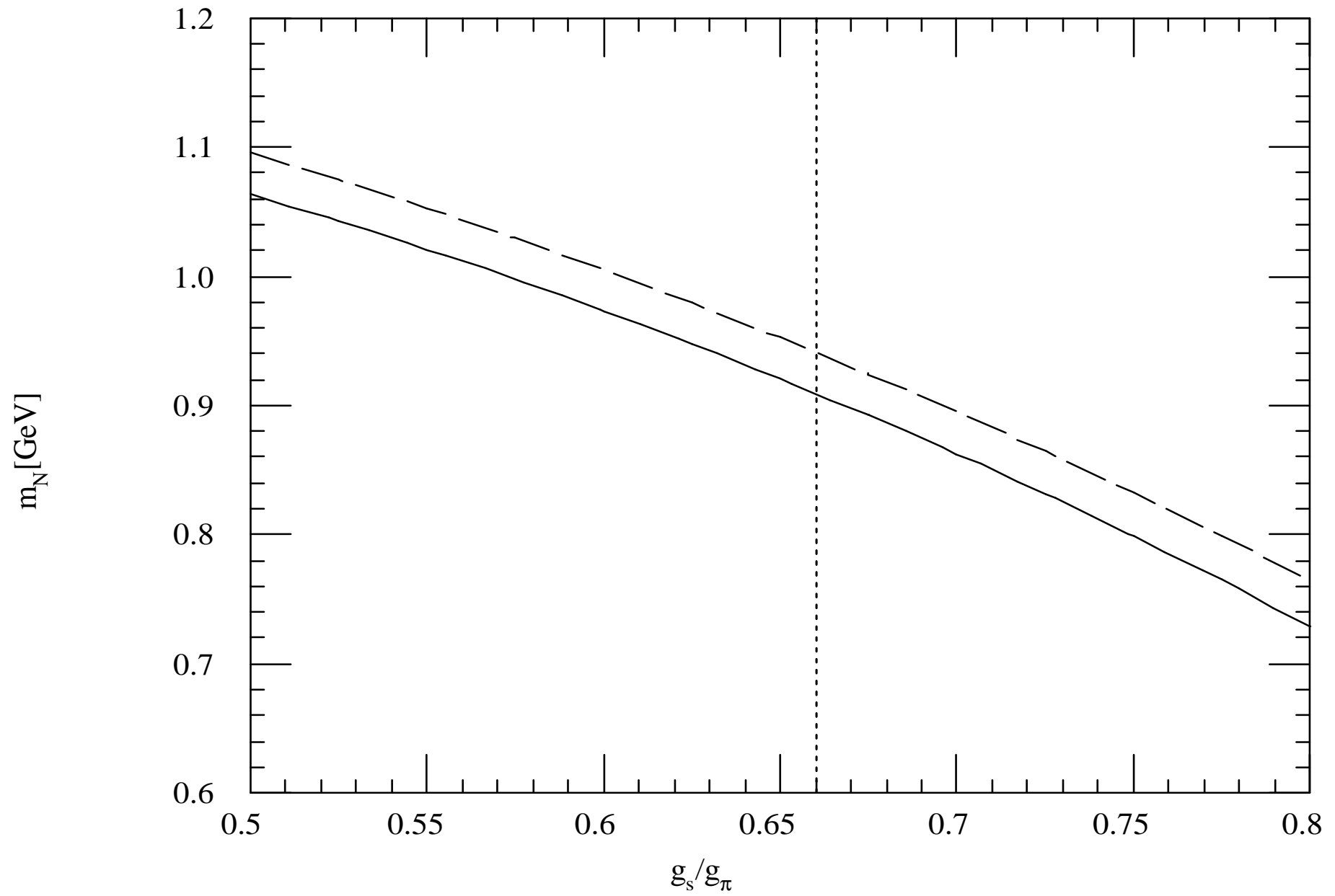




Fig.20

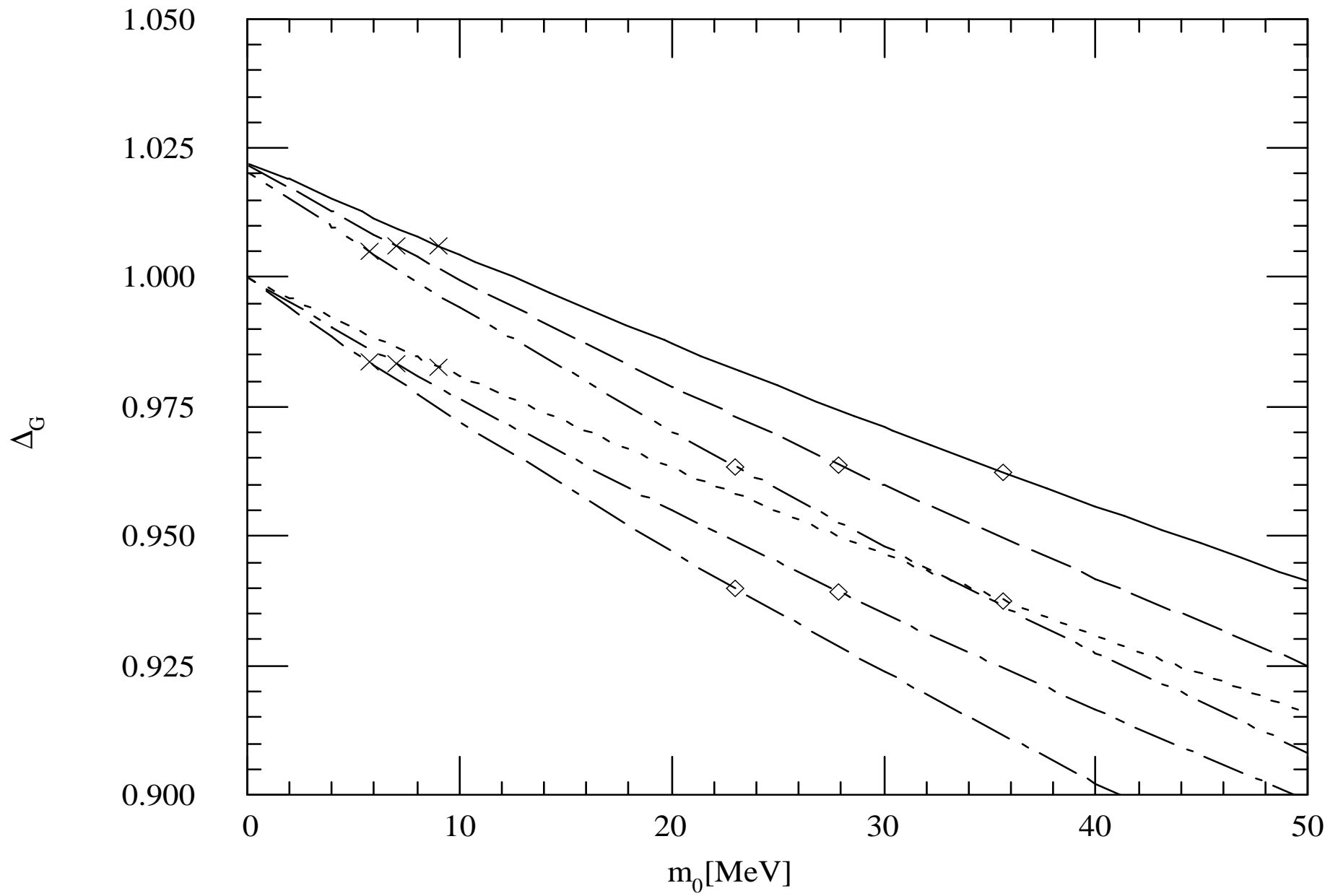


Fig.12

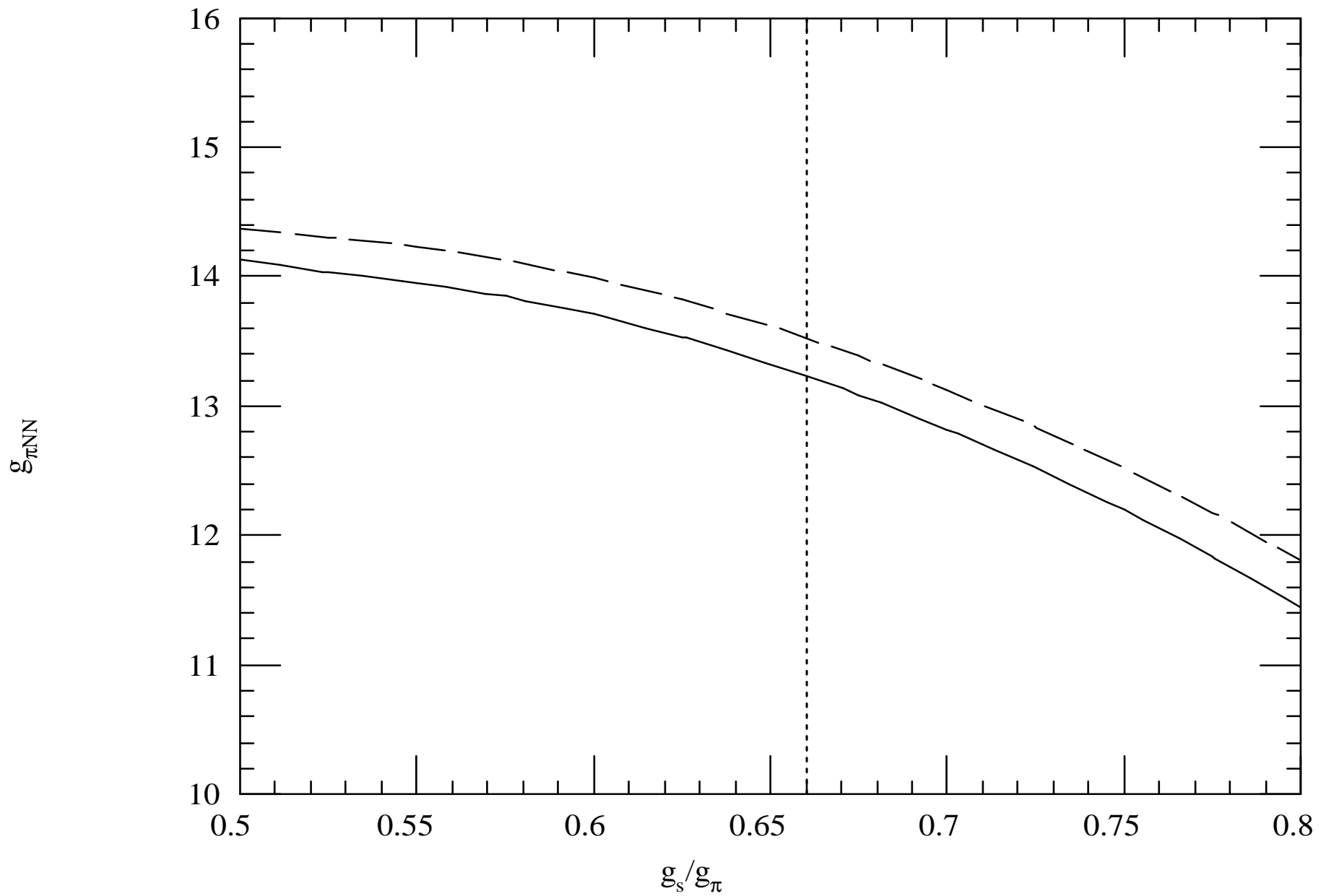


Fig.21

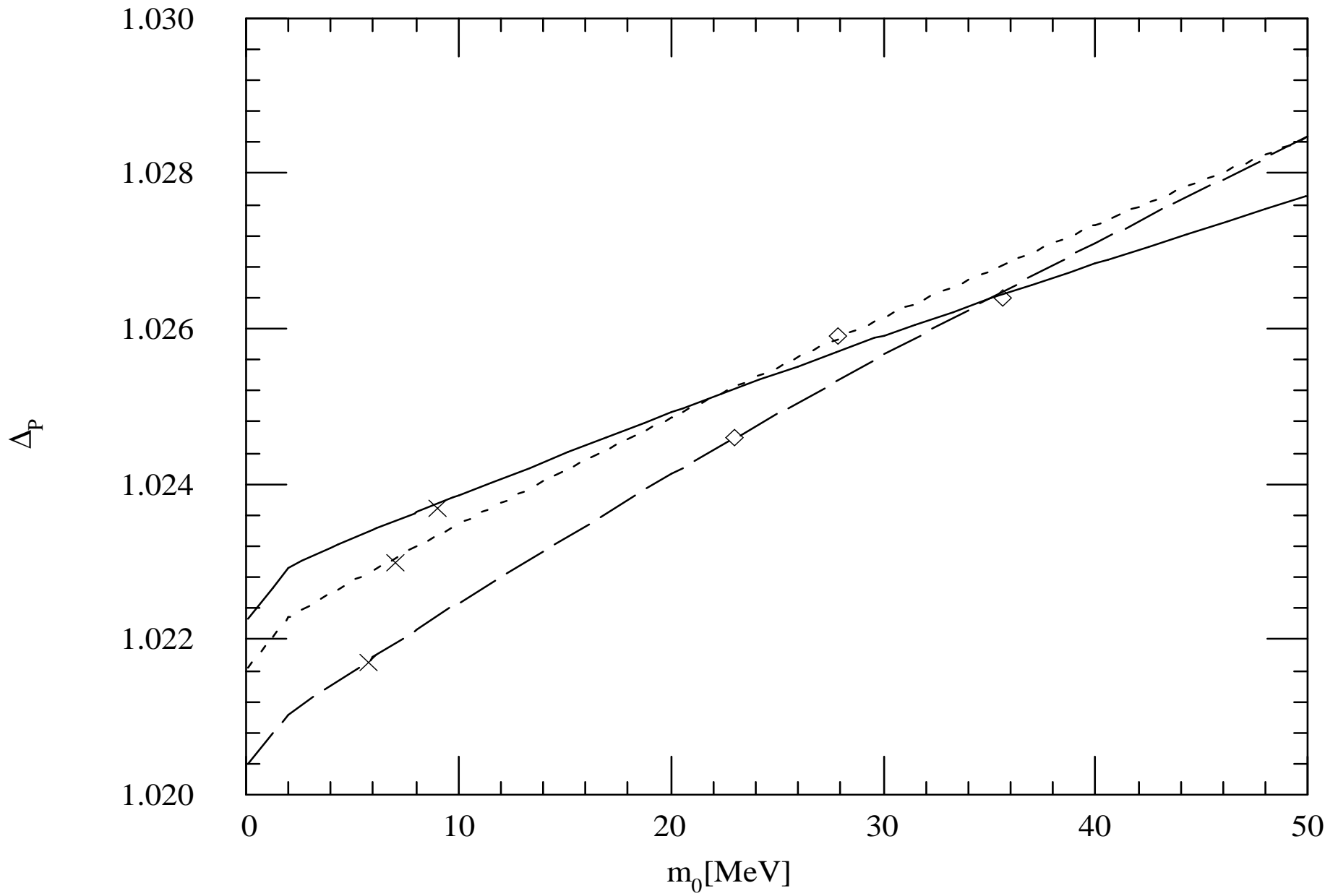


Fig.13

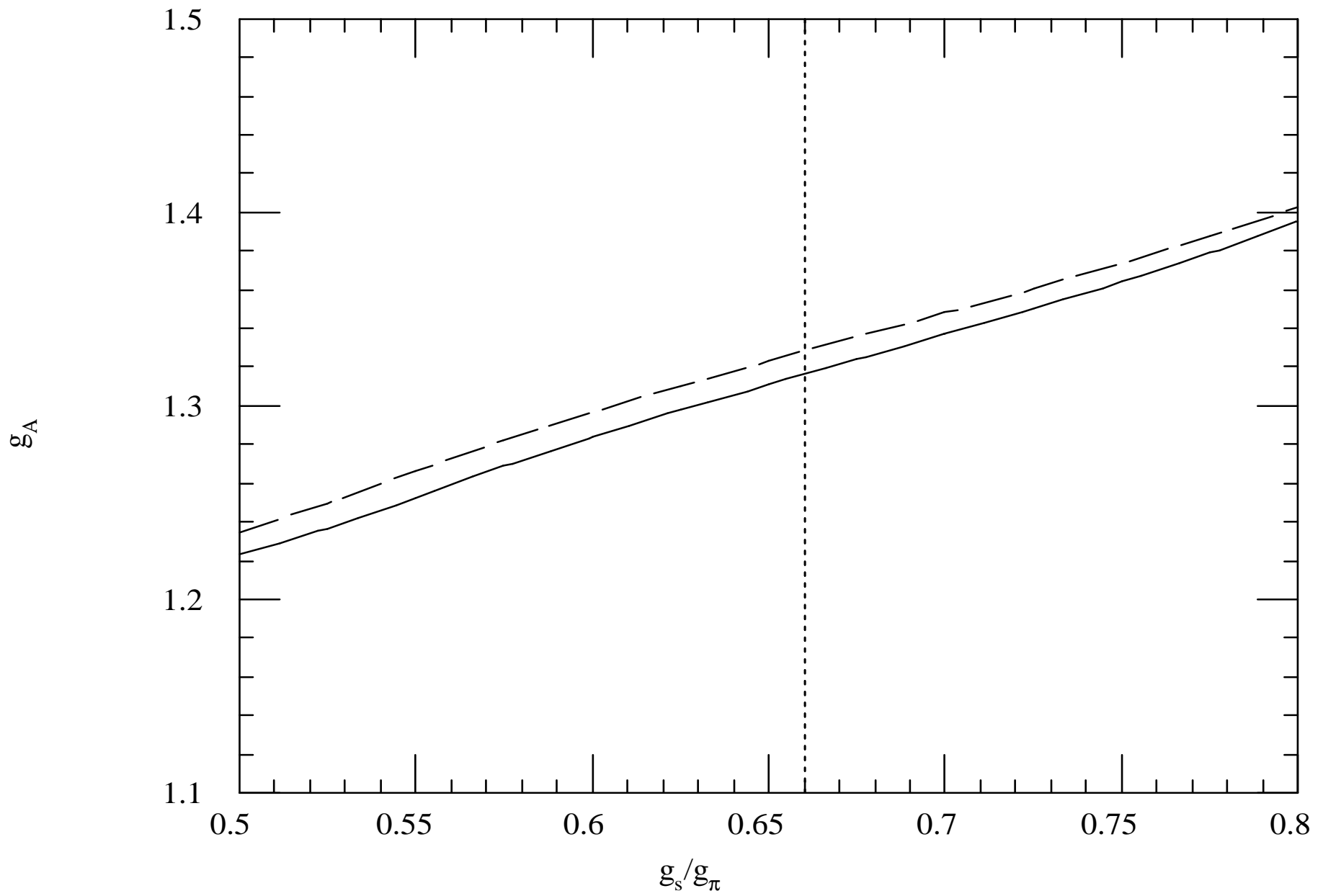


Fig.14

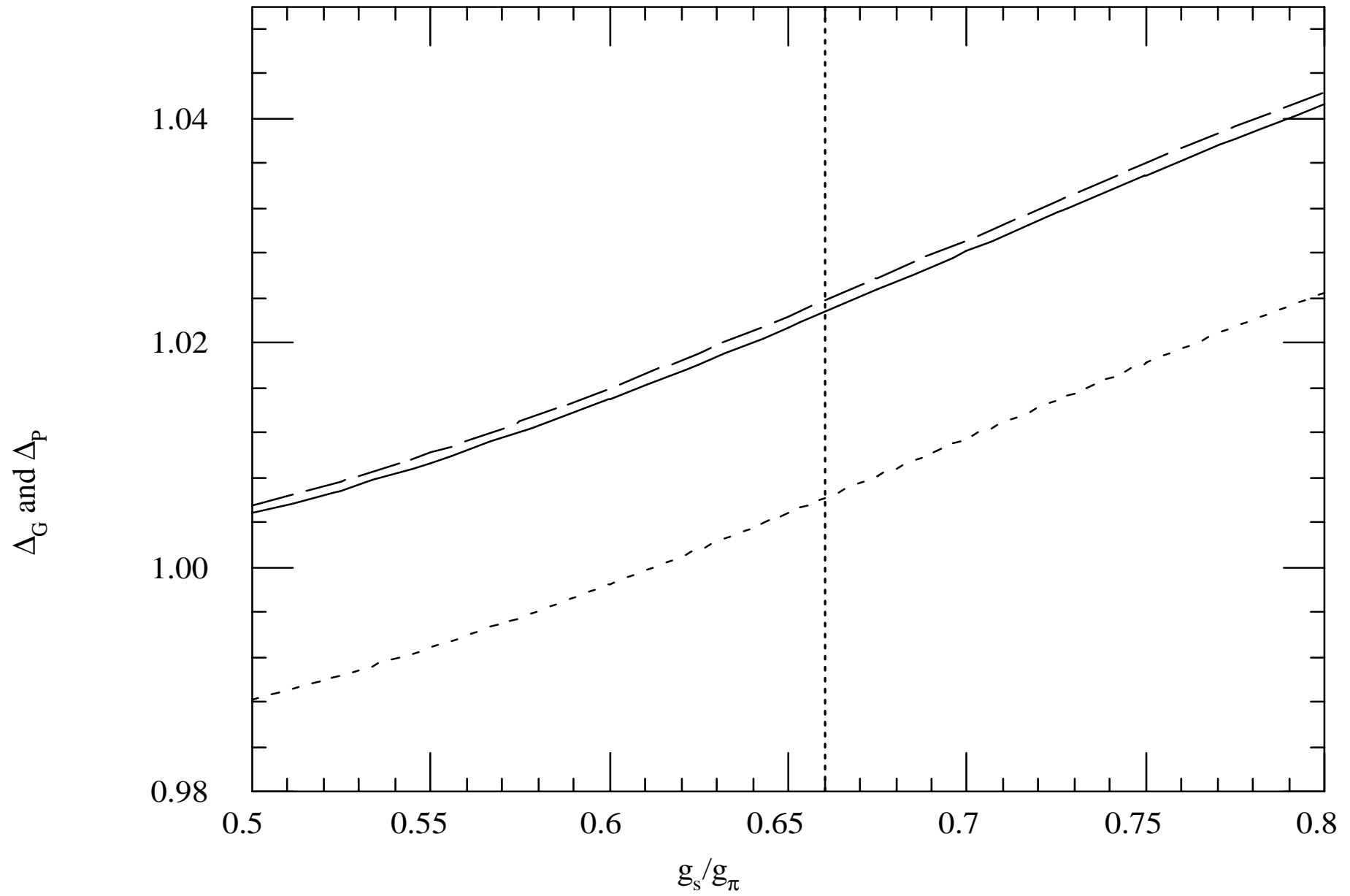


Fig.15

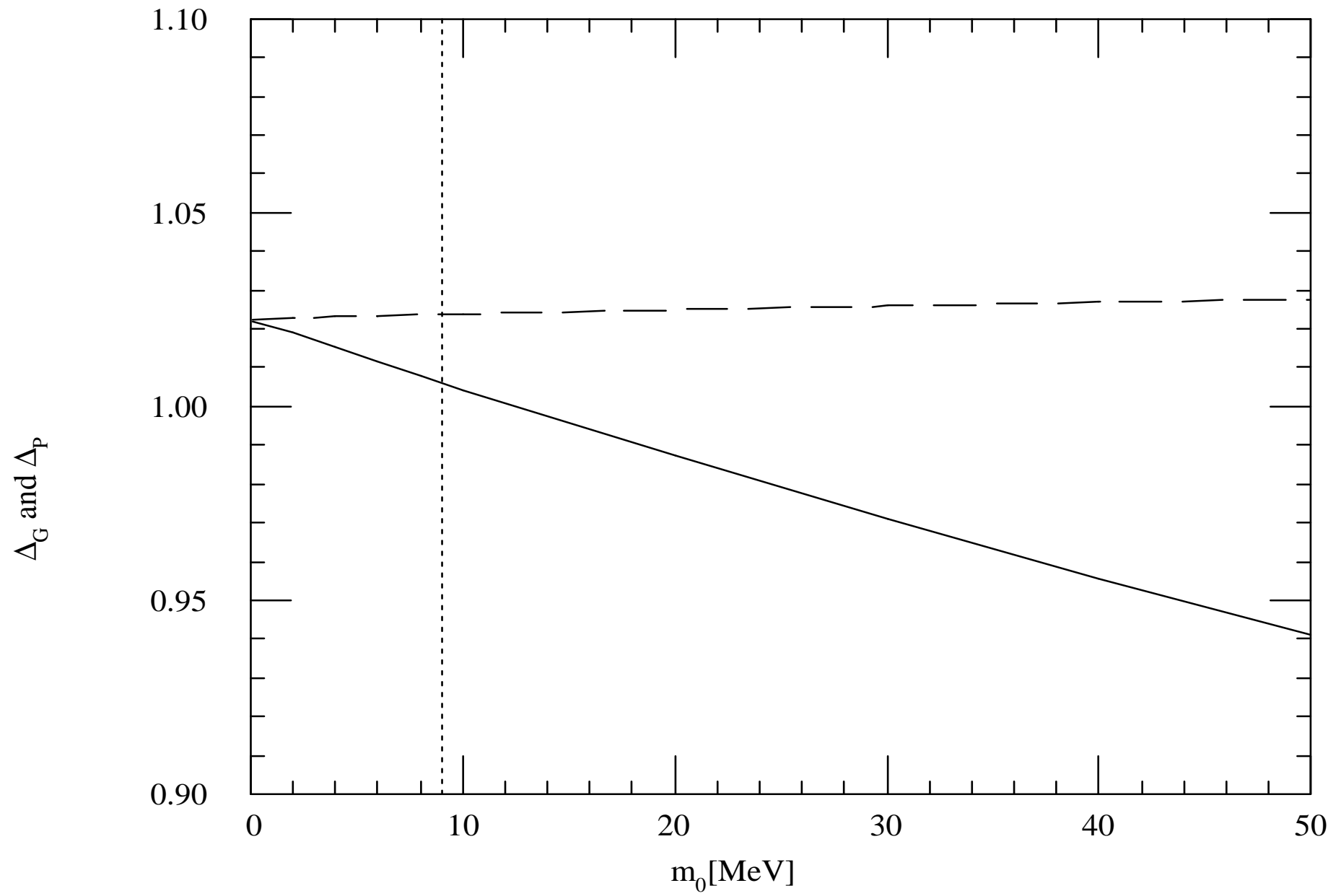


Fig.1

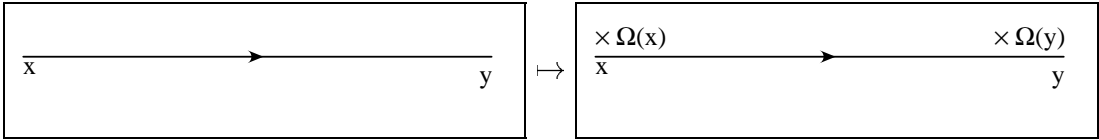
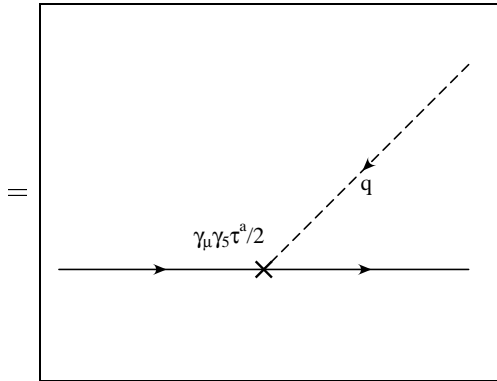
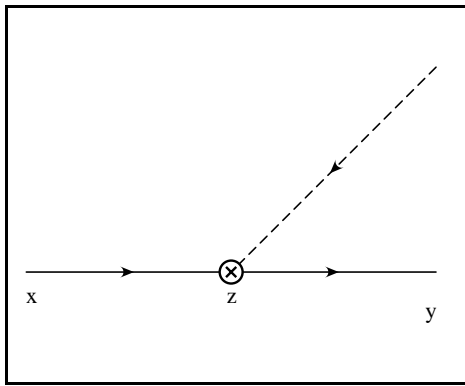


Fig.2.a



+

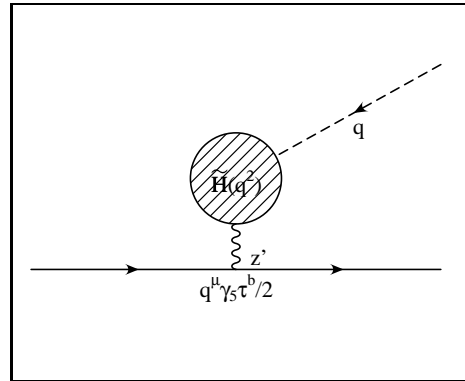
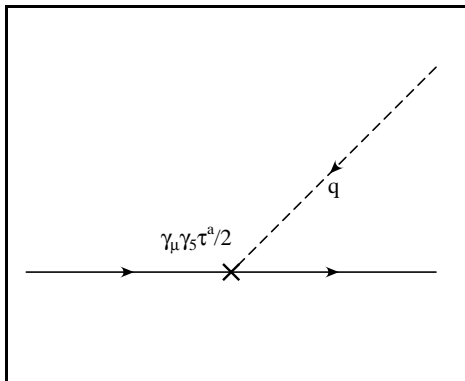
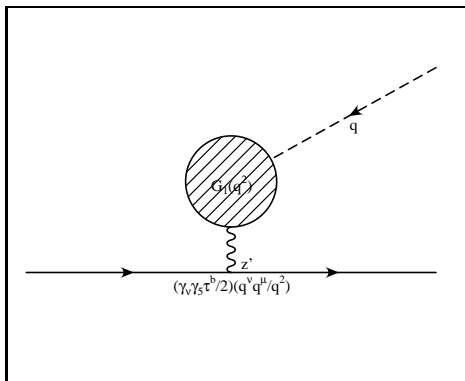
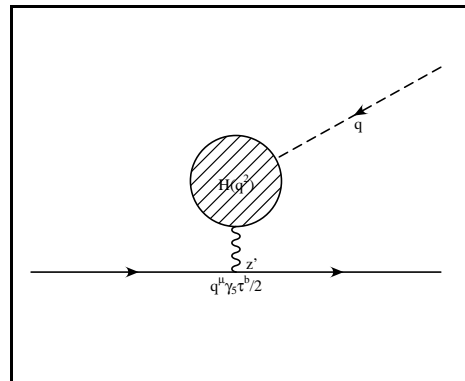


Fig.2.b



+



+

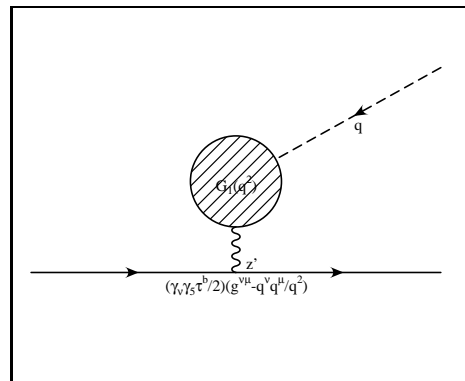




Fig.3.a

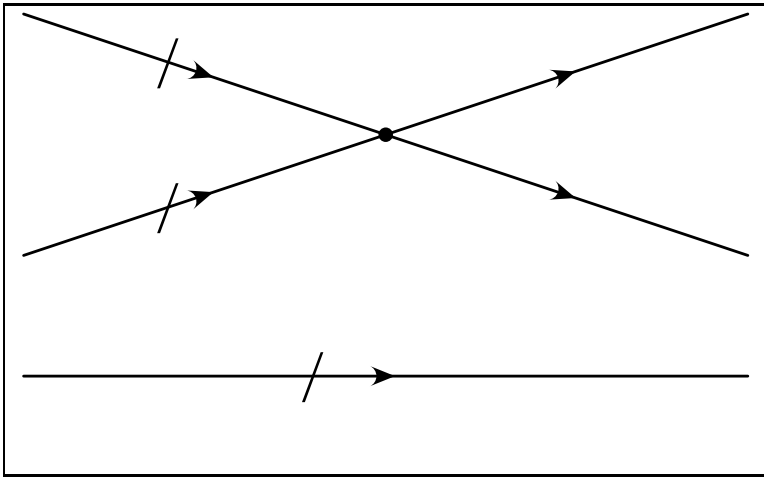


Fig.3.b

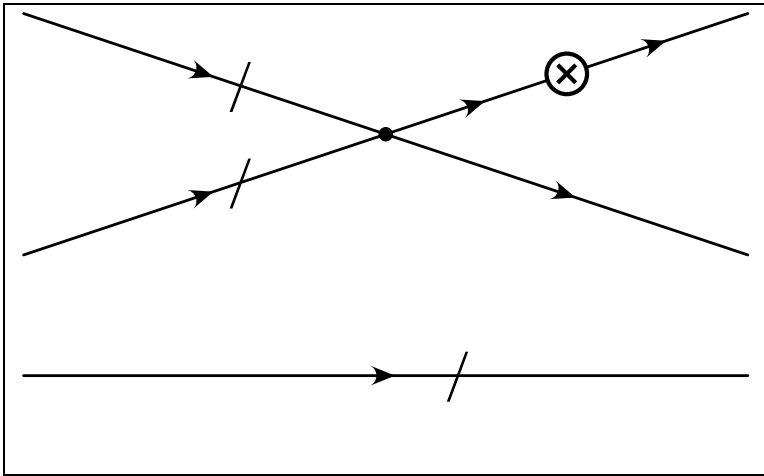


Fig.4.a

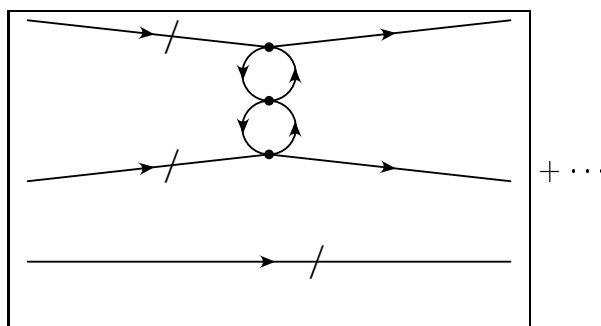
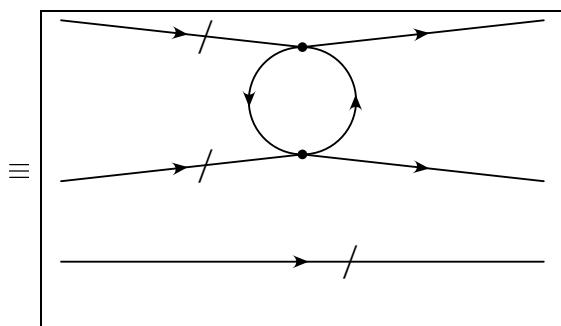
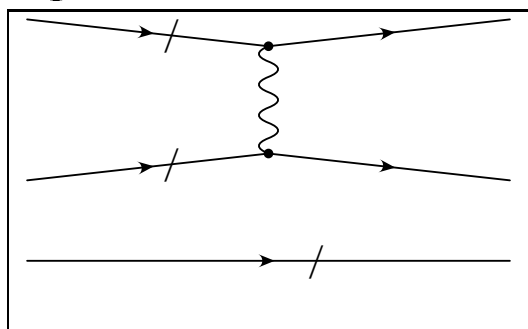


Fig.4.b

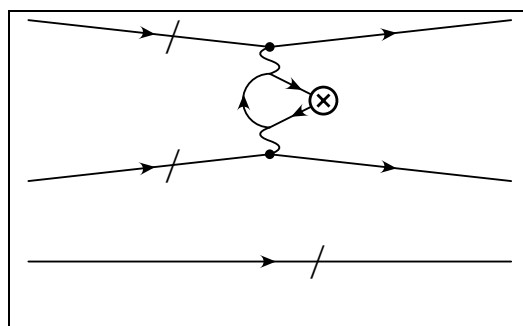
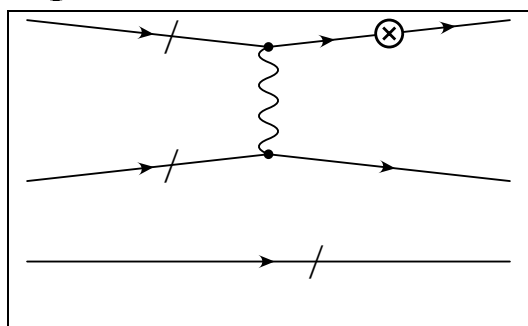


Fig. 3

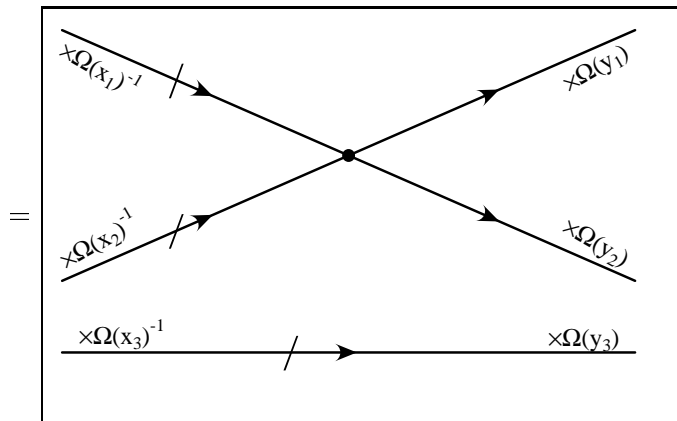
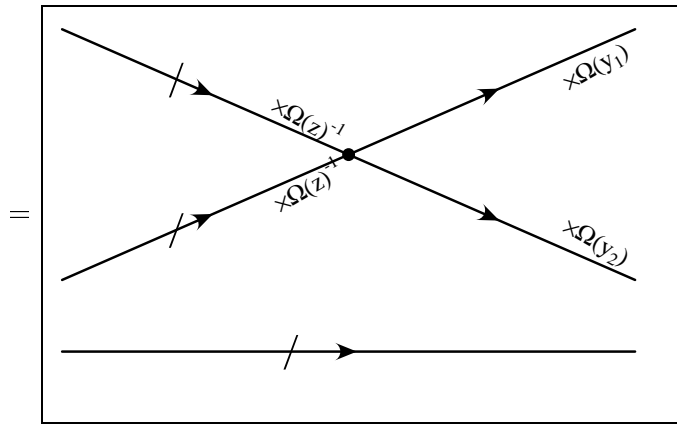
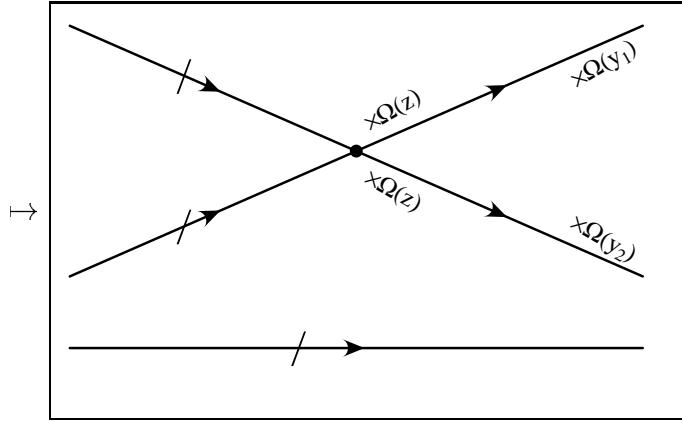
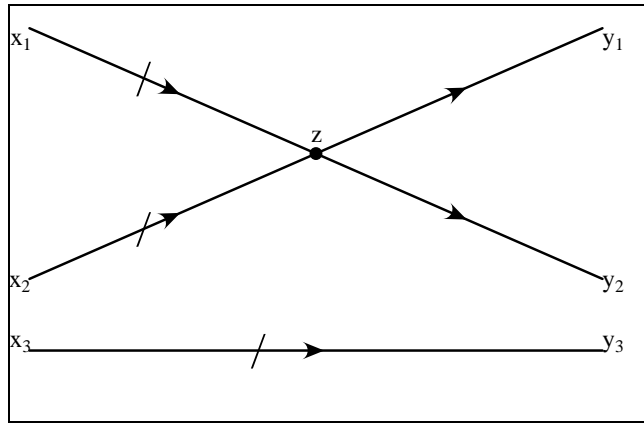


Fig. 6

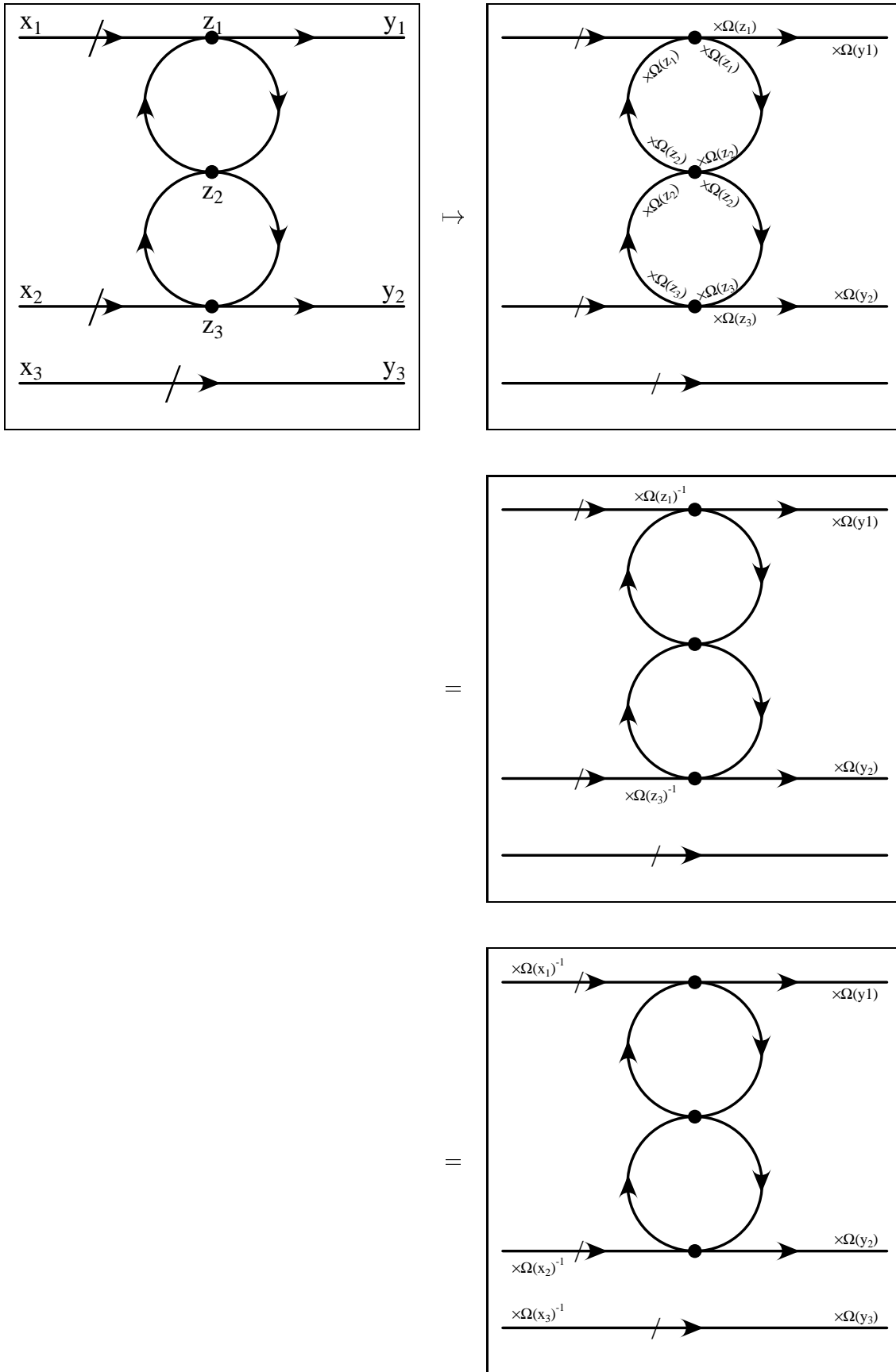


Fig. 7.a

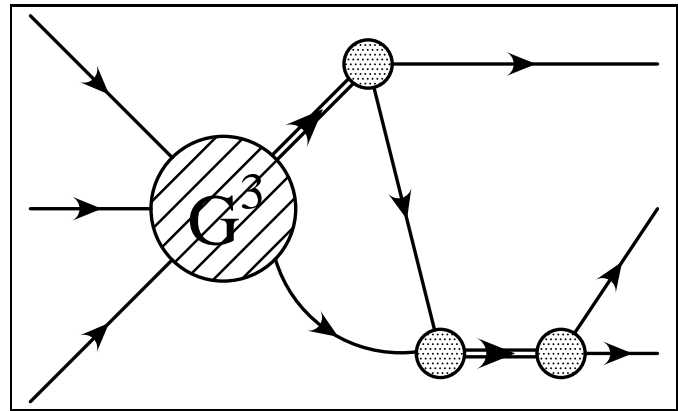
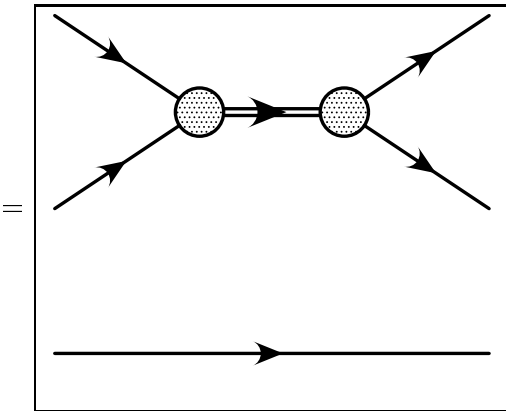
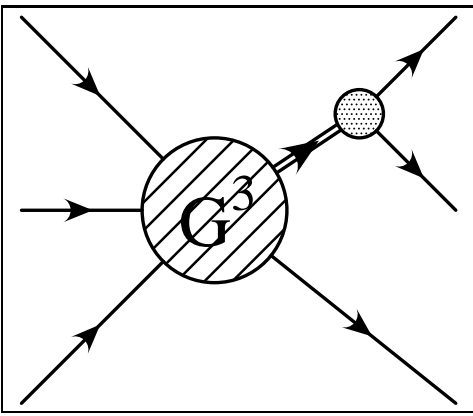


Fig. 7.b

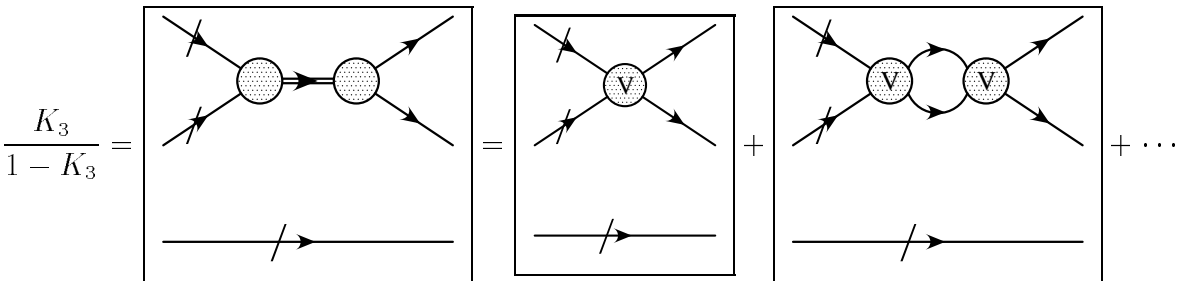


Fig.8.a

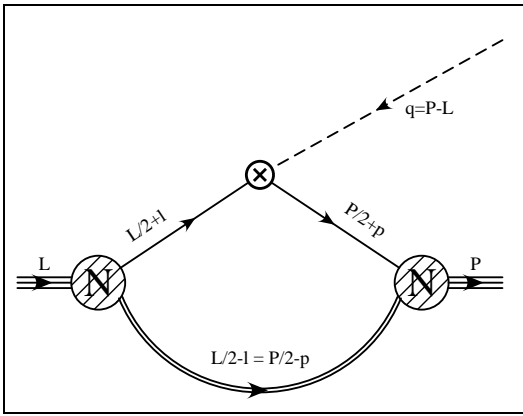


Fig.8.a'

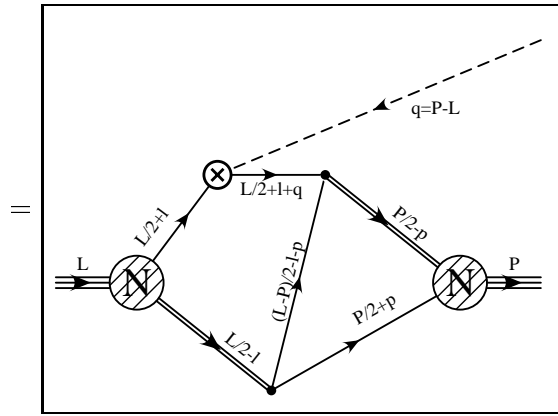


Fig.8.b

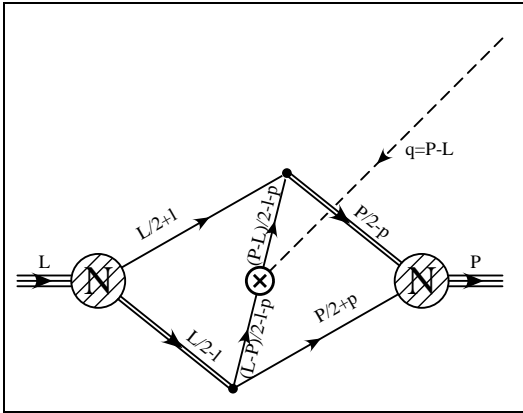


Fig.8.c

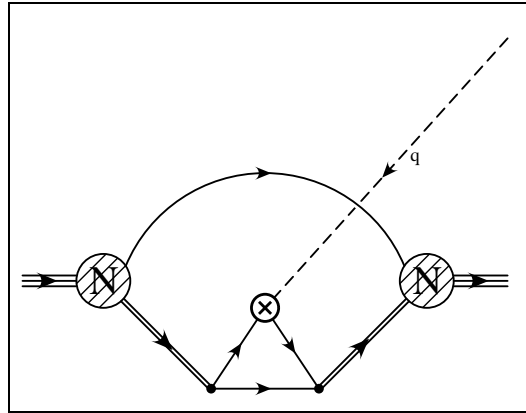


Fig.8.d

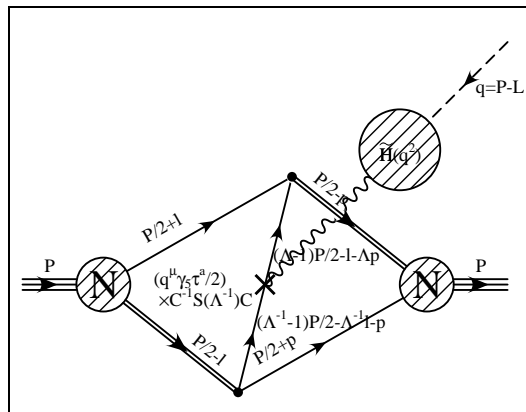
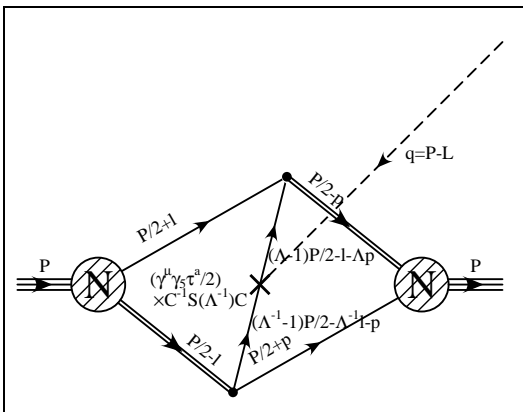
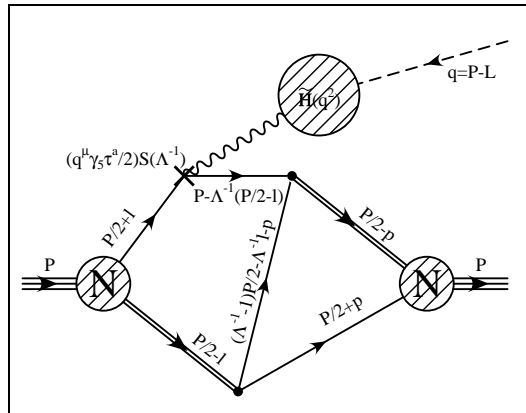
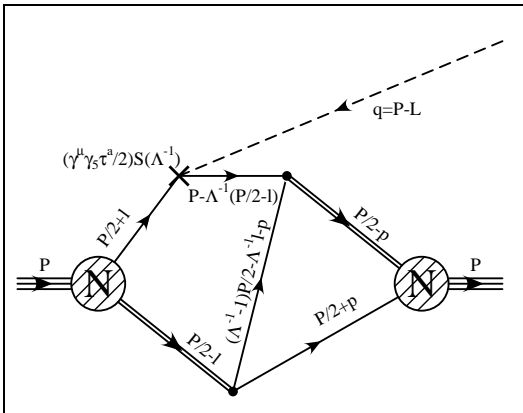


Fig.9

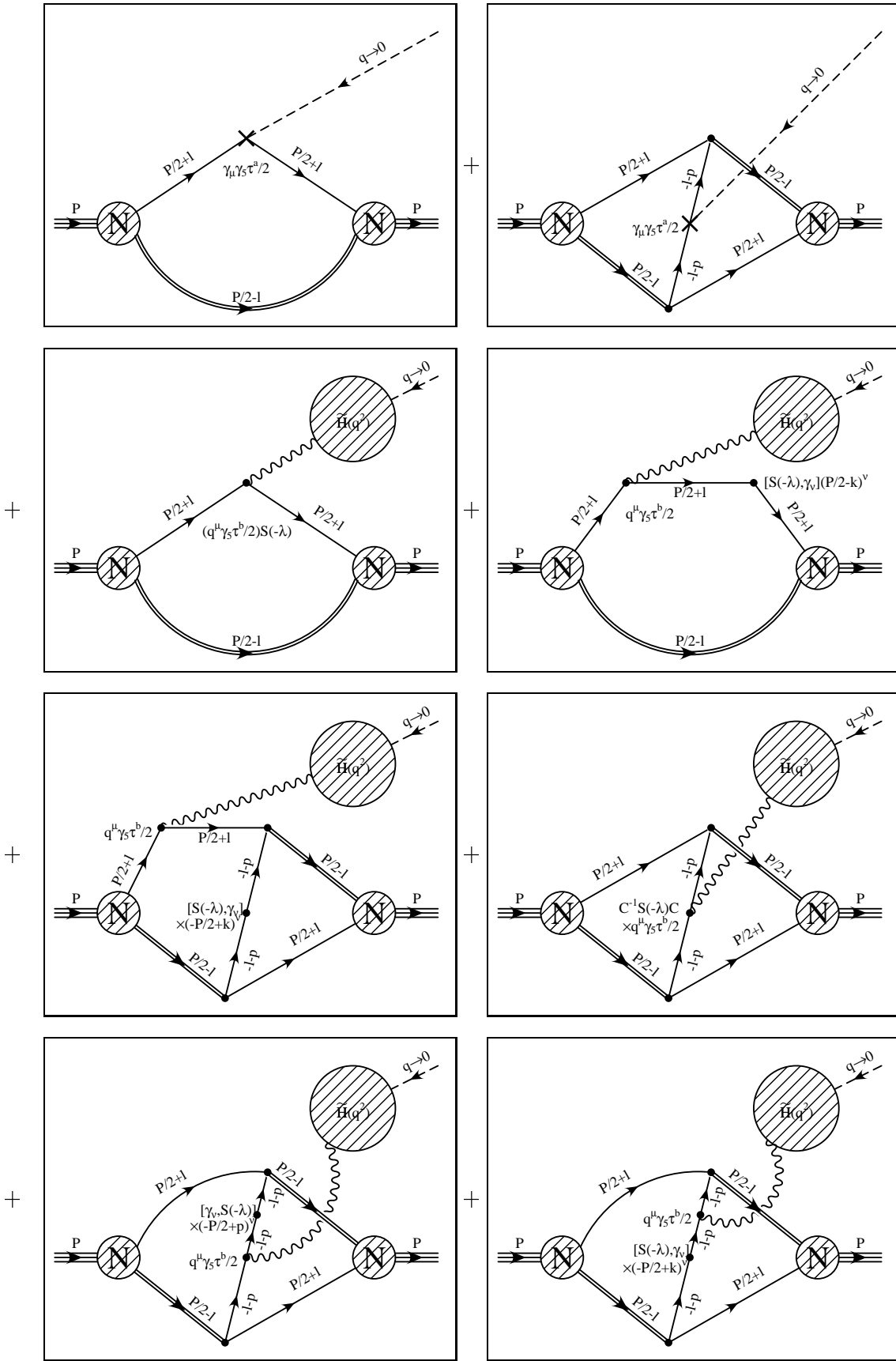


Fig.16.a

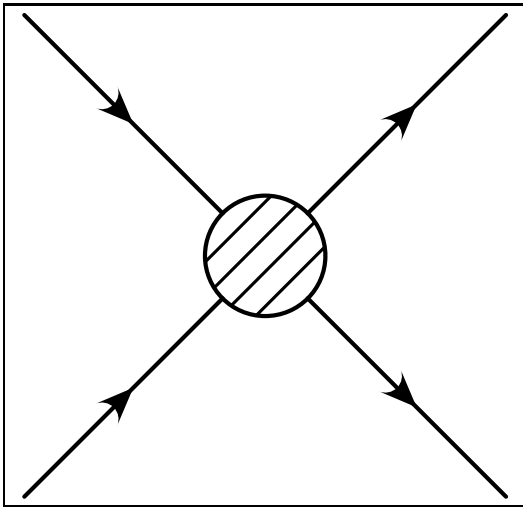


Fig.16.b

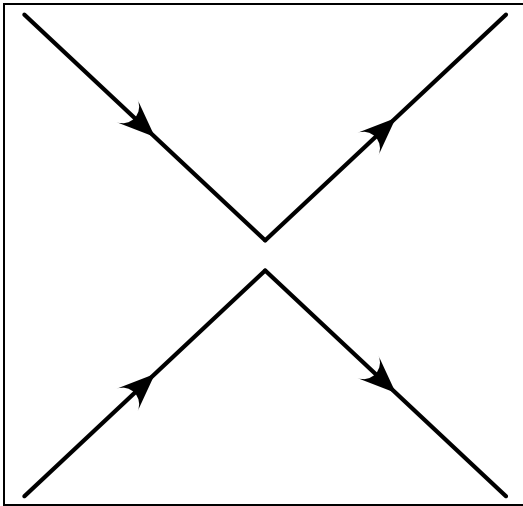


Fig.16.c

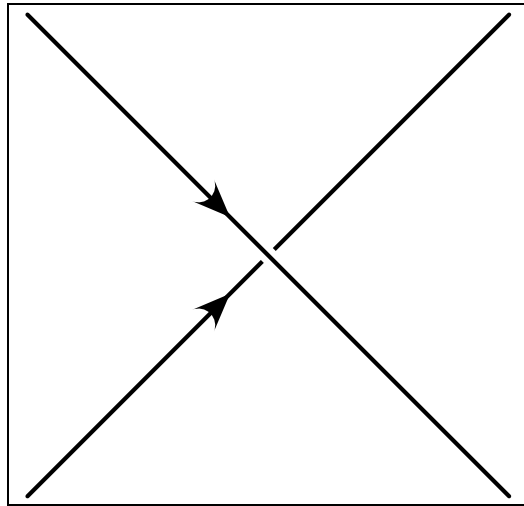


Fig.16.d

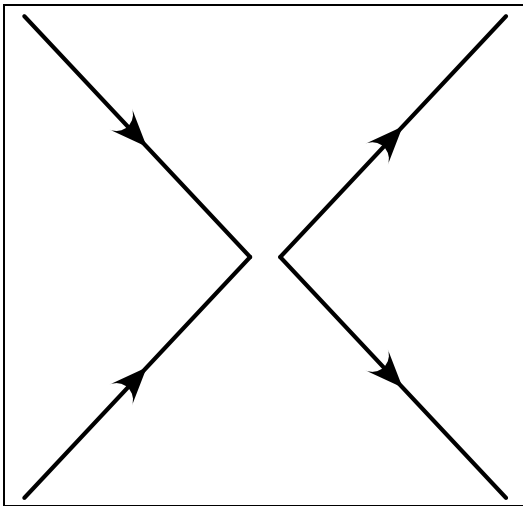
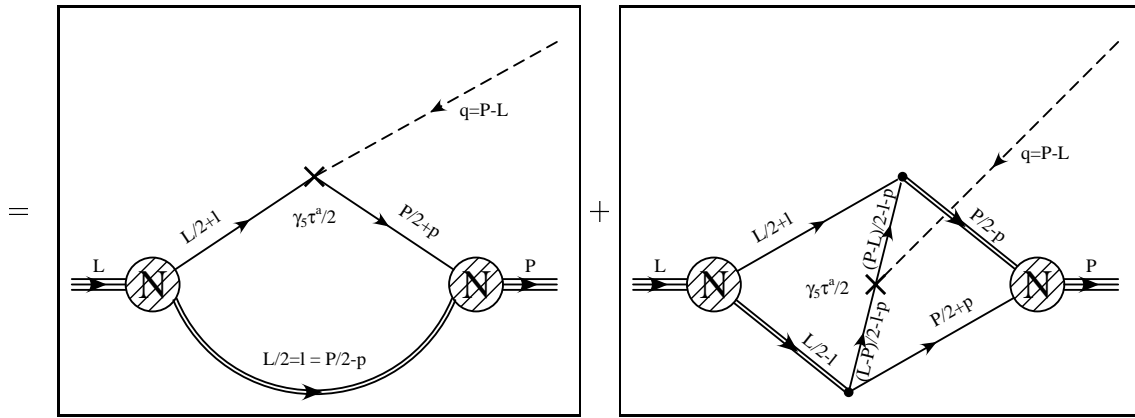




Fig.17

$$B_P(q^2) \left( \bar{u}(P) \gamma_5 \frac{\tau^a}{2} u(L) \right)$$



$$B_A(q^2) \left( \bar{u}(P) \gamma^\mu \gamma_5 \frac{\tau^a}{2} u(L) \right)$$

